MECHANISM OF SELF-HEALING OF AMPLIFIED SPONTANEOUS EMISSION IN THE DYE-DOPED POLYMER DISPERSE ORANGE 11 DYE IN PMMA POLYMER

By

NATNAEL B. EMBAYE

A dissertation submitted in partial fulfillment of
the requirements for the degree of

DOCTOR OF PHILOSOPHY

WASHINGTON STATE UNIVERSITY
Department of Physics

December 2007

To the Faculty of Washington State University:

The members of the Committee appointed to examine the dissertation of Natnael B. Embaye find it satisfactory and recommend that it be accepted.

_____

Chair

_____

_____

_____

ACKNOWLEDGMENTS

I would like to thank my advisor, Prof. Mark G. Kuzyk, for all his guidance and advise as well as for his patience. Thanks also to my lab mates and classmates for all the fruitful discussions. Thanks to Shiva Ramini for the valuable discussions we had. Thanks to my committee for reading the thesis and giving me positive feedback. I am indebted to Dr. Rick Lytel and Prof. Koen Clays for their insightful discussions and to Edward W. Taylor for providing us with gamma-irradiated samples. I appreciate the staff of the Physics Department for their help during my education, and the Air Force and the National Science Foundation for their support. Dr. Gordon Johnson for making my teaching assistant life simple. I would also like to thank the machine and electronic shop personnel.

Thanks to my brother Dr. Abel B. Embaye for his encouragement and financial help in time of need and all my family for their love and prayers. I would also like to thank all the people that I came to know through the years starting from my first grade until now for their friendship. Especially, the friends in my O.T.B., A.I.F. as well as in my local Church here in Pullman Presbyterian Church for their sincere encouragement and prayers. Foremost, I would love to thank The Lord Jesus Christ for His everyday Grace and Mercy in my life.

MECHANISM OF SELF-HEALING OF AMPLIFIED SPONTANEOUS EMISSION IN THE DYE-DOPED POLYMER DISPERSE ORANGE 11 DYE IN PMMA POLYMER

Abstract

by Natnael B. Embaye, Ph.D.
Washington State University
December 2007

Chair: Mark G. Kuzyk

We study the mechanisms of photodegradation and self-healing of 1-amino-2-methylanthraquinone (Disperse Orange 11) in solid poly(methyl methacrylate) under 532nm Nd:YAG laser excitation as measured by amplified spontaneous emission (ASE). We used photochromism in conjuction with ASE dynamical studies to gain an understanding of the character of species formed during photodegradation. Based on our experiments, we propose the mechanism of dimer formation from dipole coupled tautomers and summarize our results with an energy level diagram that is consistent with the full set of measurements. We use a simple population dynamics model to explain the proposed mechanism. As expected from our proposed mechanisms,

we find an intensity-dependent photodegradation rate and a constant recovery rate. This understanding can be used to design materials for devices that are more robust against the common problem of photodegradation.

Contents

List of Figures

Chapter 1

Introduction

A dye is an organic molecule containing at least one carbon-hydrogen bond and by definition exhibits color in the visible. While the observation of color is a complex physiological process, generally, the color that is observed is from the light not absorbed by the molecule. In ancient times, dyes were commonly used to impart their colors to clothes, artwork and decorations. Today, strongly-colored dyes are used as a lasing medium in nonlinear devices and many other applications because they interact strongly with light. Dye molecules typically have structures rich in chains of alternating single and double bonds, called conjugation, as is shown in Figure 1.1. Excitation of such molecules result in charge transfer from one end of the dye to the other through the conjugate chain. Similarly, when a molecule de-excites, it will emit light when the charge transfers along the conjugated bonds. Highly conjugated, π-electron, organic molecules that absorb light in the visible spectrum are sometimes

called chromophores.

Dye lasers typically use a dye in solution as a medium. The first dye laser was reported by Sorokin and Lankard[1] about forty years ago. They used a solution of phthalocyanine dye dissolved in the chloroaluminum solvent as a laser medium. Since then, researchers have reported stimulated emission, the process by which a photon causes excited dyes to emit light in step with that photon, from many classes of organic compounds. Rhodamines and Coumarines are some of the most popular and heavily studied and used classes of organic compounds. Dye lasers are attractive because they are tunable, i.e. the stimulated emission wavelength can be tuned throughout the broad fluorescence spectrum of the dye. A large number of available dyes can be dissolved in solution or in solid matrices like the common polymer, polymethylmethacrylate (PMMA). The host materials, whether they are liquids or solids, act as passive supports of the dyes. The cost of the organic dyes used as an active medium is negligible compared to that of inorganic solid-state lasers, though dyes degrade over time and need to be replenished.

Soffer and McFarland in 1967 demonstrated the first solid-state dye lasers[2], which have many advantages over their liquid counterparts. They are nonflammable, nontoxic and can be made into a desired shape and thus eliminate the need for dye flow hardware. In liquid systems, large reservoirs along with a circulation apparatus are needed to supply fresh molecules to the active region in order to avoid thermal problems and the build up of photodegraded dye molecule which decreases the lasing

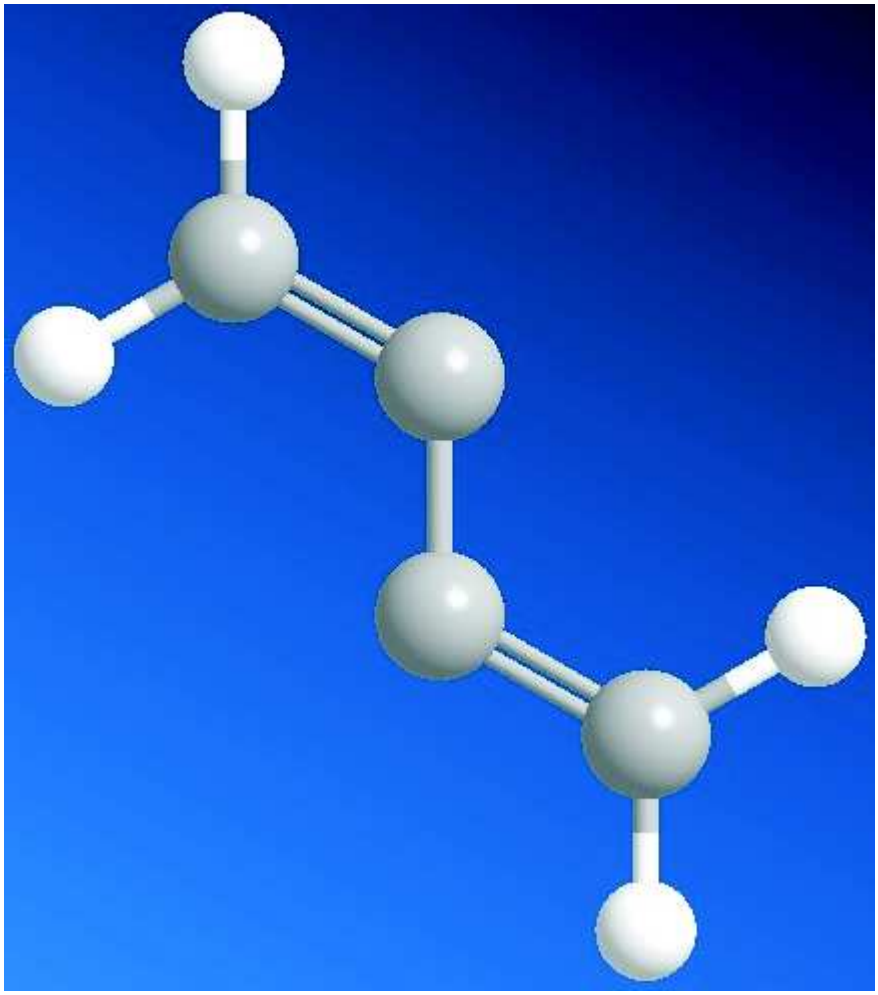

Figure 1.1: Butadine as an example of a conjugated bond, which has at least two double bonds that straddle a single bond. The big spheres are carbon atoms and the smaller ones are hydrogen.

efficiency. Because of their limited life time, dye solutions have to be replaced often, which requires significant maintenance. Furthermore, such maintenance exposes the user to toxic waste. There are no such problems in solid-state dye lasers since they contain no liquid. Many solid-state host materials can be used to make a laser. However polymer matrices are the simplest to fabricate and use, and therefore the least expensive choice. Most importantly, polymers posses many favorable optical properties compared to other types of solid materials.

The problem of photodegradation of dye molecules is well known to high-intensity applications[3]. Organic laser dye molecules usually experience irreversible photodegradation during optical pumping. Even though laser dyes have been under use and investigation for decades, a detailed understanding of the processes responsible for dye stability and maintenance of their lasing properties from photodegradation under high pump repetition rates is still vague. Some explanations suggest the formation of dimers[4] (two mutually bonded molecules) or thermal breakdown due to local heat accumulation[5]. These mechanisms result in the lasing efficiency continuously and permanently decreasing in short periods of time, rendering the dye-doped polymer useless as a lasing medium due to the laser's limited operational life time. Attempts have been made to delay the photodegradation process using additives in the polymer matrices[6, 7] or by rotating the pumped medium[8, 9, 10] thereby continually changing the location of excitation.

Peng and coworkers[11] reported on fluorescence decay and partial recovery in dye

doped PMMA. Peng found that under high intensities and exposure time, the degree of photodegradation was not reversible even if it was kept in dark for a long period of time. Partial recovery was observed for medium intensities. Reversible photodegradation of two-photon fluorescence in a dye-doped polymer was also reported by Zhu and coworkers[12]. Zhu's photodegradation and recovery data was explained using simple rate equations. In both reports the mechanism of reversible photodegradation of the fluorescence is not yet known. Undoubtedly, finding the mechanism for reversible photodegradation of the fluorescence will have interesting applications.

Amplified Spontaneous Emission (ASE) can also recover. Howell and Kuzyk found that the ASE signal of DO11 dye-doped PMMA (DO11/PMMA) polymer would completely recover when left in the dark for 48 hours[14]. In liquids however, there was no recovery[15]. In the solid state experiments, the degradation rate decreased and the recovered amplified spontaneous emission efficiency increased with subsequent cycling of degradation and recovery, suggesting that it may be possible to harden a material against photodegradation by such cycling. The recovery mechanisms were attributed to phototautomerization followed by dimer formation[16]. All experiments were done using a Continuum PY Series mode-locked Nd-yttrium-aluminum-garnet(Nd:YAG) pulsed laser operating at 10Hz with picosecond laser pulses at 532nm(second harmonic of Nd:YAG).

In my research, I found results that are similar to those of Howell and Kuzyk for the self-healing of ASE of the DO11/PMMA, using an Nd-yttrium-aluminum-

garnet(Nd:YAG) pulsed laser operating at 10Hz and having nanosecond-timescale pulses at 532nm. With the help of these new results, we were able to study the mechanisms of self-healing of ASE in DO11/PMMA as suggested by Kuzyk[16] by using simple coupled rate equations. We were able to explain the photodegradation and recovery processes using population dynamics. The results of the fitting of the data to the theory shows that the degradation process is linear with intensity but the recovery process is independent of the intensity. Zhu[12] found similar results for TPF in AF455 dyes, but the mechanism is not yet known. Based on molecular structure, should not be the same as DO11/PMMA. Our goal is to use rate equations to understand degradation and recovery.

The work of this dissertation is organized in the following manner. Chapter 2 presents the theory and principles that we propose underlie the degradation and self-healing of DO11/PMMA. We derive the spontaneous and stimulated decay rates for use in the rate equations. Chapter 3 shows the experimental procedures that were used in formulating the mechanisms and in getting complementary data in order to explain the mechanism. Chapter 4 discusses the results and discuss their implications. Finally, in Chapter 5 we summarize our work and discuss future work that we believe will shed light on self-healing of dye doped polymers.

Bibliography

[1] M. Maeda, Laser Dyes, *Properties of Organic Compounds for Dye Lasers*, Academic Press, Inc., Orlando, Florida, 1984, pp. 1.

[2] K. Kuriki, T. Kobayashi, N. Imai, T. Tamura, S. Nishihara, Y. Nishizawa, A. Tagaya, Y. Koike, Y. Okamoto, Appl. Phys. Lett. **77**, 331 (2000).

[3] S. Popov, Appl. Opt. **37**, 6451 (1998).

[4] K.H. Drexhage, *Structure and Properties of Laser Dyes in Topics in Applied Physics, Dye Lasers*, SpringerVerlag, Berlin, Germany 1990, pp. 21-22, 167-169.

[5] F. Amat-Guerri, A. Costela, J.M. Figuera, F. Florido, R. Sastre, Chem. Phys. Lett. 209, 352 (1993)

[6] R. Duchowicz, L.B. Scaffardi, A. Costela, I. Garcia-Moreno, R. Sastre, A.U. Acuna, Appl. Opt. **39**, 4962 (2000).

[7] K. Dyumaev, A. Manenkov, A. Maslyukov, G. Matyushin, V. Nechitailo, A. Prokhorov, J. Opt. Soc. Am. B **9**, 145,147-148 (1992).

[8] G. Somasundaram, A. Ramalingam, J. Photochem. Photobiol. A **125**, 97 (1999).

[9] G. Somasundaram, A. Ramalingam, J. Lumin. **90**, 5 (2000).

[10] G. Somasundaram, A. Ramalingam, Chem. Phys. Lett. **324**, 28 (2000).

[11] G. D. Peng, Z. Xiong, and P. L. Chu, J. Low Temp. Phys. **16**, 2365 (1998).

[12] Ye Zhu, Juefei Zhou, and Mark G. Kuzyk, Optics letters, **32**, 8 (2007).

[13] K. Dyumaev, A. Manenkov, A. Maslyukov, G. Matyushin, V. Nechitailo, and A. Prokhorov, J. Opt. Soc. Am. B **9**, 143 (1992).

[14] B. Howell and M. G. Kuzyk, J. Opt. Soc. Am. B **19**, 1790 (2002).

[15] B. Howell and M. G. Kuzyk, Appl. Phys. Lett. **85**, 1901 (2004).

[16] M. G. Kuzyk, *Polymer Fiber Optics: Materials, Physics, and Applications*, Vol. **117** of Optical Science and Engineering (CRC Press, 2006).

Chapter 2

Theory

2.1 Introduction

The purpose of this dissertation is to study the mechanisms of reversible photodegradation or self-healing of ASE in DO11-doped PMMA[1, 2]. To that end, we develop a theory using population dynamics to model the proposed mechanism of light emission after phototautemerization followed by dimer formation that quenches ASE, followed by dimer breakup back to the DO11 molecule.

Before proceeding to the formulation of our theory, the general properties of the dye molecules is reviewed in section 2.2. In section 2.3, we briefly discuss the absorption and emission processes in dye doped polymers using a two-level energy diagram. In this section, we also derive the spontaneous emission decay rate using the classical electron model. Using some simple quantum concepts, the classical results can be

transformed to their quantum mechanical form. A derivation of purely classical theories and their connection to quantum mechanics is given by Seigman[3] and Vleck and Huber[4]. Using these results, we also obtain the stimulated emission decay rate in section 2.3.4.

In section 2.3.5, we introduce phototautomerization, dimer formation and photodegradation in DO11-doped PMMA. Finally we formulate the theory using a five-level energy diagram and use simple rate equations and apply them to the processes that we postulate are relevant the self-healing of DO11-doped PMMA as measured with ASE.

2.2 General Properties of Dyes

Dyes are organic compounds which are classified as either saturated or unsaturated. Organic compounds that contain only single bonds are called unsaturated and those compounds that contain at least one double bond are called saturated. The character of the multiple bonds in organic compounds lead to a range of reactivities and spectroscopic properties. Most organic compounds that have only single bonds usually absorb light with a wavelength below 160nm, which corresponds to a photon energy of 7.8 eV. This amount of energy can easily break the bonds since most bond energies are smaller than 7.8 eV. For instance, the bond energy between H-H and C-C is 4.5 eV and 3.6 eV respectively. Therefore, such organic molecules are not suitable for a laser material. All single bonds are formed by σ electrons, but the double and triple

bonds use π electrons in addition to the σ electrons. Bonds formed with σ electrons are called σ bonds and bonds that are formed with π electrons are called π bonds. The energy of a double or triple bond is higher than the unsaturated organic compounds but the total energy of the molecule is lower[5]. Two double bonds separated by a single bond is called a conjugated chain. Dyes contain many conjugated bonds and have strong absorption in the visible part of the spectrum.

A dye absorption spectrum is a function of temperature. A dye molecule in a polymer has thermal energy, which manifests itself as vibrations of the molecules in the polymer as well as nuclear vibrations with each molecule. The thermal energy can excite a molecule to a higher energy level. As the temperature is increased, higher energy levels become populated. The energy distribution is governed by Boltzmann's law and is given by:

$$N = N_0 \exp[-E/kT], \tag{2.1}$$

where N is the number of dye molecules in a level of energy E, N_0 is the number of molecules in the ground state, $k = 1.38 \times 10^{-23} J/K$ is the Boltzmann's constant when E is in units of Joules, and T is the absolute temperature in K. At room temperature, T=293K and for a molecule with an excitation energy in the visible part of the spectrum, say λ=500nm, the ratio $N/N_0 \approx 10^{-40}$. In the same fashion, we can also show that at a reasonable temperature there will not be a significant excited state population. This leads us to an important conclusion: the upward

excitation decay rate (i.e, from the ground state to the excited state) due to thermal energy for a molecule that absorbs light in the visible region is negligible.

2.3 Interaction of Light with Dye-Doped Polymers

2.3.1 Absorption and Spontaneous Emission

In order to understand the absorption and emission of dye molecules, it is best to start with an energy level diagram. The energy level structure of organic dyes is complex owing to the large number of electrons that interact along their extended conjugated bonds. The energy levels of an organic dye are not distinct states but form bands. The bands are due to vibrational and rotational modes of the atoms that form the dye molecule. S_0 is the lowest band and it is called the singlet state, with a total quantum mechanical spin of zero. The dye molecule can absorb or emit energy by undergoing transitions upwards or downwards between its energy levels. Figure 2.1 shows a simplified two-level energy diagram to demonstrate excitation and emission.

For example the dye molecule absorbs light and is excited from the ground singlet sub level a to the excited singlet sub level B as shown in Figure 2.1. In a few femtoseconds, the molecule decays to sub level b. The decay involves rearrangement of the total energy without emitting a photon and is therefore called a non radiative transition. After a few nanoseconds, the molecule may decay spontaneously to the singlet sub level A conserving energy in the process. This process is called spontaneous

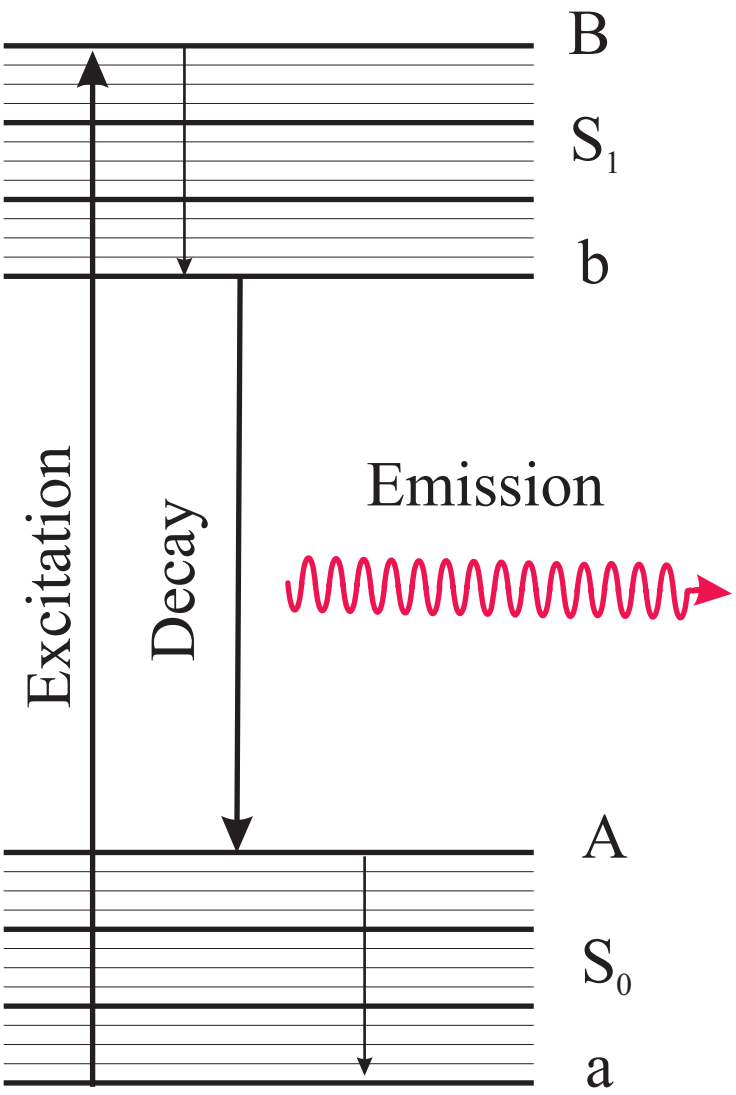

Figure 2.1: Simple two level energy diagram. S_0 and S_1 represent the singlet ground state excited state levels. Within the singlet states are vibrational levels, which are split by rotational levels.

emission or fluorescence with the photon energy matching the energy difference $E_b - E_A$ between the states. The wavelength is given by

$$\lambda_{bA} = \frac{hc}{E_b - E_A}, \tag{2.2}$$

where $h = 4.136 \times 10^{-15}\ eV \cdot s$ is Planck's constant and $c = 3 \times 10^8\ m/s$ is the speed of light. Finally the molecule decays to the sub level a or the ground state level of the singlet band S_0 without emitting a photon. For a more conceptual understanding of the absorption and fluorescence of dye-doped polymers, the reader is referred to Kuzyk[6].

In the next section, we derive the fluorescence or spontaneous decay rate, sometimes called the Einstein Coefficients, from the classical oscillator point of view and then transform the equations into their quantum counterparts.

2.3.2 The Classical Electron Oscillator (CEO).

Before we begin, let's remind ourselves about some facts about atoms in a dye molecule:

1. Dye molecules contain many atoms.

2. Atoms in turn consists of protons and neutrons in its nucleus and electrons surrounding them.

3. Molecules show energy resonances in their spontaneous emission processes.

4. The energy dispersion of resonances resemble the shape of a simple harmonic oscillator.

5. Molecules respond to electric fields and the strongest molecular transitions are those that are electric dipole transitions.

The properties mentioned above help us to use the classical electron oscillator model shown in Figure 2.2.

In an atom the electrons revolve around the nucleus. The motion of the electron is governed by the electric force between the electron and the nucleus. When an electron is displaced by $\mathbf{x}(t)$ from its equilibrium orbit, the positive nucleus exerts a restoring force that we approximate by

$$\mathbf{F} = -K\mathbf{x}(t), \tag{2.3}$$

where the corresponding potential is

$$U(x) = \frac{1}{2}Kx^2(t), \tag{2.4}$$

and where K is the force constant. The equation of motion for the electron is then

$$m\frac{d^2x(t)}{dt^2} = -Kx(t) - eE_{x(t)}, \tag{2.5}$$

which can be re-written as

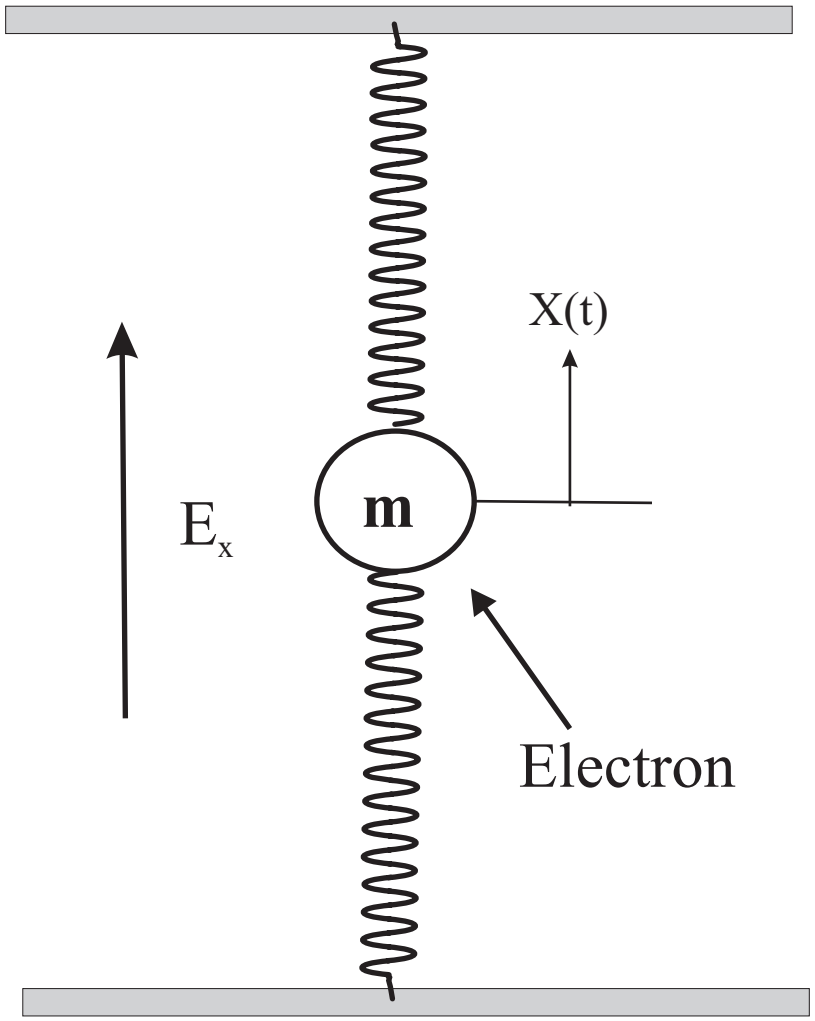

Figure 2.2: An atom can be modeled as a classical electron oscillator. The electron has mass m and charge e and when displaced a small distance $x(t)$, it experiences a harmonic force that approximates the force between an electron and positive charge of the nucleus. The electron experiences a restoring force $-Kx$.

$$\frac{d^2x(t)}{dt^2} + {w_a}^2 x(t) = -(e/m)E_{x(t)}, \tag{2.6}$$

where $w_a = \sqrt{K/m}$. This is the CEO's resonance frequency for the CEO model equivalent to the optical transition frequency $w_{12} = (E_2 - E_1)/\hbar$ of a molecular transition in real molecule.

A damping term γ must be added to the equation of motion in order to allow the oscillator to lose energy, which yields:

$$\frac{d^2x(t)}{dt^2} + \gamma\frac{dx(t)}{dt} + {w_a}^2 x(t) = -(e/m)E_{x(t)}, \tag{2.7}$$

where γ is the damping rate. The solution of equation[2.7] without the applied field is given by

$$x(t) = x(0)\exp(-\gamma/2 + iw_b)t, \tag{2.8}$$

where $w_b = \sqrt{{w_a}^2 - (\gamma/2)^2}$. The energy of the CEO model, $U_a(t)$, is

$$U_a(t) = \frac{1}{2}Kx(t)^2 + \frac{1}{2}m{V_x}^2 = U_a(0)\exp(-\gamma t) = U_a(0)\exp(-t/\tau). \tag{2.9}$$

From equation[2.9], we see that γ is the energy decay rate and $\tau = \gamma^{-1}$ is the energy decay time constant.

A molecule in an excited state will lose energy by making a transition to a lower state. When a photon is emitted from a single molecule in vacuum, the process is called spontaneous emission or fluorescence. We define γ_{rad} to be this pure radiative decay rate. In addition, energy can be transferred to the surrounding, which we characterize by the non-radiative decay γ_{nr}. Non radiative processes include collisions with the surrounding material or transfer of energy in the form of heat. The total decay rate is

$$\gamma = \frac{1}{U_a}\frac{dU_a}{dt} = \gamma_{rad} + \gamma_{nr}. \tag{2.10}$$

From electromagnetic theory, we can calculate the radiative decay rate by assuming that the oscillating electron in a molecule radiates electromagnetic energy in the same way as in oscillating dipole antenna. From Jackson[9] the time averaged rate at which power is radiated into the far field in all directions by a dipole antenna or by a sinusoidally oscillating charge with an electric dipole moment $\mu_x(t) = \mu_0 \cos wt$ is

$$P_{av} = \frac{{w_a}^4 {\mu_0}^2}{12\pi\epsilon v^3}. \tag{2.11}$$

Making use of equation[2.10] and equation[2.11] and using $U_a = \frac{1}{2} m {w_a}^2 {x_0}^2$ we get

$$\gamma_{rad} = \frac{{w_a}^2 e^2}{6\pi\epsilon m v^3}, \tag{2.12}$$

where ϵ is the permittivity of the material and v is the speed of light in the material. Recall that the refractive index of a material $n = \sqrt{\frac{\epsilon}{\epsilon_0}}$ or $n = c/v$ and the frequency of oscillation measured in Hz is given by $f_a = \frac{c}{\lambda}$. Putting all these together, the radiative decay rate is

$$\gamma_{rad} = \frac{2\pi e^2}{3\epsilon m c^3} n {f_a}^2 = \frac{1}{\tau}, \tag{2.13}$$

where c is the speed of light in vacuum.

It is important to note that the purely radiative decay for strongly allowed transitions of real molecules is of the same order of magnitude as the radiative decay rate for the CEO for the same resonant frequency. Let's take one practical example of the Rhodamine 6G dye molecule which is used as a laser medium. It has a radiative decay rate of $\frac{1}{10ns}$ from an S_1 to S_0 transition, which corresponds to a wavelength of 620nm, which is about $\frac{1}{11ns}$[3] by using the CEO model. Therefore, the CEO is a good way of estimating the radiative decay rates of real molecules.

The radiative decay rate has a value $\gamma_{rad,CEO} \approx 10^8 sec^{-1}$ for an optical excitation in the visible frequency range of $w_a = 4$ x 10^{15} sec^{-1}. Therefore the decay rate is very small compared to the oscillation frequency.

Equation[2.13] is used later to estimate the spontaneous radiative decay rates of various energy levels.

2.3.3 Stimulated Emission

When a photon energy matches the transition energy between two states in a molecule which is in an excited state it will induce the molecule to emit light in phase with that photon. The probability of emission will increase in proportion to the number of photons in the incident field. This process is called stimulated emission. Only photons with energy equal to the energy difference between the allowed transition states of the molecule can stimulate emission in an excited molecule. Figure 2.3 shows a diagram of stimulated emission.

If there are more molecules in the excited state than in the ground state (inverted population), a photon that is emitted by spontaneous emission is amplified through stimulated emission. As the number of photons builds, the amplification process snowballs. In this way, a few photons are amplified into many photons that are coherent with each other. This amplification process is the phenomenon underlying lasers (Light Amplification by Stimulated Emission of Radiation). A laser requires a cavity to reinforce coherent emission. Without a cavity this process is called Amplified Spontaneous Emission (ASE). For a more conceptual understanding of ASE of dye doped polymers, the reader is again referred to Kuzyk[6].

2.3.4 Stimulated Emission Rate

This stimulated emission rate ω_s depends on a number of factors such as cross-sectional area of the pump beam at the sample, the stimulated emission cross section

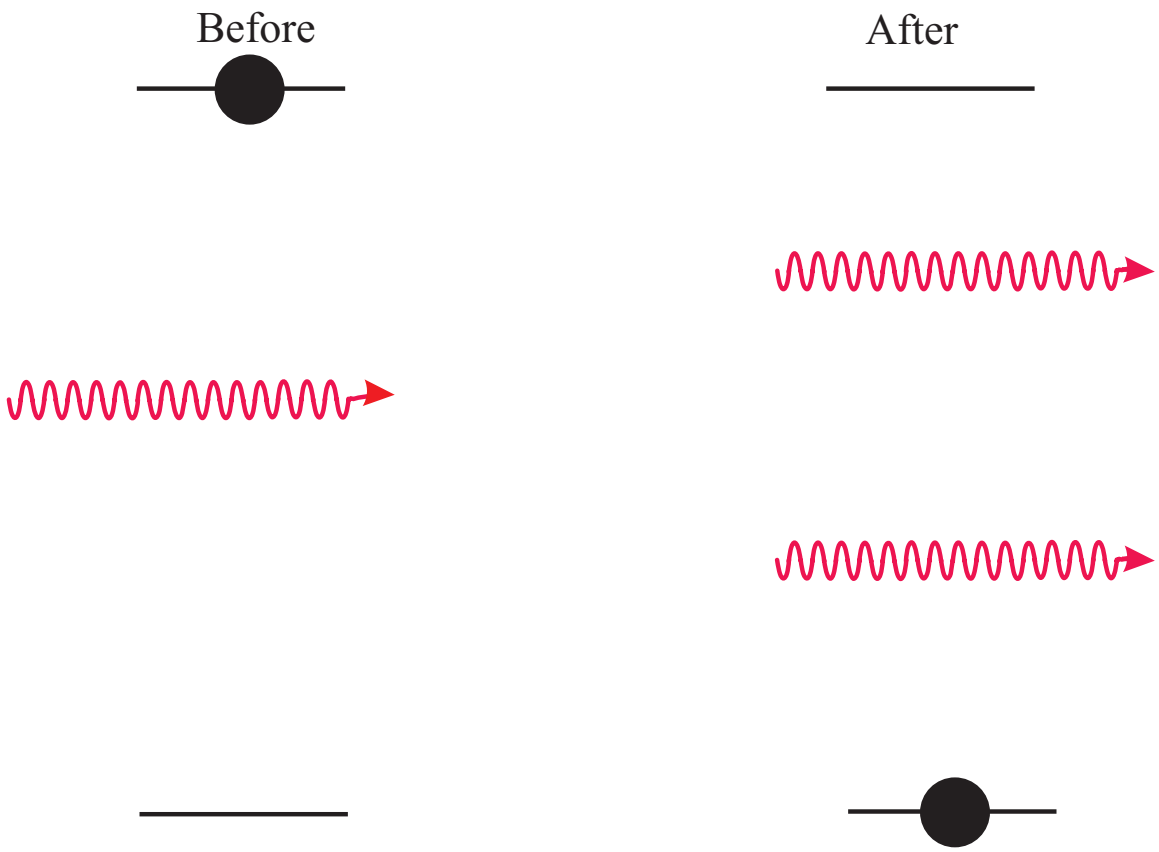

Figure 2.3: A photon of appropriate energy interacts with a molecule already in an excited state. In the process, the photon is not destroyed but creates another photon with the same energy and phase.

σ_s, the inverted population number density N^i and finally the spontaneous decay rate due to the excited state molecule to its ground state. The derivation that follows brings all these factors together to get an expression for the stimulated decay rate ω_s.

Consider a rod of length L and diameter 2a as in Figure 2.4 that is uniformly filled with an inverted population density N^i.

The power of the spontaneous emissions will be emitted in all directions from each small volume element of the medium. The power per unit volume will be given by $N^i\ \gamma_{32}\hbar\omega$. For L>>a, the contribution to the amplified spontaneous intensity dI_{ASE} arriving at the output end of the rod from any small slice of width dz near the input end of the rod can then be written as

$$dI_{ASE} = \frac{\pi a^2 N^i \gamma_{32}\hbar\omega}{4\pi L^2} \exp\left[2\alpha_m(L-z)\right]dz, \tag{2.14}$$

where $2\alpha_m \equiv N^i\sigma$ is the power amplification coefficient in the rod. If we sum over the spontaneous emission from all volume elements over the entire length of the rod, the total ASE intensity at the output end will be

$$I_{ASE} \approx \frac{N^i \gamma_{32}\hbar\omega a^2}{4L^2} \exp\left(2\alpha_m L\right) \int_0^L \exp\left[-2\alpha_m z\right]dz. \tag{2.15}$$

Integrating equation[2.15] we get:

$$I_{ASE} \approx \frac{\gamma_{32}\hbar\omega a^2}{4\sigma L^2}(\exp\left[2\alpha_m L\right] - 1). \tag{2.16}$$

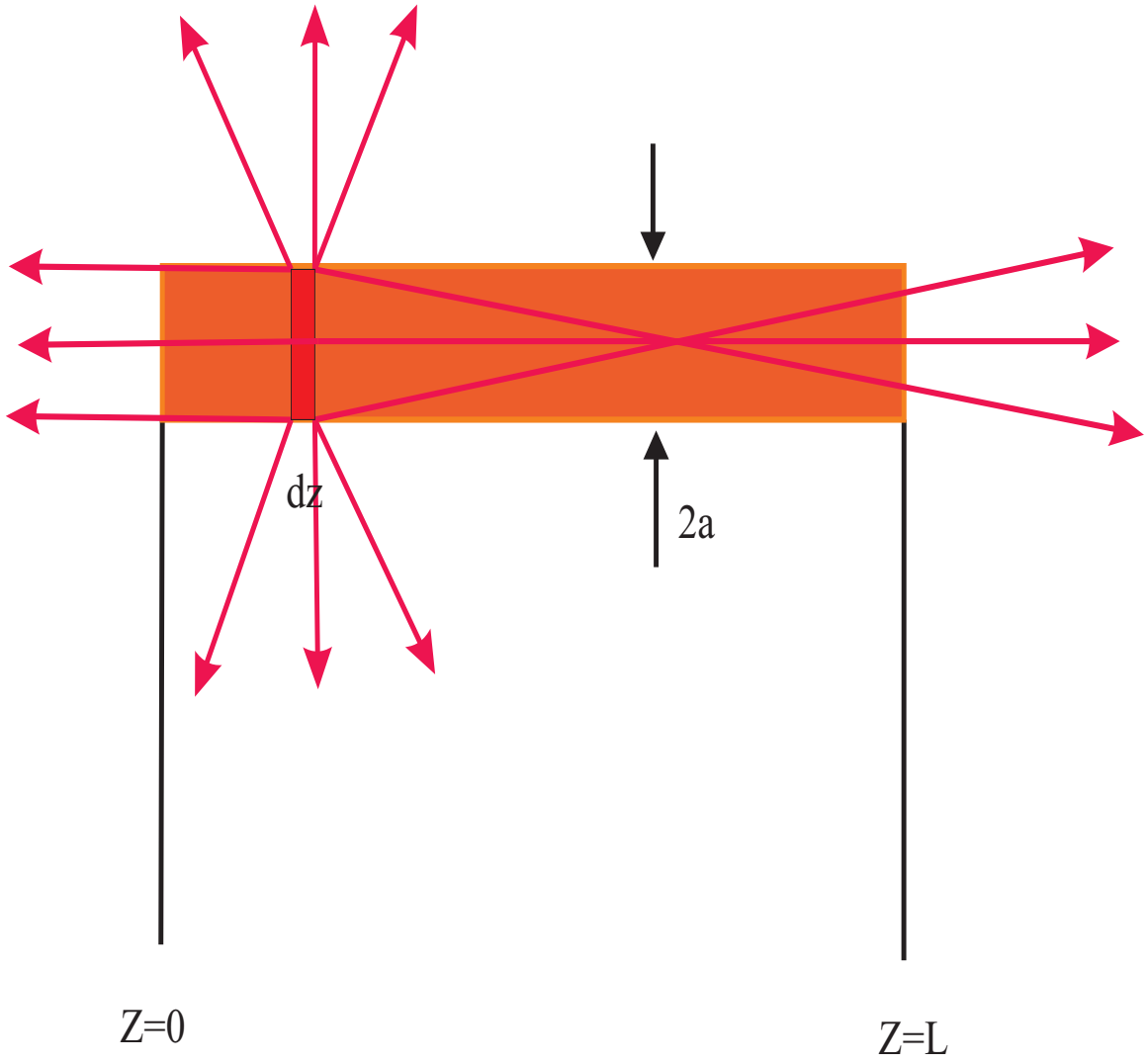

Figure 2.4: The population in the excited state is greater than in the ground state. The rod has length L and diameter 2a. Spontaneous emission for a volume element at dz will be emitted equally in all directions while stimulated emission will travel preferentially in the direction of the inverted population, i.e., parallel to the rods axis.

From the Classical Molecule Oscillator we know that the ω_s is related to I_{ASE} by

$$\omega_s = \frac{\sigma I_{ASE}}{\hbar\omega} = \frac{\gamma_{32}a^2}{4L^2}(\exp\left[N^i\sigma L\right] - 1). \tag{2.17}$$

Our experiment measures the ASE signal which is related to the number density using equation [2.17]. Note that the ASE power is an exponential function of the number density. The fluorescence which is a linear function of the population of excited molecules.

2.3.5 Phototautomerisation, Dimer Formation and Photodegradation

In the previous sections we discuss how light interacts with dye molecules to induce transitions. Phototautomerisation and Dimer formation are other processes by which a molecule non radiatively decays to a different species. Phototautomerisation is the intra molecular transfer of a proton (H^+) from one part of a dye molecule to another. Alternatively a proton can transfer to other dyes or to the polymer. Phototautomerization can be initiated by an absorption of a photon and results in a large energy shift of the electronic state. Tautomerization is made evident in the anomalously large shift toward longer wavelengths of the fluorescence spectrum.

The formation of a pair of molecules is called a dimer. The DO11 molecule, which is the focus of this dissertation, has a considerably large dipole moment in its tautomeric state than for the neutral state. Thus, we postulate that tautomers

can readily form dimers, i.e, $tautomer + tautomer \rightleftharpoons Dimer$. This dimer is a new species with a new absorption and fluorescence spectrum. Figure 2.5 and Figure 2.6 shows schematic diagrams of dimer formation and the absorption spectrum of the monomer(singlet molecule) and the expected spectrum of a dimer species respectively.

Figure 2.6 shows that the dimer has an absorption spectrum with two peaks that results from splitting of the monomer peak. As a monomer is converted to a dimer, the monomer peak gets smaller while the two dimers peaks grow. The dimer thus has two transition moments from the ground state. One is strong and the other is weak[7]. It is well known that transition moments are related to the lifetimes of the energy levels. Since the lower dimer energy level has practically vanishing transition moment and since this results in long lifetime of the level, the fluorescence yield will be very small. In such cases, the fluorescence in the dimer is quenched. A dimer in its ground state can decay to the lower-energy ground state of the monomer when the dimer disassociates.

Much research has been devoted to finding more robust materials that are resistant to photodegradation. Our work is focused on understanding the mechanism of a new phenomena of self-healing, where a photodegraded molecule comes back to life. We will see how the formation of dimers are a key part of the photodegradation process and how recovery depends on dimer disassociation.

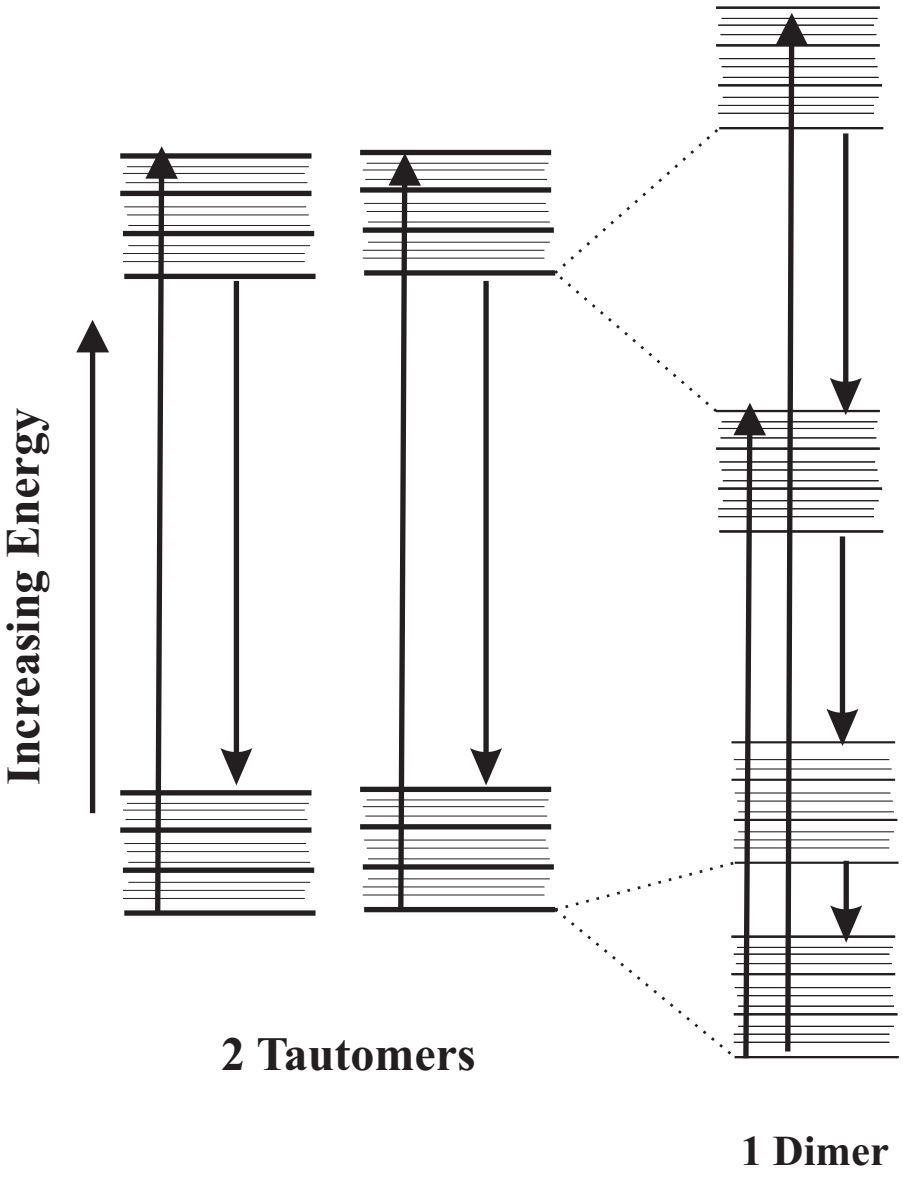

Figure 2.5: Schematic diagram of dimer formation from two tautomers. Considering, a two state model for each tautomer, interactions will cause the ground state and the excited states split. The dimer also absorbs light in the visible range at two wavelengths.

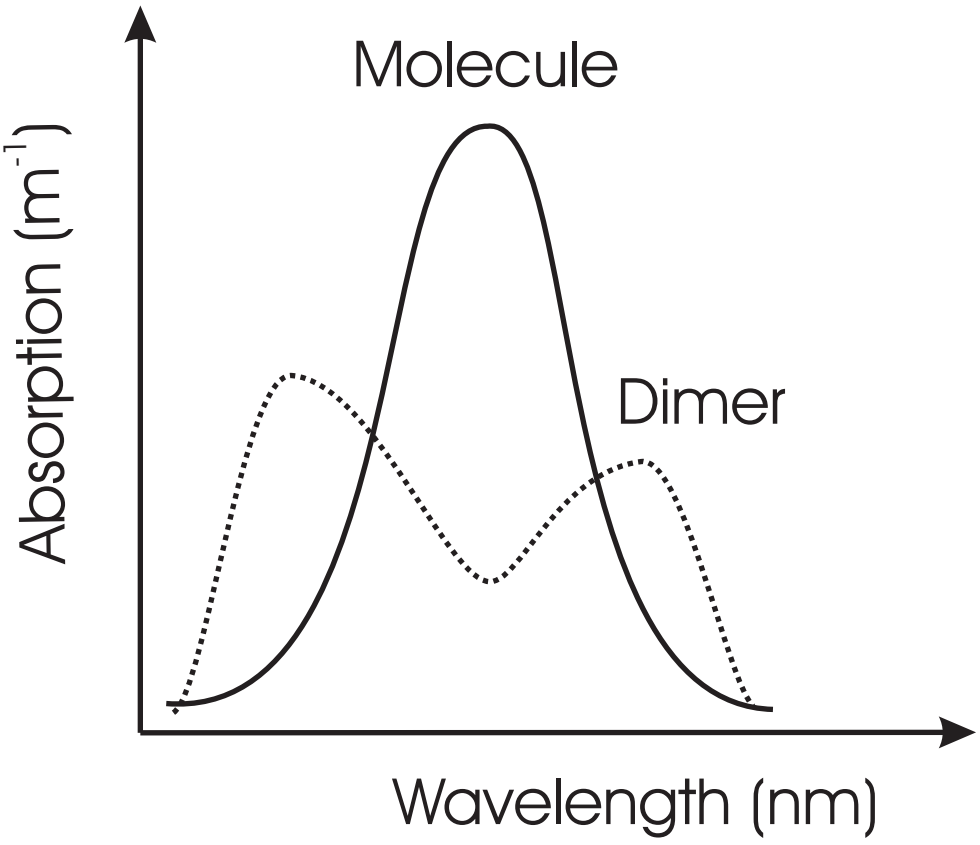

Figure 2.6: The absorption spectrum of a monomer near its dominant absorption peak. When dimers are formed the excited state splits, resulting in two distinct peaks. The creation of the dimers are evident when the main absorption peak changes when monomers is depleted and an increase at the short and long wavelength peaks corresponds to the two dimer states.

2.4 Mechanism of Self-Healing of ASE in a Nonlinear Dye-Doped Polymer

One of the nonlinear optical molecules that showed self-healing of ASE at Washington State University in the nonlinear optics lab is the Disperse Orange 11 (DO11)dye doped poly(methyl methacrylate) (PMMA) polymer[1, 2, 10]. In this section, we propose a theory that explains the mechanism of self-healing of ASE after photodegradation in the dye-doped system of DO11/PMMA. To the best of our knowledge, this theory is the first one to model self-healing of ASE in a dye doped polymer. Our theory has the following assumptions:

1. The ground state of the system is for the case of a DO11 molecule in its singlet ground state S_0. As such, the initial state of the system is a collection of DO11 molecules in the state S_0.

2. A photon in the visible spectral range can excite the molecule only into the excited state S_1.

3. The excited singlet state can decay back either radiatively to its ground state S_0 or non radiatively to the excited state of the tautomer T_1 by phototautomerization.

4. The excited state tautomer T_1 can decay back to the tautomer ground state T_0 radiatively by spontaneous or stimulated emission.

5. The tautomer in its ground state can decay non radiatively either to the singlet ground state of the monomer or it can interact with another tautomer in the ground state to form a dimer D_0.

6. The ground state and the excited state energy levels of the tautomer are each split by the interaction between tautomers in the dimer.

7. The dimer slowly decays back to the ground state of the molecule by thermal tunneling.

Furthermore, we define the following terms:

1. w_p is the pumping rate, defines as the number of photons absorbed per unit time by a DO11 molecule in its ground state and is given by

$$w_p = \frac{\sigma\ I_p}{\hbar\omega}, \tag{2.18}$$

where σ is the one photon absorption cross section, I_p is the pump intensity, $\hbar$ is Planck's constant divided by 2π and ω is the photon frequency, which is resonant with the $S_0 \rightarrow S_1$, excitation of the DO11 molecule.

2. γ_{41} is the spontaneous decay rate of the excited DO11 molecule to its ground state ($S_1 \rightarrow S_0$) and is estimated using the CEO model.

3. γ_{43} is the phototautomerization rate of the DO11 molecule excited state to the excited state of the tautomer($S_1 \rightarrow T_1$) and the corresponding time constant is

in the picosecond range [8].

4. γ_{32} is the spontaneous decay rate of the excited state tautomer to its ground state $T_1 \rightarrow T_0$ and is estimated from the CEO model.

5. γ_{25} is the rate of dimer formation from the ground state tautomer to the dimer $T_0 \rightarrow D_0$.

6. γ_{21} is the reverse phototautomerization rate of the ground state tautomer to the DO11 molecule ground state $T_0 \rightarrow S_0$ similar to γ_{43} but less in decay rate value since dimers are also forming from the same level.

7. γ_{51} is the rate of dimer dissociation, i.e the rate of formation of ground state DO11 molecules from the dimers $D_0 \rightarrow S_0$.

We propose that photodegradation in the DO11/PMMA system originates in the formation of dimers. As we will show in the experimental section, the linear absorption spectrum of a degraded sample is consistent with the depletion of DO11 molecules and the formation of species with an absorption spectrum similar to the dotted curve in Figure 2.6.

The proposal that dimers are formed by the attraction of metastable tautomers is consistent with the fact that a tautomer has a large dipole moment when compared with DO11 molecules. Since the process of generating ASE light is associated with emission from a tautomer, we propose that the origin of photodegradation is through the formation of dimers. Since a dimer can dissociate to the level energy

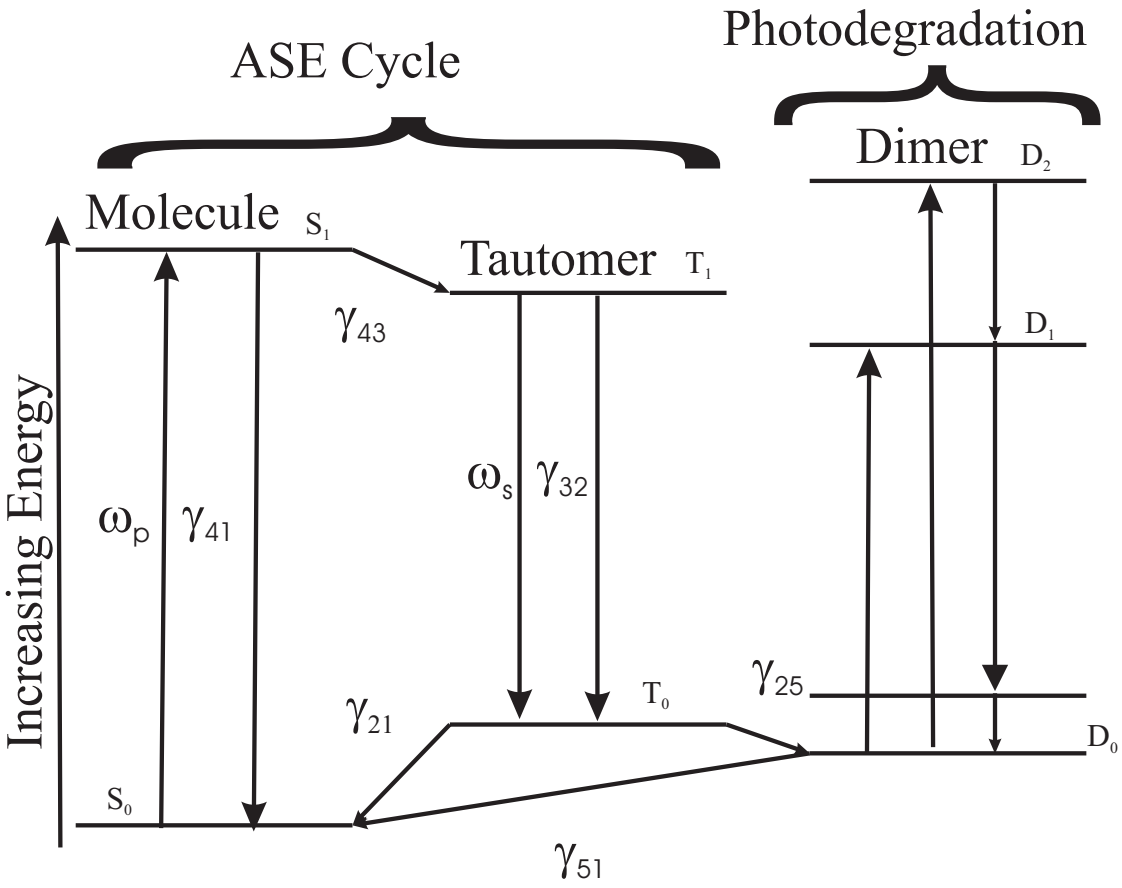

Figure 2.7: Proposed energy level diagram, of the ASE process, photodegradation and recovery.

DO11 molecules, the process is reversible. Figure 2.7 shows the proposed energy level diagram responsible for the photodegradation and recovery processes.

2.4.1 The Rate Equation Model

A population dynamics model can be expressed by coupled differential equations that describe the rates of population changes in response to a pump field. Unfortunately, there are too many unknown parameters for a fit of this kind of theory to the data to make sense. So we must make simplifying assumptions to decrease the size of the parameter space. Our approximations are consistent with what is typically observed.

First, we assume that the stimulated emission rate ω_s that we have derived in section 2.3.4 must be smaller than the transition line width $\Delta\omega_a$. In organic dye lasers, $\Delta\omega_a$ is as large as a few nanoseconds and as small as a few picoseconds. The inverse line width for these materials are even shorter, e.g., typically $1/\Delta\omega_a = 10^{-13}$s.

Organic dye molecules have a large number of energy levels E_i with time varying populations $n_i(t)$. Pump light may be applied at frequencies near several different transition frequencies $w_{ji} = (E_j - E_i)/\hbar$ and relaxation transitions can occur between all possible pairs of levels in the system. We will limit the number of states in our dynamics model to the five energy levels S_0, S_1, T_0, T_1, and D_0.

In Figure 2.7, $n_i(t)$ represents the population in state i, so $n_1(t)$ is the monomer ground state population, $n_2(t)$ is the ground state population of the tautomer, $n_3(t)$ is the excited state tautomer population, $n_4(t)$ is the excited state DO11 molecule

population, $n_5(t)$ is the ground state dimer population. While the tautomer ground state is split into two levels, we assume that only one is populated. Furthermore, we assume that the excited states of the dimer (D_1 and D_2) do not get populated during ASE generation or degradation. However, we will separately measure the population of dimers through linear absorption spectroscopy with excitation to states (D_1 and D_2). Given the above definitions, the rate equations for the population in each state are,

$$\frac{dn_1(t)}{dt} = -\omega_p n_1(t) + \gamma_{41} n_4(t) + \gamma_{21} n_2(t) + \gamma_{51} n_5(t), \tag{2.19}$$

$$\frac{dn_2(t)}{dt} = (\gamma_{32} + \omega_s) n_3(t) - (\gamma_{21} + \gamma_{25}) n_2(t), \tag{2.20}$$

$$\frac{dn_3(t)}{dt} = -(\gamma_{32} + \omega_s) n_3(t) + \gamma_{43} n_4(t), \tag{2.21}$$

$$\frac{dn_4(t)}{dt} = \omega_p n_1(t) - (\gamma_{43} + \gamma_{41}) n_4(t) \tag{2.22}$$

and

$$\frac{dn_5(t)}{dt} = \gamma_{25} n_2(t) - \gamma_{51} n_5(t). \tag{2.23}$$

Where ω_s is the number of photons of the ASE per second. We assume that the total

number of molecules N is fixed, i.e at t=0, $n_1(0) = N$ and at any instant of time, we have

$$n_1(t) + n_2(t) + n_3(t) + n_4(t) + n_5(t) = N. \tag{2.24}$$

Since N is fixed, we have only four independent rate equations where any one variable $n_i(t)$ can be derived from the negative sum of the remaining four rate equations. Using typical values of the parameters, we can solve the five coupled first order linear ordinary differential equations using Mathematica 5.2. Figures 2.8 to 2.12 show plots of the populations as a function of time for $\omega_p = 1.5 \times 10^{10}$ per second, $\gamma_{41} = 4.0 \times 10^8$ per second, $\gamma_{21} = 1 \times 10^{10}$ per second, $\gamma_{32} = 2.5 \times 10^8$ per second, and $\gamma_{43} = 1.0 \times 10^{11}$ per second. For how the typical values are calculated, please refer to Appendix A. These plots show that a full inverted population is reached and that the population is dominated by dimers when ASE disappears.

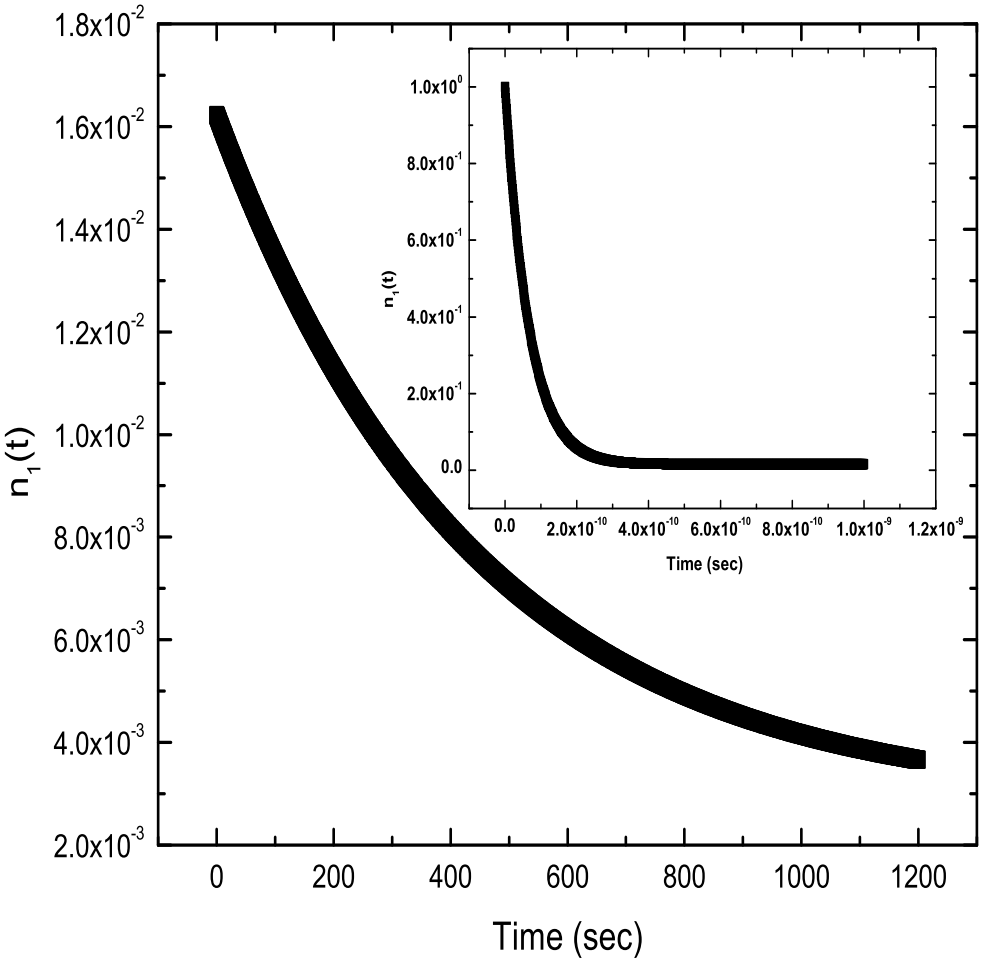

Figure 2.8: The population of the ground state of the DO11 molecule as a function of time during pumping ($\omega_p = 1.5 \times 10^{10}$ per second) well after population inversion is reached. The inset shows during population inversion.

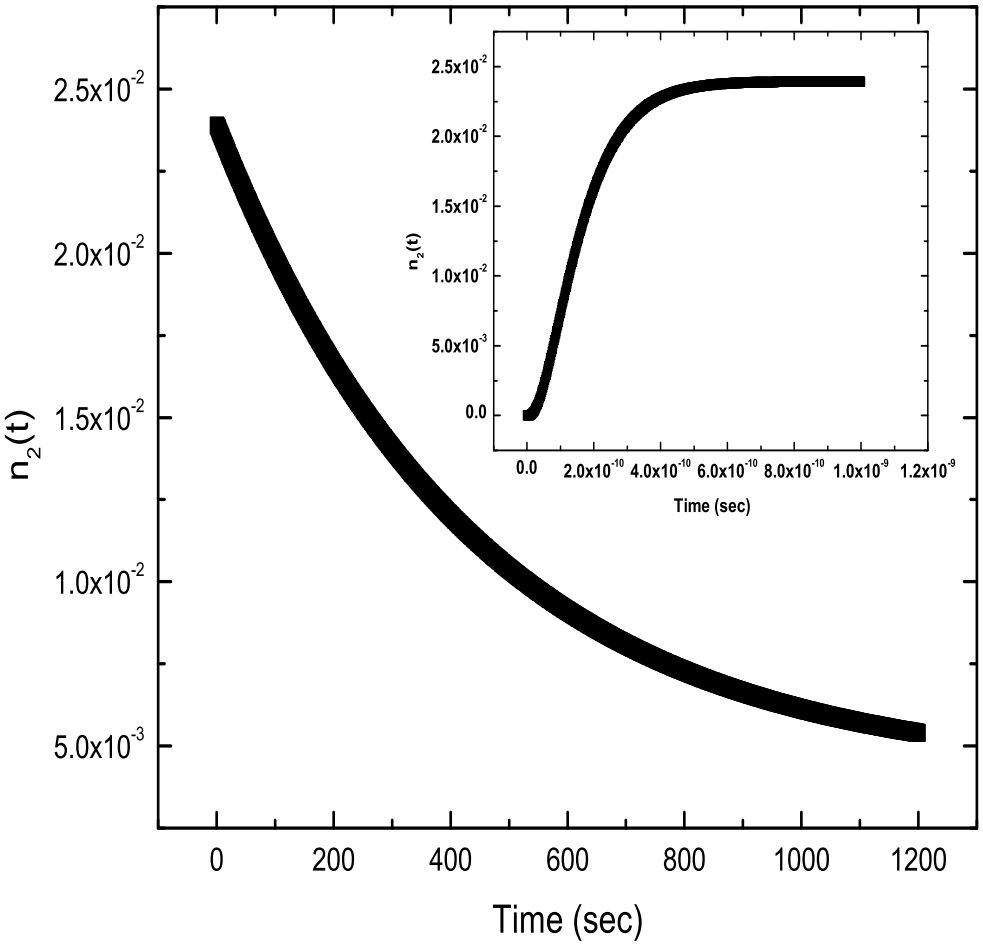

Figure 2.9: The population of the ground state of tautomer as a function of time during pumping ($\omega_p = 1.5\times10^{10}$ per second) well after population inversion is reached. The inset shows during population inversion.

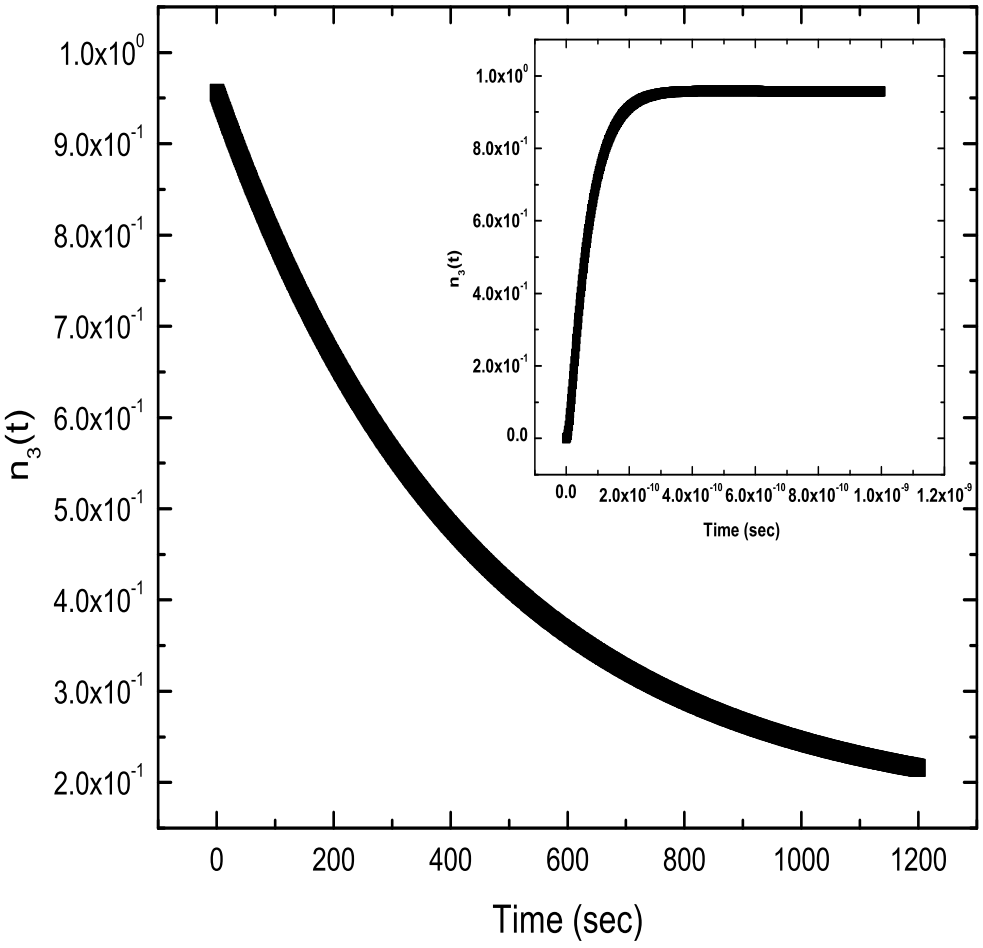

Figure 2.10: The population of the excited state of the tautomer as a function of time during pumping ($\omega_p = 1.5 \times 10^{10}$ per second) well after population inversion is reached. The inset shows during population inversion.

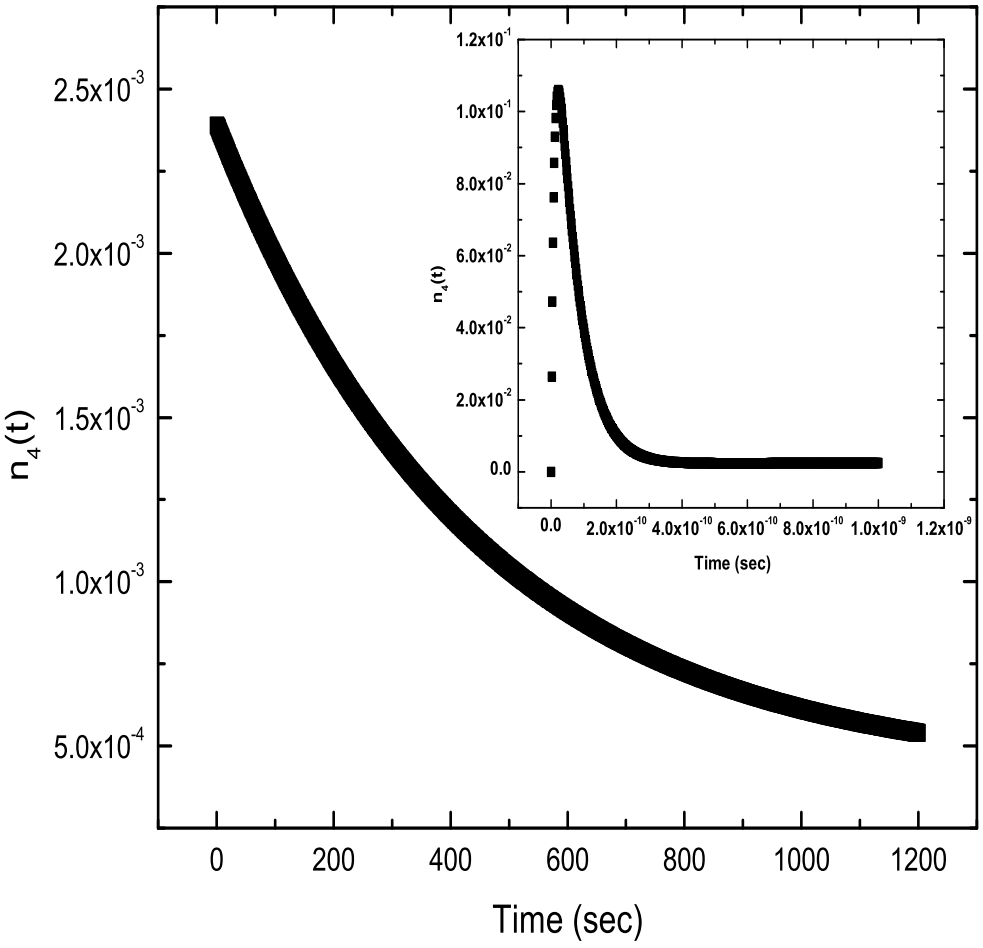

Figure 2.11: The population of the excited state of the DO11 molecule as a function of time during pumping ($\omega_p = 1.5 \times 10^{10}$ per second) well after population inversion is reached. The inset shows during population inversion.

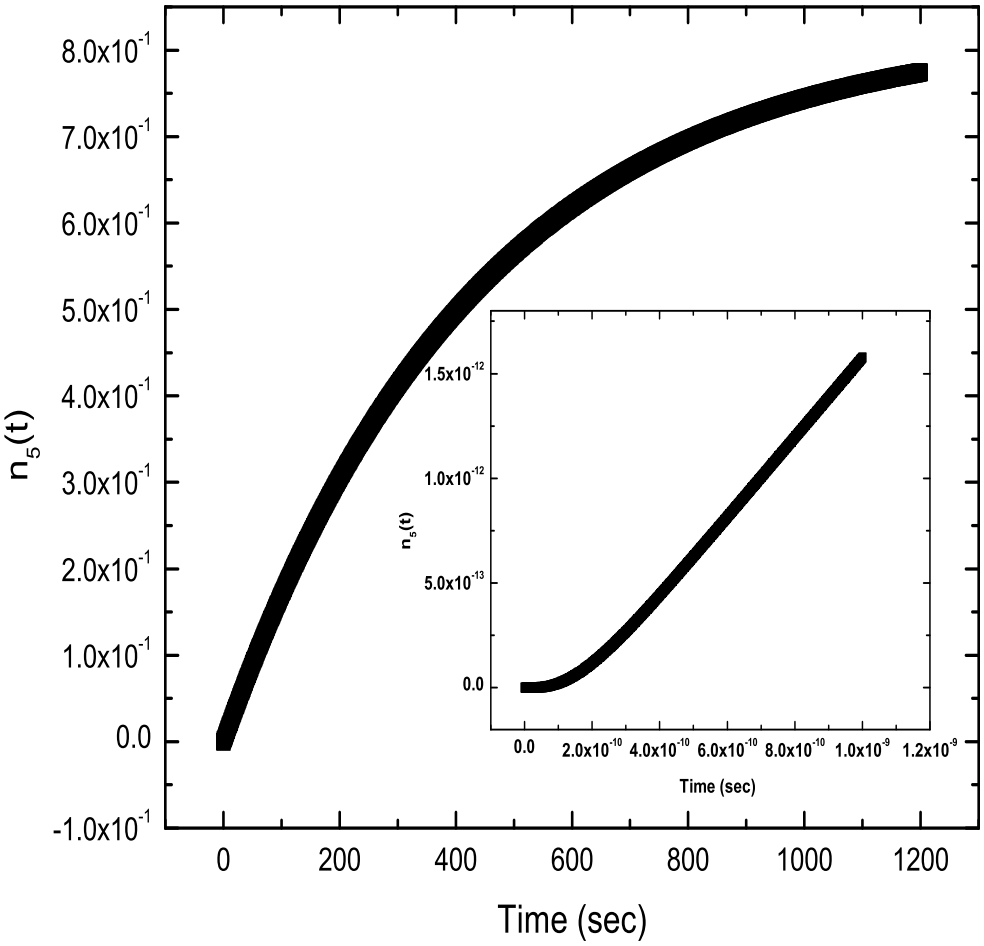

Figure 2.12: The population of the ground state of the dimer molecule as a function of time during pumping ($\omega_p = 1.5 \times 10^{10}$ per second) well after population inversion is reached. The inset shows during population inversion.

Bibliography

[1] B. Howell and M. G. Kuzyk, J. Opt. Soc. Am. B **19**, 1790 (2002).

[2] B. Howell and M. G. Kuzyk, Appl. Phys. Lett. **85**, 1901 (2004).

[3] Siegman, *Lasers*, University Science Books, Mill Valley, California, 1986.

[4] J. H. Van Vleck and D. L. Huber, "*Absorption, emission, and linebreadths: A semihistorical perspective*," Rev. Mod. Phys. **49**, 939-959(October 1977).

[5] K.H. Drexhage, Structure and Properties of Laser Dyes in Topics in Applied Physics, *Dye Lasers*, SpringerVerlag, Berlin, Germany 1990.

[6] M. G. Kuzyk, *Polymer Fiber Optics: Materials, Physics, and Applications*, Vol. **117** of Optical Science and Engineering (CRC Press, 2006).

[7] K.H. Drexhage, Structure and Properties of Laser Dyes in Topics in Applied Physics, *Dye Lasers*, SpringerVerlag, Berlin, Germany 1990, pp. 22.

[8] N. P. Ernsting and B. Nikolaus, Appl. Phys. B **39**, 155-164 (1986).

[9] J. D. Jackson, *Classical electrodynamics*, 3rd ed. (Wiley, [New York], 1999).

[10] B. Howell, *TRANSIENT ABSORPTION AND STIMULATED EMISSION OF THE ORGANIC DYE DISPERSE ORANGE 11*, Master's thesis, Washington State University, 2001.

Chapter 3

Experiment

3.1 Introduction

This chapter describes the experiment that we use to study the mechanism of self-healing of DO11/PMMA as measured with ASE. Section 3.2 focuses on sample preparation for ASE and absorption measurements. Section 3.3 explains the time dependent ASE measurement and section 3.4 describes how we characterize photodegradation and recovery. Section 3.5 describes absorption measurements and how the time and temperature dependent is determined. The sample response as a function of the light polarization is also discussed.

3.2 Sample Preparation

3.2.1 Sample Preparation for ASE Measurement

Our samples are dye-doped polymers where the dye is about one percent by weight in PMMA (polymethyl methacrylate) polymer. The first step in making a sample is to prepare a pure liquid of the Methyl Methacrylate (MMA) monomer. The MMA that we purchase from Sigma-Aldrich contains a small amount of inhibitor to prevent the monomers from polymerizing. We run the MMA through alumina powder in a column to remove the inhibitor. The MMA is collected from the column to a fresh bottle. We call the resulting MMA 'filtered'. The filtered MMA is mixed with the dye and the bottles placed in an ultra-sonic bath for an hour until the dye is fully dissolved (see Figure 3.1).

The bottle containing the dye and MMA is covered with aluminum foil to avoid polymerization induced by room light. After the dye is completely dissolved, we add about 3.3μ l/ml of CTA (chain transfer agent) and initiator. The initiator induces polymerization by making a monomer molecule chemically active, which starts a cascade of reactions that causes a chain of molecules to link together until the chain runs into CTA molecule that terminates further polymerization. Thus the average length of a polymer chain is limited in proportion to the concentration of CTA. All these reactions take place in a chemical fume hood for protection.

The mixture is filtered to a test tube using a disk filter of 0.2μm GHP ACRODISC

Figure 3.1: The Ultra-Sonic bath used for dissolving DO11 in MMA. The heating system of the bath is turned off to avoid polymerization. Polymerization in the ultrasonic bath yields solution that are difficult to filter and eventually to bad sample quality.

to eliminate pre-polymerized clusters or dust particles larger than 0.2μm. Test tubes with liquid dye/PMMA are placed in an aluminum block (Figure 3.2) with drilled holes that provide a smug fit for the test tubes. The block is then placed in an oven (Figure 3.3) at 95^0C. Every ten minutes for at least 30 minutes the cube of the test tubes is opened and the test tube caps loosened to allow the accumulated gases that form during the polymerization process to escape. This reduces the pressure in the test tube and prevents bubble formation inside the sample. The block remains in the oven for 48-72 hours until all the samples are polymerized.

When polymerization is complete, the test tube is placed in a freezer for few hours to cause the polymer through differential contracting to separate from the test tube. Finally we break the test tube to remove the cylinder sample, which for historical reasons called preform. Preforms of 3, 5, 7, 9 and 11 gram per liter (g/l) are made in a batch.

One end of the preform is polished to optical quality using a successive sequence of 3M sandpaper of grade 150, 180, 320, 400, and 600. Grade 600 is the most fine. We polish for 20 minutes with each grade, then use an Alumina polishing suspension (agglomerate-free) for one hour. The Alumina Grades used are 3.0, 1.0, and 0.3 CR micron. The other flat side of the preform is left unpolished. The curves surfaces of the cylindrical rods are optically smooth from contact with the test tube inner smooth surface during polymerization.

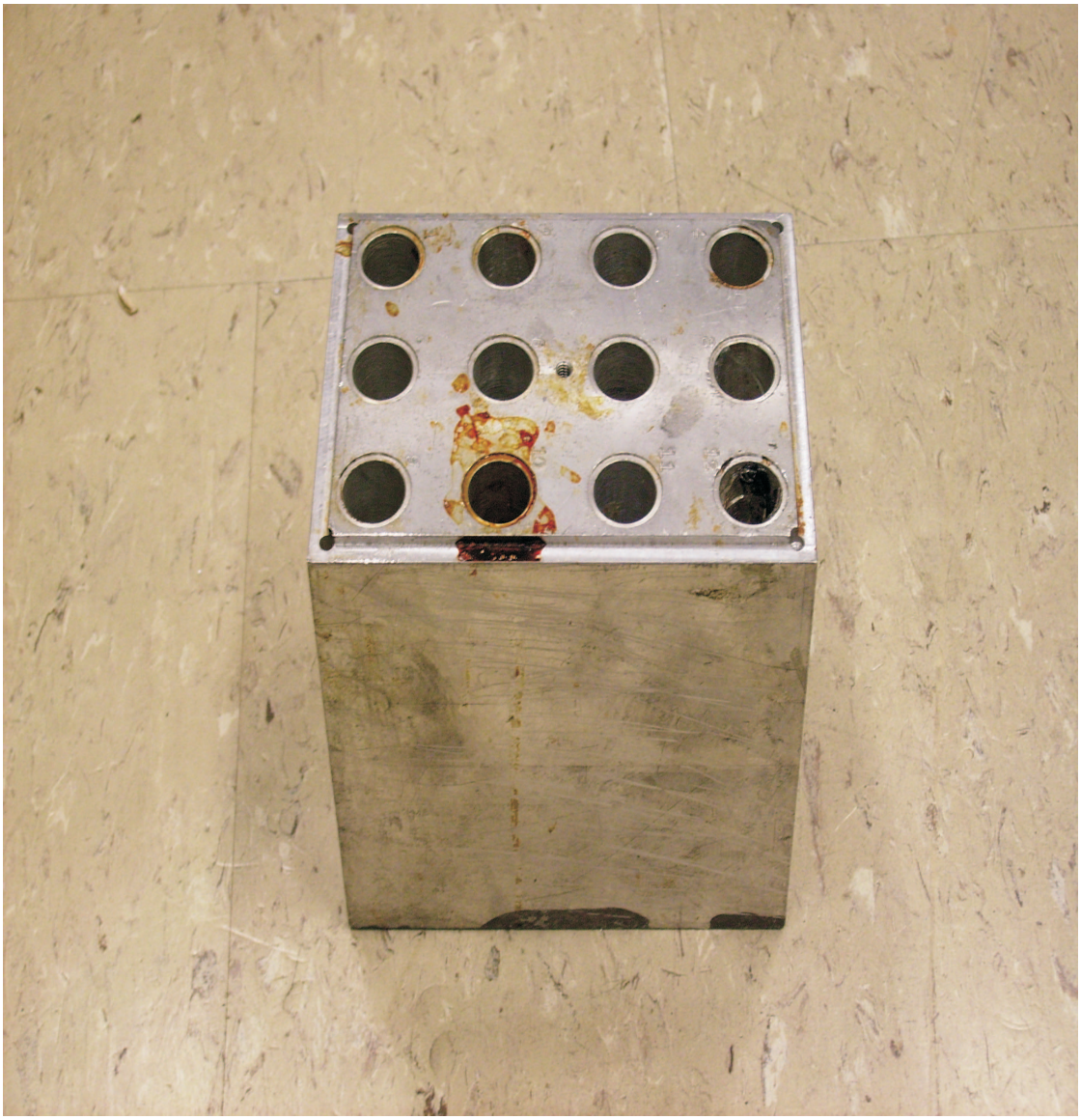

Figure 3.2: Aluminum block with drilled holes for holding the test tubes.

Figure 3.3: Oven used to polymerize sample.

3.2.2 Sample Preparation for the Absorbance Measurement

In order to make measurements consistent, we have processed thin films from preforms by cutting a small piece from the unpolished side of the sample and placing it between two glass slides. The sandwich structure is placed in an oven (shown in Figure 3.4) and pressed to form thin films. We used temperature controller unit (Model Omega CN-2010) to control the thickness of the sample by setting the temperature at 8 different set points for different values of temperature as shown in Figure 3.5). To measure the thickness of the film sample, we use a high precision digital micrometer to determine the thickness of the film. Only the 9g/l thin film is processed by this method since it shows superior reversible photodegradation.

3.3 The ASE Experiment

Amplified spontaneous emission (ASE) is the fundamental process that is the basis of lasing. Figure 3.6 shows the experiment used to measure the ASE intensity. We use a continuum Surelite II Nd:Yttrium-Aluminum-Garnet (Nd:YAG) pulsed laser operating at 10Hz with nanosecond-scale pulses at 1064nm (fundamental) as a light source. The fundamental light beam from the laser pumps a Second Harmonic Crystal (SHC) (INRAD model 531-120) to generate green second harmonic light (532nm). The optical damage threshold of the crystal is greater than 3GW/cm^2.

The maximum peak intensity from the surelite II laser at the fundamental wave-

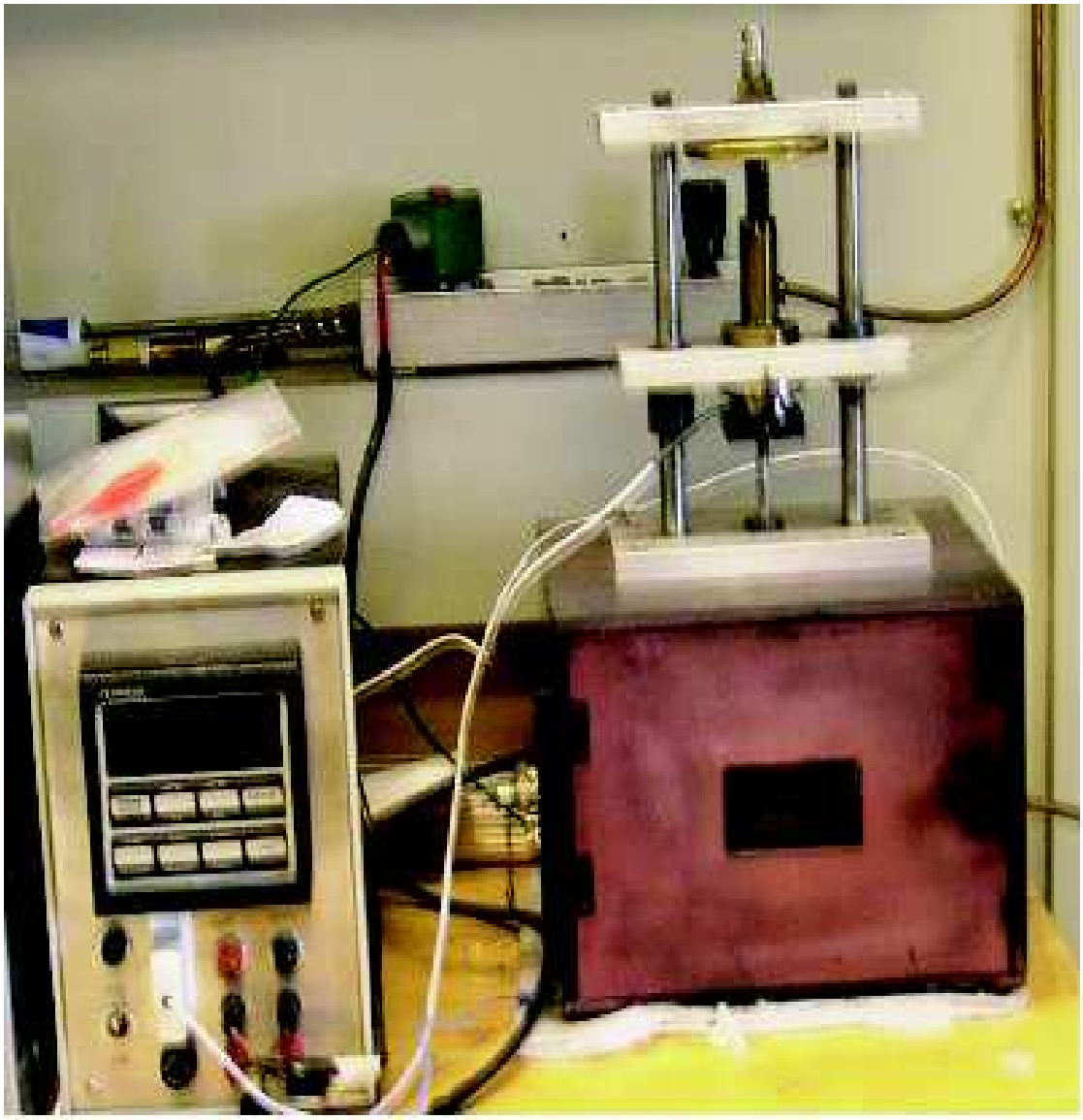

Figure 3.4: Oven (right) used to press samples. The mechanism above the oven is used to apply pressure and the unit to the left is the temperature controller.

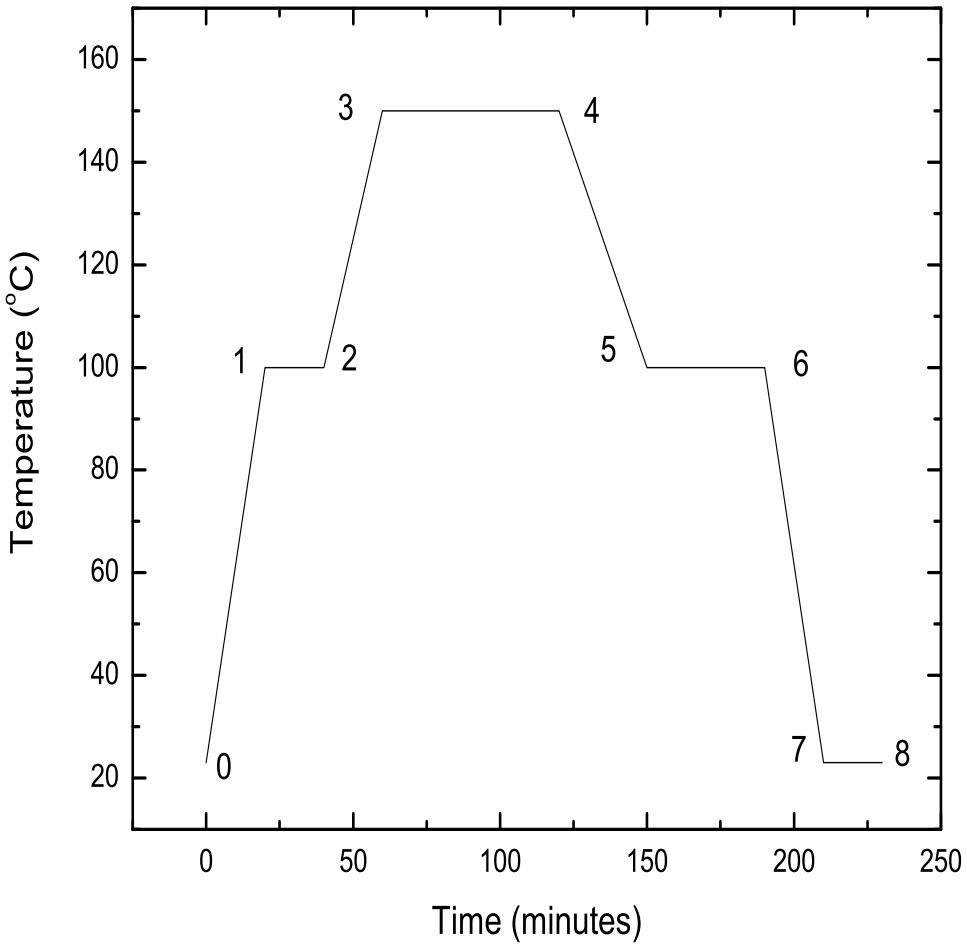

Figure 3.5: The plot shows temperature as a function of time for 8 different set points in the temperature controller unit.

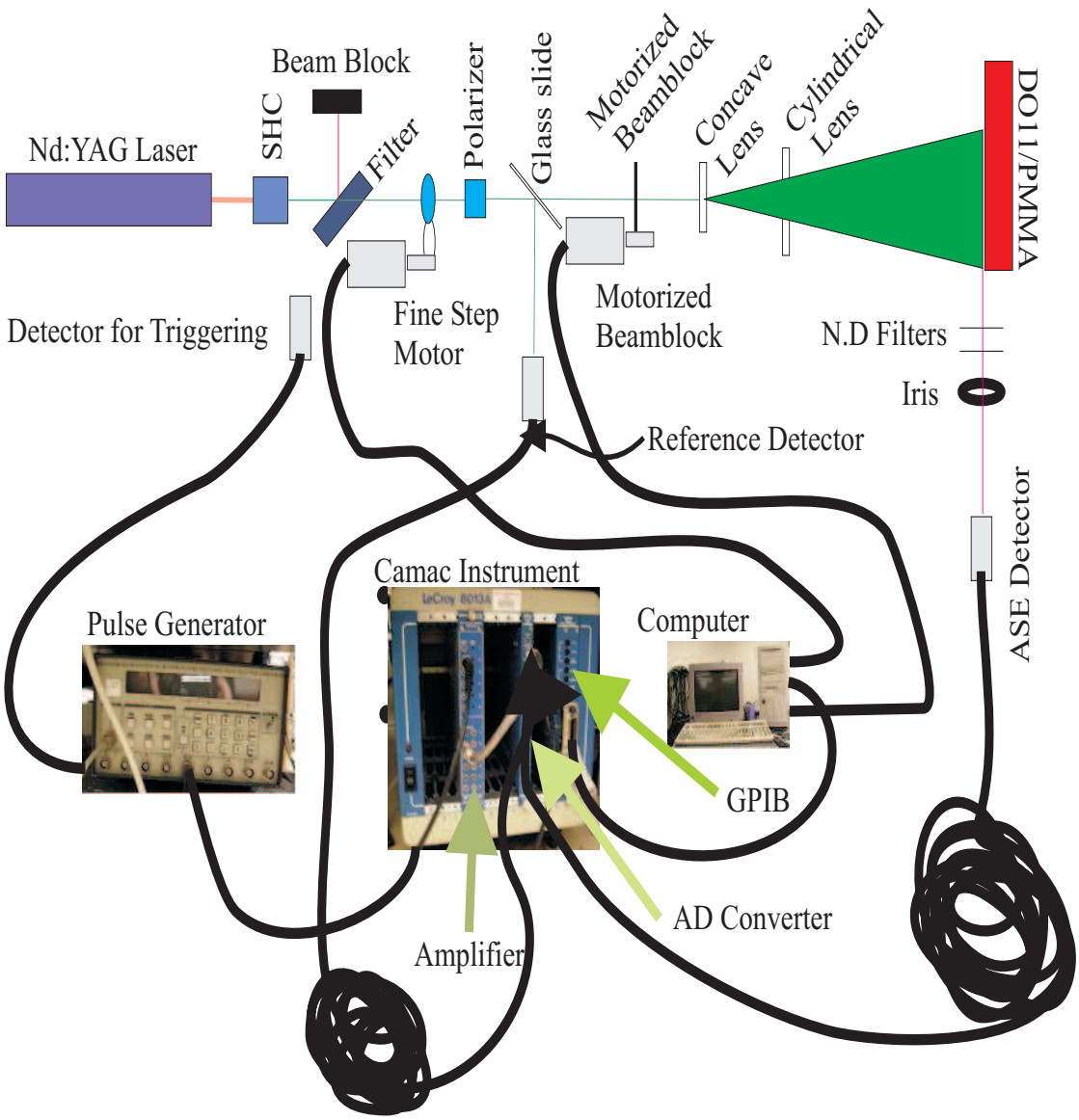

Figure 3.6: The ASE experiment. All the detectors, the pulse generator, the camac instrument and the motorized half-wave plate are computer controlled, for automation.

length with 6ns pulses and a 7mm diameter beam is about 0.3GW/cm^2. Even though the intensity from the laser at the KD*P crystal (SHC) is about 10 times smaller than the damage threshold, one must be careful not to focus the fundamental beam on the crystal. To learn how the SHC converts the fundamental beam to the second harmonic, the reader is referred to Boyd's book on nonlinear optics[1]. We have measured the temporal width (Figure 3.7) of the 532nm beam using an oscilloscope and find it to be the same as specified by the Surelite II laser system's documentation. The pulse width is used to determine the intensity incident on the sample.

Following the SHC is a filter that is set at 45^0 to reflect the unconverted 1064nm light and pass the 532nm light. The light reflected from this filter is blocked by a brick. Next a motorized half-wave plate (HWP) and fixed polarizer is used to adjust the intensity of the beam without affecting its polarization. The polarization of the light after it passes the polarizer is perpendicular to the optical table, so is called the transverse polarization direction. We use a glass slide to deflect a portion of the light to monitor the stability of the pump light. A motorized beam block is used as a shutter to block the beam without turning of the laser. We use a concave lens to expand the beam and a cylindrical lens to focus the beam into a line of dimension 0.1mm $\times$ 10mm. The line shape is measured using a beam profile at the surface of the sample. The sample then generates ASE light at a wavelength of about 645nm and is detected by silicon photo-diode detector. A similar detector is used for the reference and triggering pulse. However, a faster detector (1ns rise time) is used for

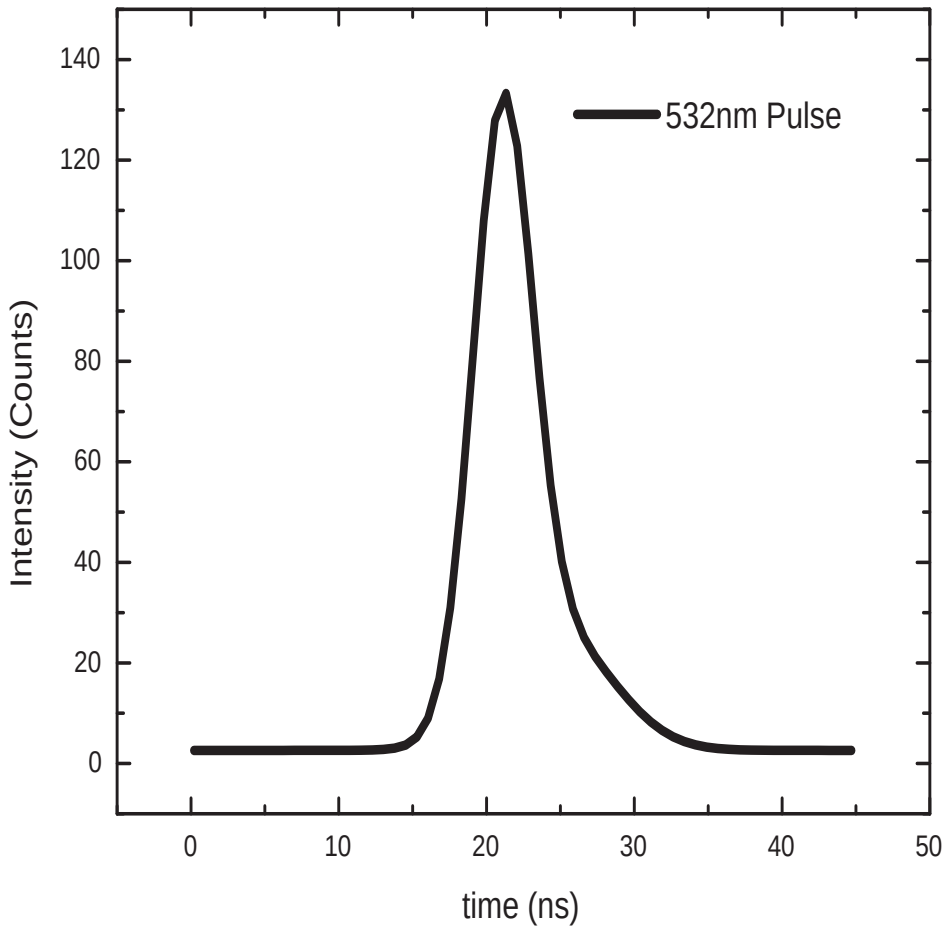

Figure 3.7: The second harmonic (532nm) pulse intensity as a function of time, measured using an oscilloscope.

the triggering. Figures 3.8 shows ASE generation using a cubic sample. The ASE threshold is about 40μJ for the line size we use. As it is shown in Figure 3.10, ASE saturates above about E = 0.5mJ.

The triggering detector near the SHC detects the scattered 532nm light and sends a signal to the digital delay/pulse generator (Model DG535, Stanford Research Systems). The output voltage from this detector, which is an input to the pulse generator, should not exceed 10V so as not to damage the pulse generator electronics. This generator is programmed to produce an output of NIM pulse of 100ns width which is sent to the camac instrument Model LeCroy 612AM amplifier. We amplify the pulse from -0.4V to about -0.8V because the Model 2249W A/D converter gate opens only if the amplitude of the trigger is greater than or equal to -0.6V. The A/D converter integrates the charge from the ASE and reference detectors over a 100ns time interval corresponding to the time the gate remains open. The integrated charge signals are then sent to the camac gateway then to the Model 8901A GPIB interface and then to the computer's GPIB which processes by the Labview software program.

This Labview program performs several functions. It controls the motorized half wave plate based on the reading of the reference detector to keep the intensity of the 532nm pump constant. This function is critical because small changes in the pump introduces large variations in ASE.

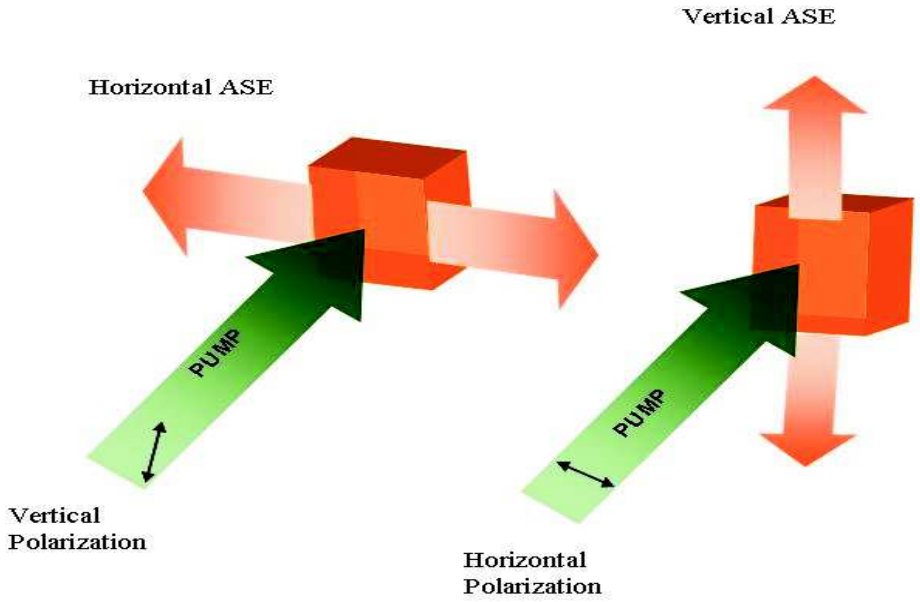

Figure 3.8: ASE generation for horizontal and vertical polarization.

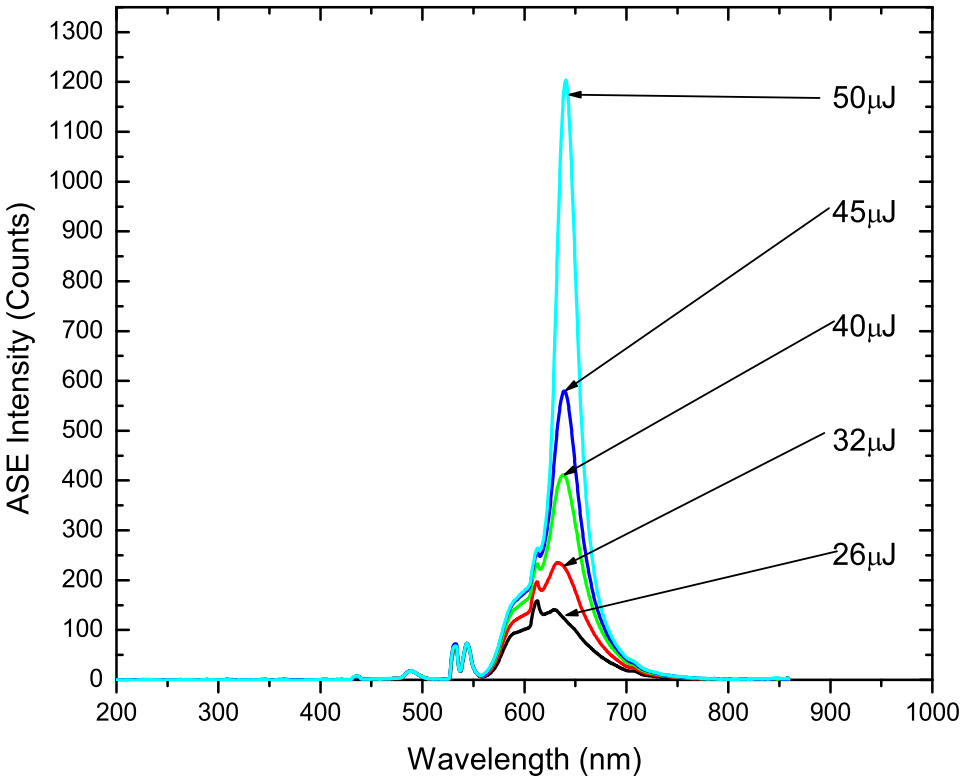

Figure 3.9: ASE Threshold is about 40μJ for the 9g/l DO11/PMMA.

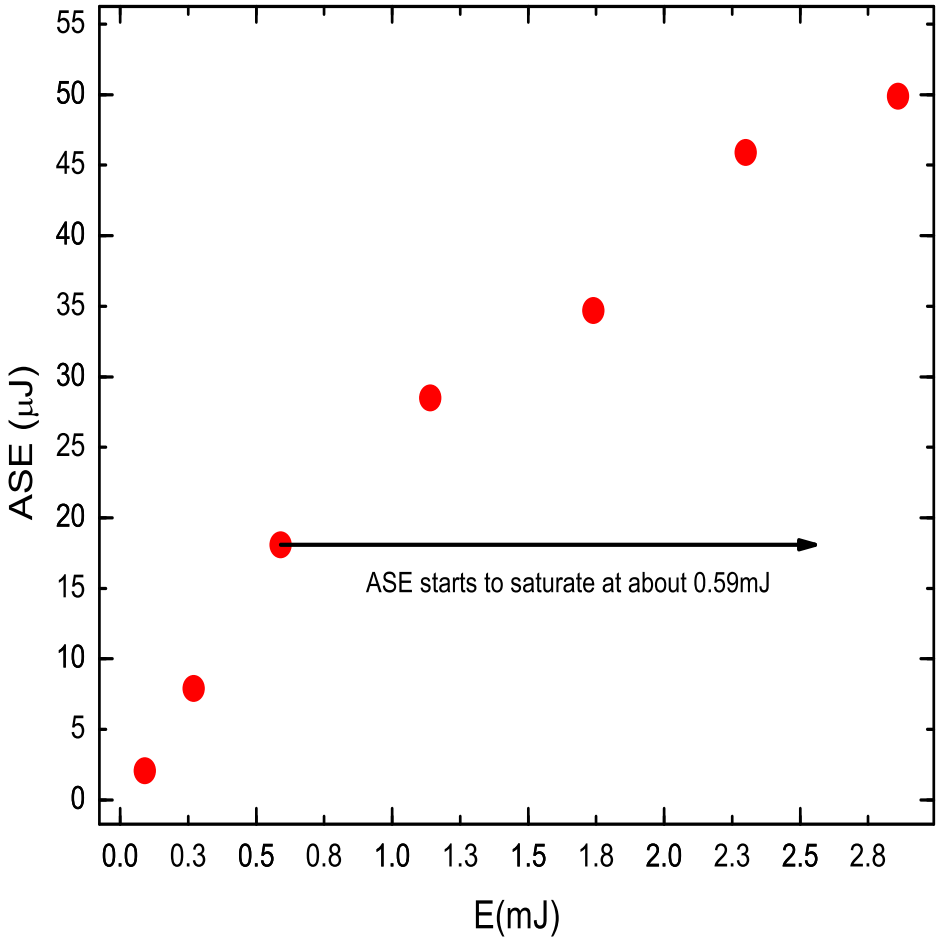

Figure 3.10: ASE saturates at a pump energy of about 500μJ for a 9g/l DO11/PMMA sample.

3.4 Photodegradation and Recovery Measurements

The ASE set-up described in section 3.3 is used to get data for the photodegradation, when the sample is constantly pulsed, and recovery where the sample is kept in the dark and only probed occasionally. Because the experiment is automated, degradation and recovery experiment can be run for long periods of time without human intervention. The computer control allows the flexibility for programming any desired time profile. This is convenient given that the recovery process takes more than 24hrs. For example, the sample can be made to degrade to any desired value, say 50%, at which time the beam is blocked with the motorized beam block and opened every one hour for 10 seconds to monitor recovery.

To determine the pump intensity at the sample in units of W/cm^2 from the angle of the HWP, we did the following procedure. We adjusted the HWP, and measured the pump intensity at the sample position with a laser probe radiometer and the reference beam intensity is recorded with the photodiode detector using Labview. By knowing the reference detector intensity in counts and the calibration factor in W/cm^2 per count, we can convert it to an intensity at the sample in units of W/cm^2. This allows us to determine the absolute pump intensity. From this calibration, we can also determine how the intensity changes when the labview program sends the stepper motor the command to move a single step, thus adjusts, HWP by the smallest possible

increment. The absolute intensity as a function of ADC counts and as a function of motor steps are shown in Figure 3.11, Figure 3.12 and Figure 3.13

3.5 Absorbance Experiment

Absorption measurements give the energy levels of the material under study, as well as any atomic or molecular transition moments. We measure the static and dynamic (i.e. under pumping) absorption spectra of the DO11 molecule in PMMA polymer of 9g/l concentration to gain insight into the species involved. The set-up for absorbance measurement is shown in Figure 3.14

An Ocean Optics miniature deuterium tungsten halogen light source with a spectral range of 200nm-1100nm was used to probe the spectrum. We have found that this light source (Figure 3.15) useful because it spans three separate absorption peaks in our sample. Measurement of the change in absorbance is one important basis for studying the mechanism of population dynamics. We use an Ocean Optics fiber (model QP400-025-SR) of 400μm diameter that transmits UV spectrum to collect the light and measure the spectrum. It is important to note that most of the UV light that comes from the light source is absorbed by the glass components in the set-up such as lenses and glass slides used to make the thin films. A neutral density (ND) filter was used to attenuate the light source. This light source acts as a probe and needs to be as weak as possible so that the absorption spectrum of the sample is not affected by this broad-spectrum source. Over a 24 hour run, we didn't find any

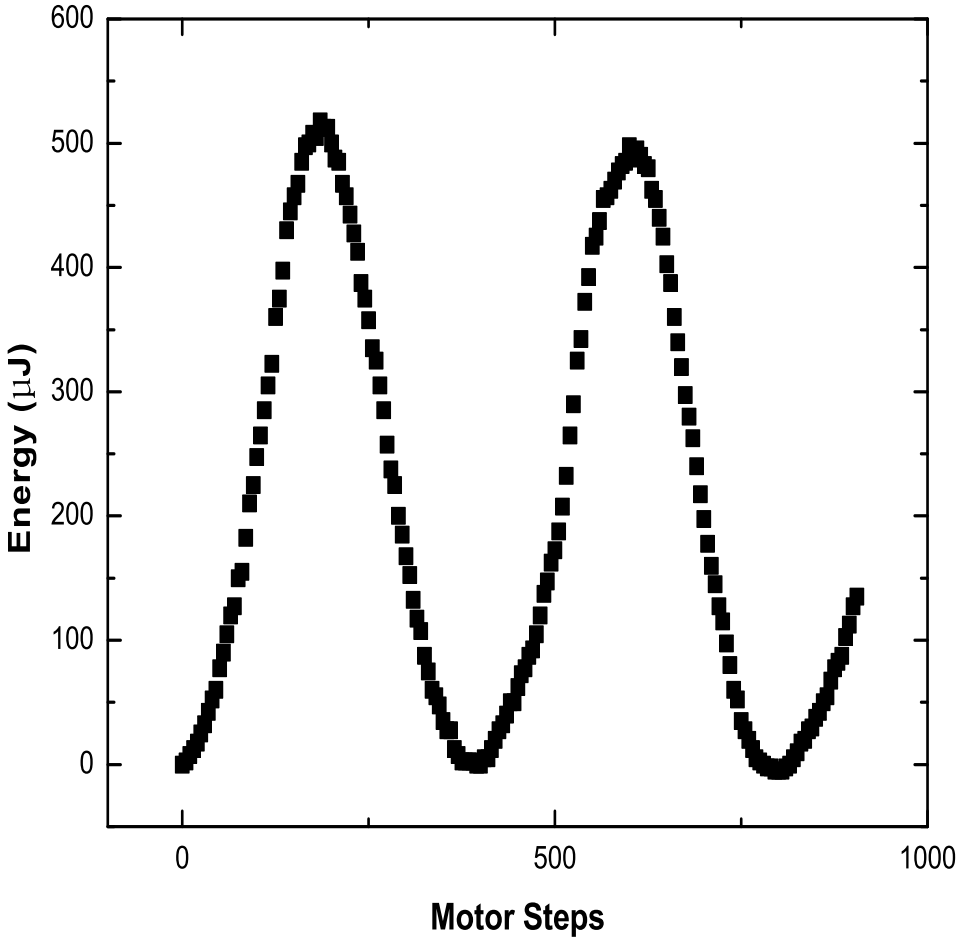

Figure 3.11: Energy meter as a function of motor steps for more than one cycle of HWP rotation.

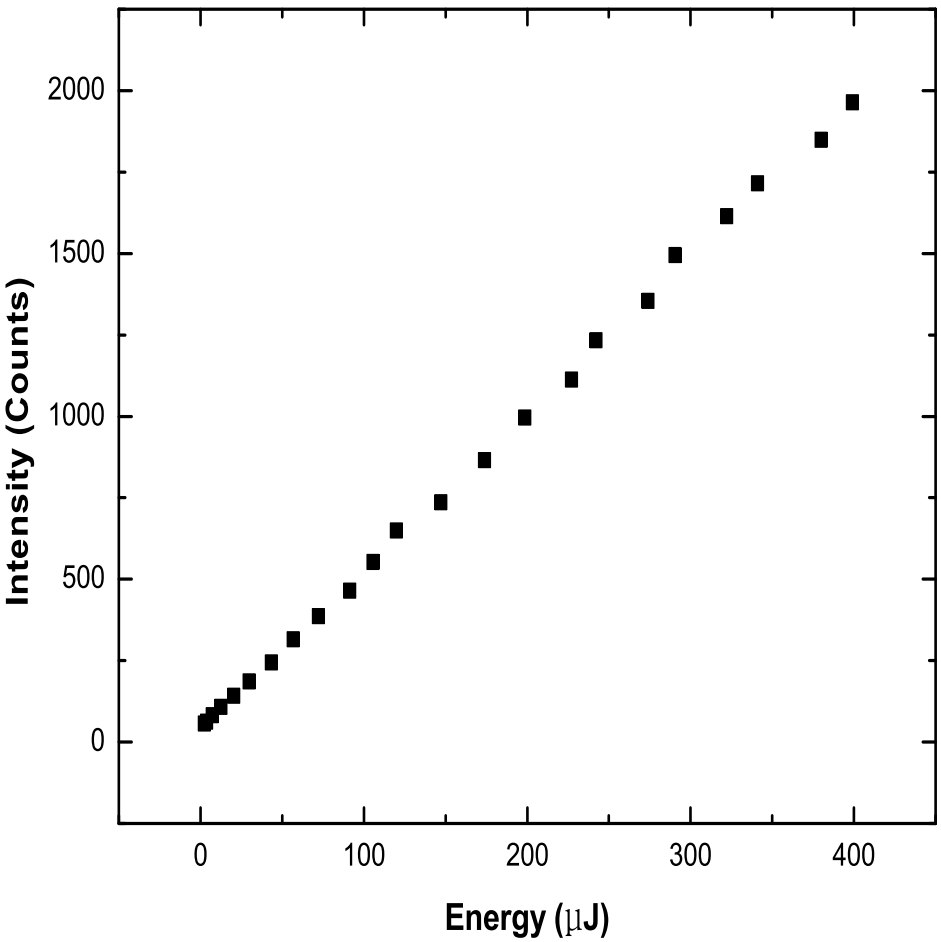

Figure 3.12: ADC counts as a function of pulse energy.

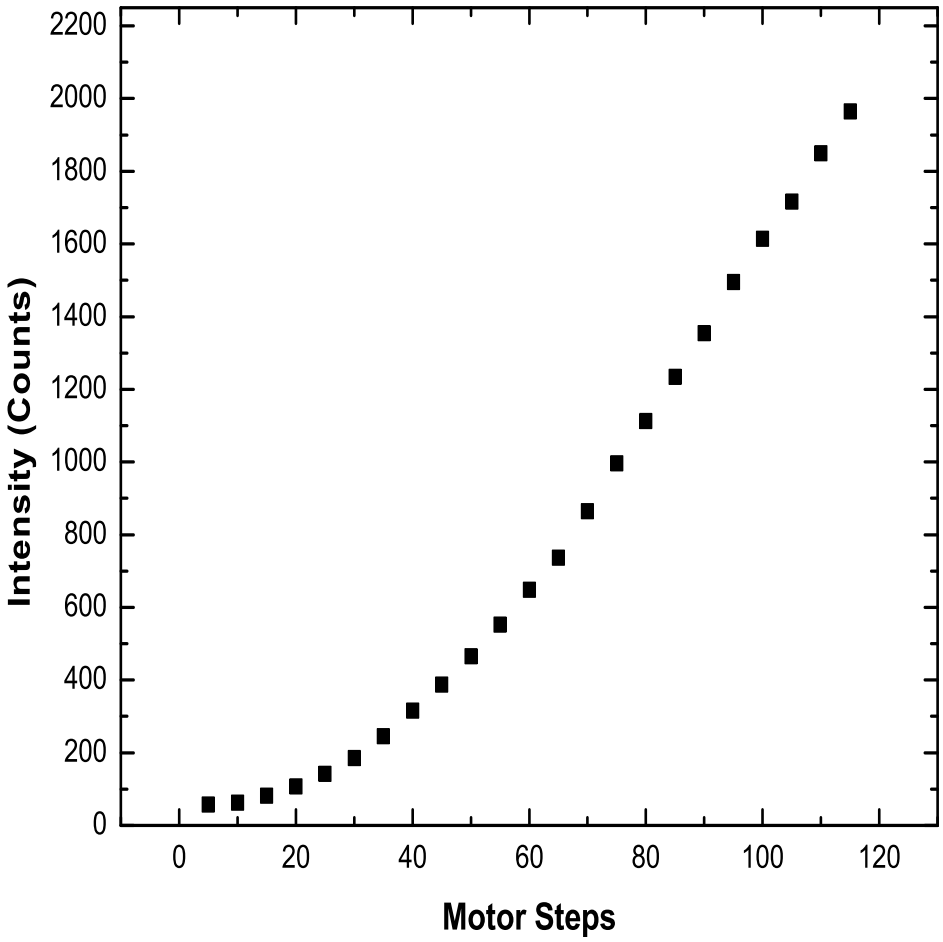

Figure 3.13: ADC counts as a function of the number of motor steps.

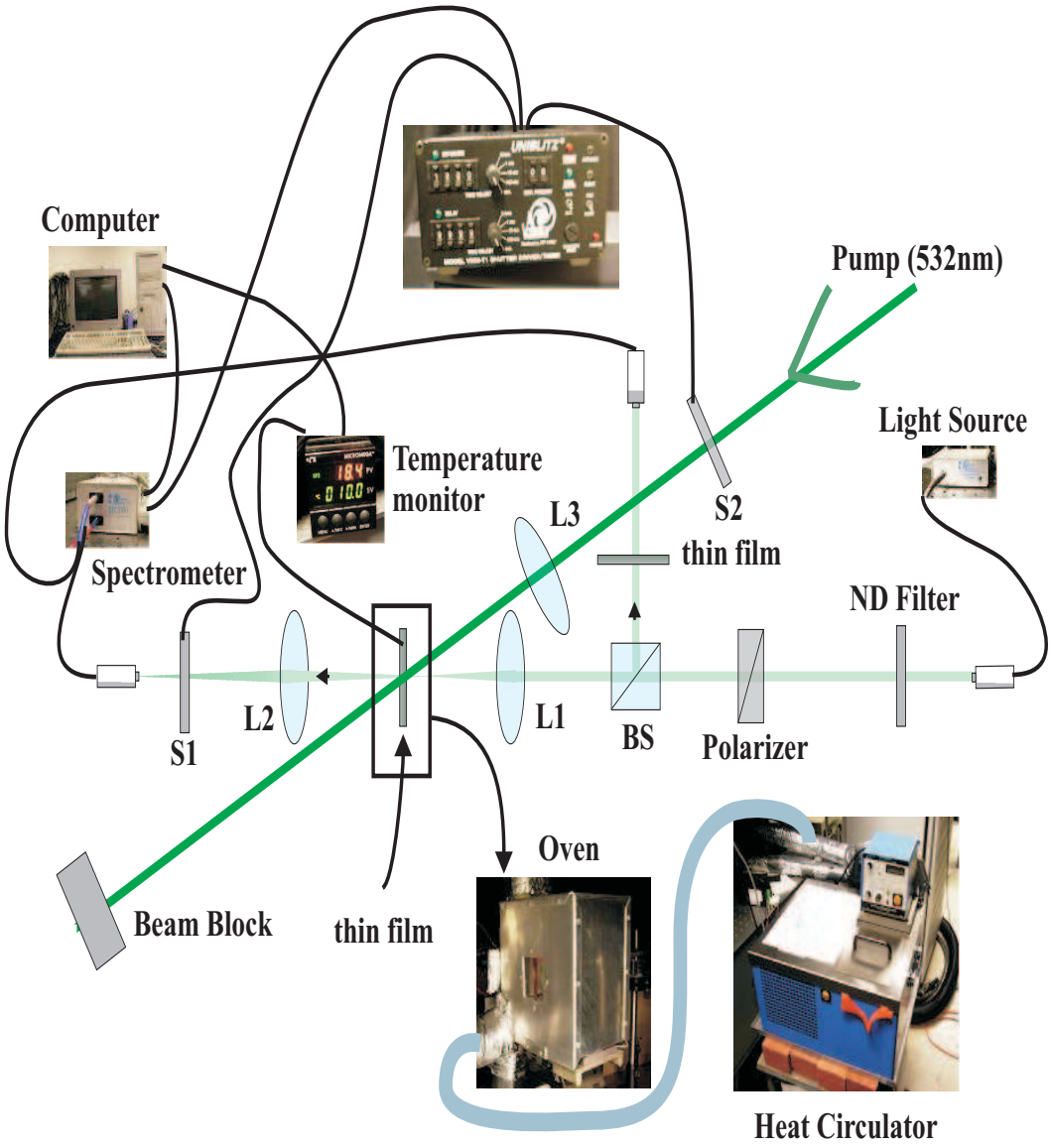

Figure 3.14: The absorbance experiment.

change in the absorption spectrum due to the probe. The light source is unpolarized, so we used a Prinz 37mm polarizer that we have adjusted to set the probe polarization to be the same as the pump, which is perpendicular to the optical table. The beam splitter (BS) was also used to divert one part to the sample and the other one to the reference. Lens (L1) is used to make the diameter of the probe at the sample to be smaller than the pump diameter so that all the molecules probed will be exposed to the excitation source. The size of the excitation pulse beam is measured using a beam profiler and found to be 0.5cm in diameter. L2 was used to focus all the light into the spectrometer fiber detector. L3 was used to decrease the size of the pump beam to get the desired intensity at the sample.

The scattered pump light from the sample can damage the spectrometer detector. For that reason we use a shutter at two positions. Shutter one (S1) is placed after the sample and shutter two (S2) is placed before the sample. This way we can pump the sample and while making sure that no scattered light is going to the spectrometer detector by closing S1. In our experiment, we close S1 and open S2 simultaneously to pump the sample for 10 minutes and then open S1 and close S2 for 1s to acquire the absorption spectrum data.

3.6 Data Acquisition

The sample is placed in an oven as shown in Figure 3.14 for temperature dependent measurements. A circulator is used to pump hot oil to an oven that houses the sample.

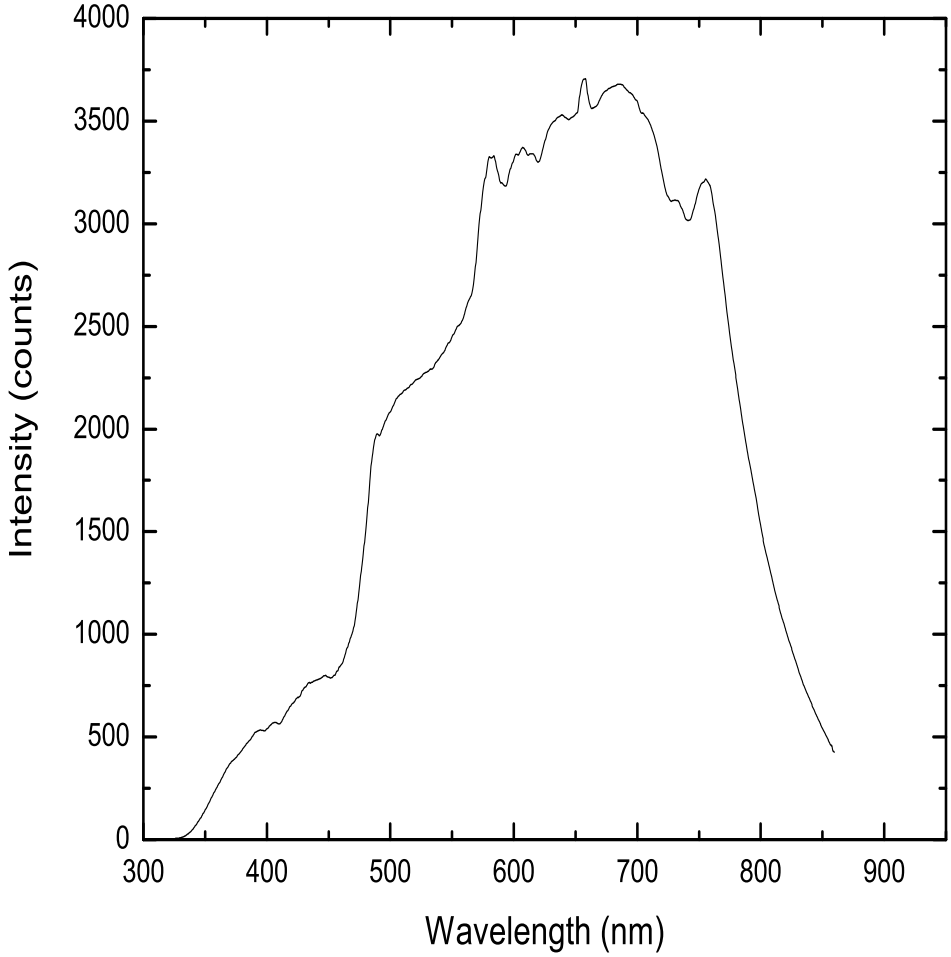

Figure 3.15: Spectrum of the deuterium tungsten halogen light source.

A thermometer is attached to the sample using conducting paste in order to read the temperature at the sample surface. We use an Omega CN7700 model temperature controller to monitor the temperature. This controller is connected to the computer with appropriate software[2] to record the temperature as a function of time as part of an automated process.

Labview[3] software for the Ocean Optics spectrometer was used to acquire data for the absorption change measurements. The software is modified so that the spectrometer and the shutter can be controlled and the data stored automatically. Thus, our software program controls the spectrometer and the shutters by way of the shutter controller. When running the pump-probe measurements at room temperature, the software makes the shutter controller open S1 and close S2 for 1 second while a spectrum is being accumulated. The computer cycles through the process every 5 minutes for 2-4 hours.

As a second experiment, we determined the temperature dependence of the absorption spectrum with the pump off. Therefore, our custom software uses Labview for spectrum acquisition and separate software that records the temperature. Both must acquire data at the same time so that a specific temperature can be associated with each spectrum. When running with the pump, and measuring the spectrum or ASE, the pump power stabilization software is used for all measurements.

Bibliography

[1] R.W. Boyd, *Nonlinear Optics*, Academic Press Inc., New York, NY 1992, pp. 69-78.

[2] Newport Electronics Inc., *iSeries Serial Communication Version 1.0*, Copyright(c) 1999.

[3] National Instruments, *Labview 4.01 (Graphical programming for instrumentation)*, Copyright(c) 1996. Newport Electronics Inc., iSeries Serial Communication Version 1.0, Copyright(c) 1999.

Chapter 4

Results And Discussion

In this Chapter we start by discussing the optical properties of DO11/PMMA. Then we analyze how photodegradation and recovery is affected by concentration, polarization, temperature and intensity. We also discuss how the recovery of DO11/PMMA is influenced when it is pre-irradiated with gamma rays. Finally, we bring together all of our results to formulate an understanding of the self-healing mechanism in DO11/PMMA.

4.1 Absorption, Fluorescence and ASE Spectrum

The first step in studying a dye molecule is to know the character of its excited states, which can be deduced from measurements of its absorption and fluorescence spectrum. Additionally, knowledge of the absorption spectrum of a dye helps to select the pump wavelength to best excite the molecule. Figure 4.1 shows the absorption, fluorescence

and ASE spectra of DO11/PMMA and the absorption spectrum of PMMA. The absorption peak of DO11/PMMA as shown in Figure 4.1(a) is found to be centered at 470nm. There is no absorption peak for PMMA as shown in Figure 4.1(b). All hydrocarbons have a dip at 650nm due to C-H stretch overtones, but compared to the absorbance of our sample, it is negligible. When using fibers made of PMMA kilometers length, then the absorption loss of PMMA is measurable.

The fluorescence as shown in Figure 4.1(c) has a centered peak at 580nm. The ASE light in Figure 4.1(d) peaks at 645nm and the small peak at 532nm is the scattered pump beam. The Stokes Shift, i.e, the separation between the absorption peak and fluorescence peak is 110nm. Similarly the separation between the absorption peak and the ASE peak is 175nm which is unusually large.

A class of dyes that are known for their large Stokes Shift are the coumarine dyes, which have a Stokes Shift of less than 100nm[1]-smaller than for our molecule. Since the shift between absorption and ASE is large, little reabsorption of the ASE by the bulk sample is expected. In addition to the large Stokes Shift, the fluorescence spectra is also nearly a mirror image but broader than the absorption spectrum. These features suggest that an intramolecular charge transfer or excited-state proton transfer[2, 3] is responsible.

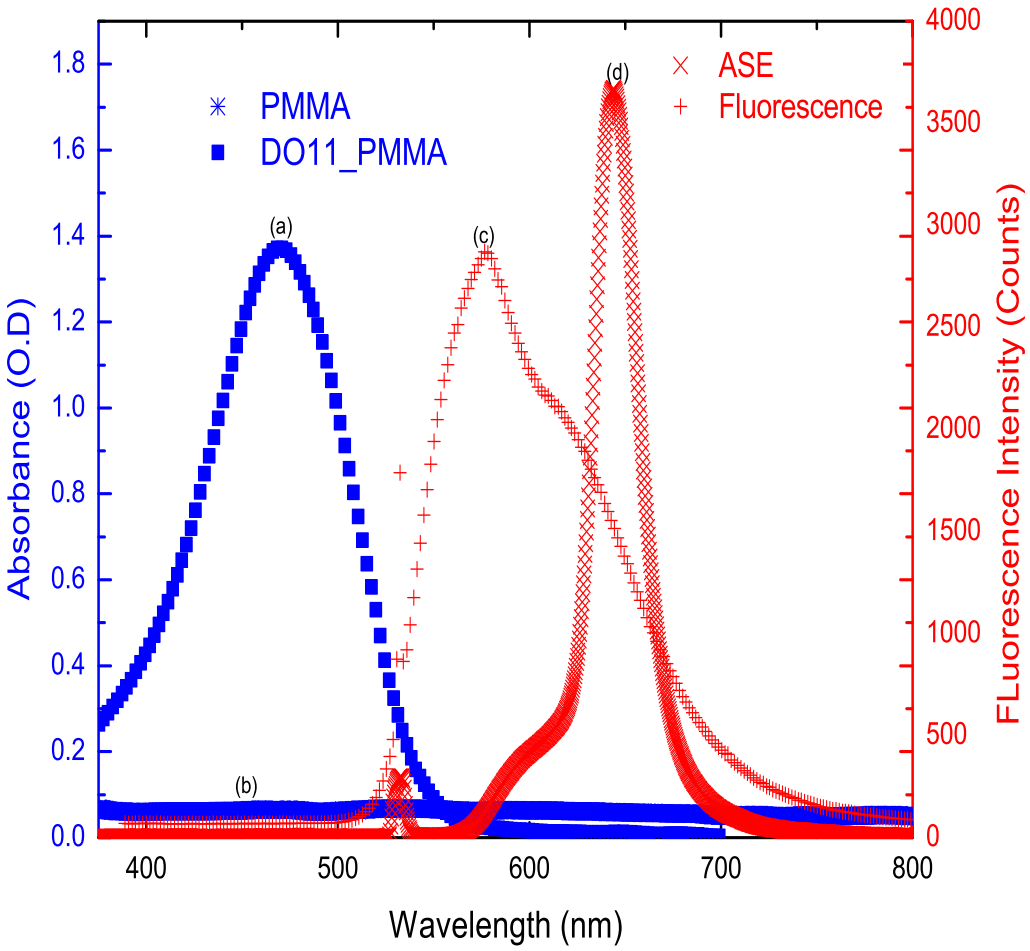

Figure 4.1: Absorption, fluorescence (pumped with 20μJ/pulse) and ASE spectrum (pumped with 20μJ/pulse) of DO11/PMMA of 9g/l concentration. There is no absorption peak for PMMA in the wavelength range shown. Since the Stokes Shift is large, fluorescence reabsorption by the bulk sample is small.

4.2 Concentration Dependent Measurements

The concentration of a dye-doped polymer is easily controlled in the polymerization process described in section 3.2.1. However, for high concentration, the dye aggregates, forming crystals. Depending on the concentration, a dye molecule can take the form of a monomer, dimer, H- or J-aggregate [4]. UV-Visible absorption spectroscopy is common method to obtain quantitative data on the monomer/dimer composition [5]. When two dye molecules form a dimer, the resulting spectrum is blue-shifted leading to a peak at shorter wavelength. An H-aggregate is formed when dye molecules aggregate in a vertical stack and also is characterized by a blue shift in the absorption spectrum. When dye molecules arrange in a slanted stack, this structure is called a J-aggregates and the resulting spectrum is red-shifted [6].

As we will show, aggregation is a desirable property that is central to self-healing. In our experiment, we study dye aggregation by using linear absorption spectrometer while measuring decay and recovery of ASE as a function of pump energy.

In order to increase the likelihood of interaction between neighboring molecules, the concentration of dyes must be high, but not so high that the material is populated by aggregates when not exposed to light. Since ASE is quenched when the molecule aggregates, a measure of the ASE signal as a function of concentration characterizes the point when aggregates begins. Figure 4.2 shows such a plot, when the intensity dependence is also shown.

Howell [7] carefully measured the ASE as a function of pump energy for 3, 6 and

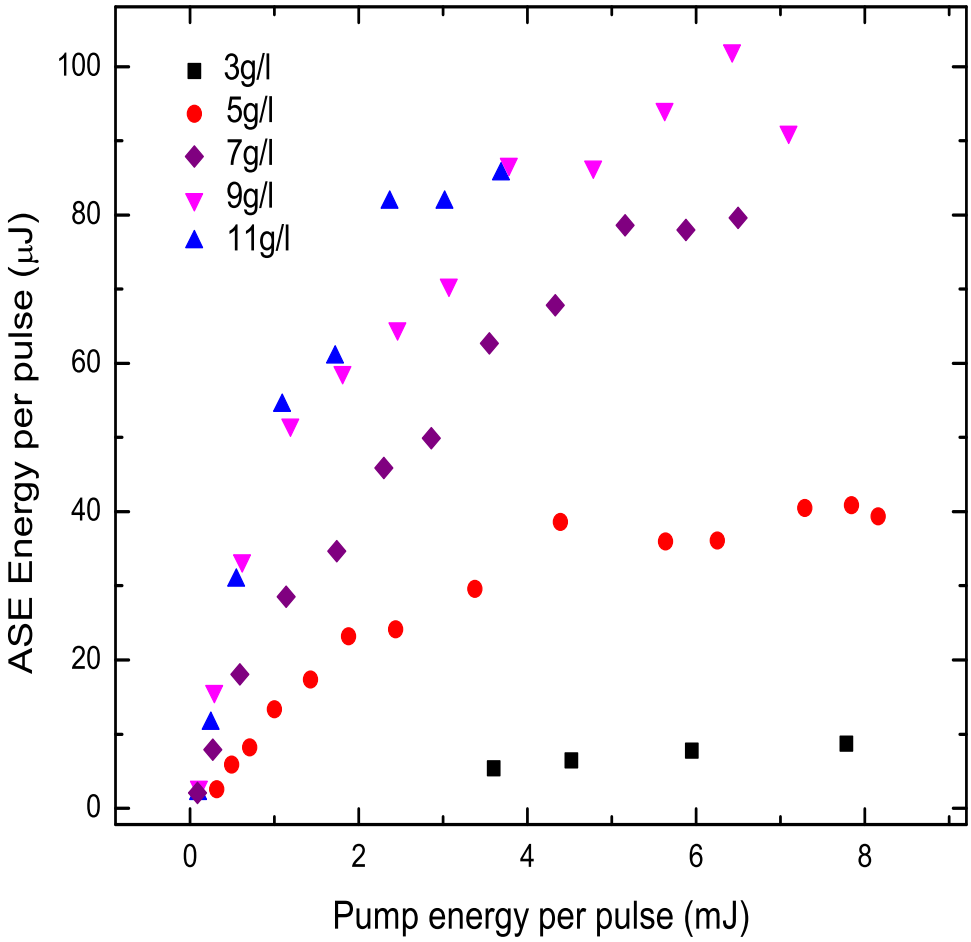

Figure 4.2: ASE as a function of energy for 3, 5, 7, 9 and 11g/l concentrations.

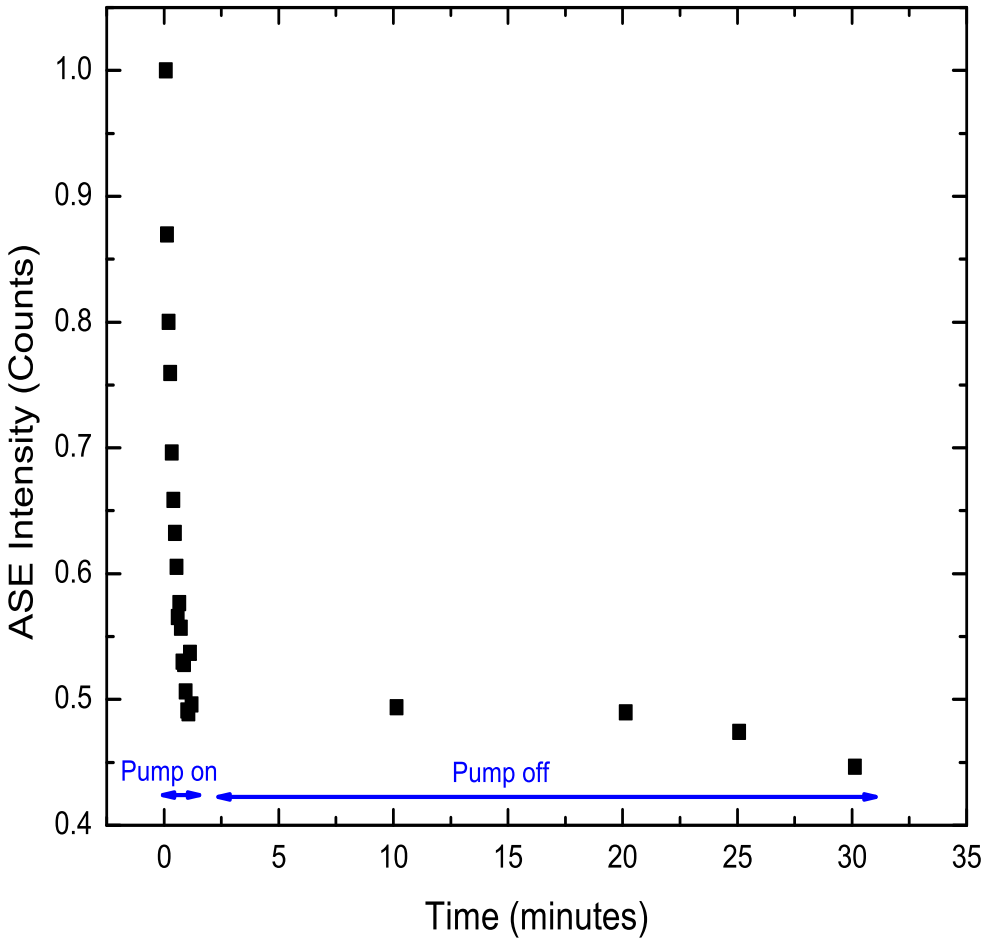

Figure 4.3: ASE intensity as a function of time with pump on and off for a 3g/l DO11/PMMA sample. The pump energy is 2mJ per pulse.

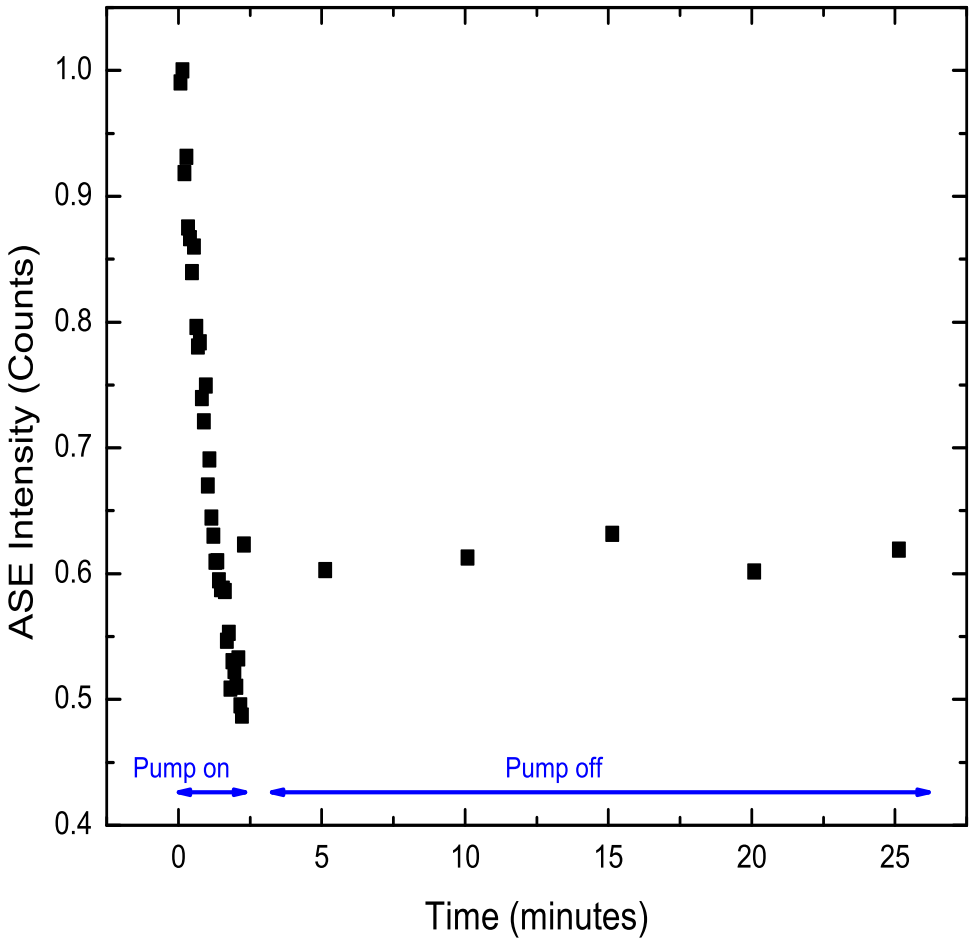

Figure 4.4: ASE intensity as a function of time with pump on and off for a 5g/l DO11/PMMA sample. The pump energy is 2mJ per pulse.

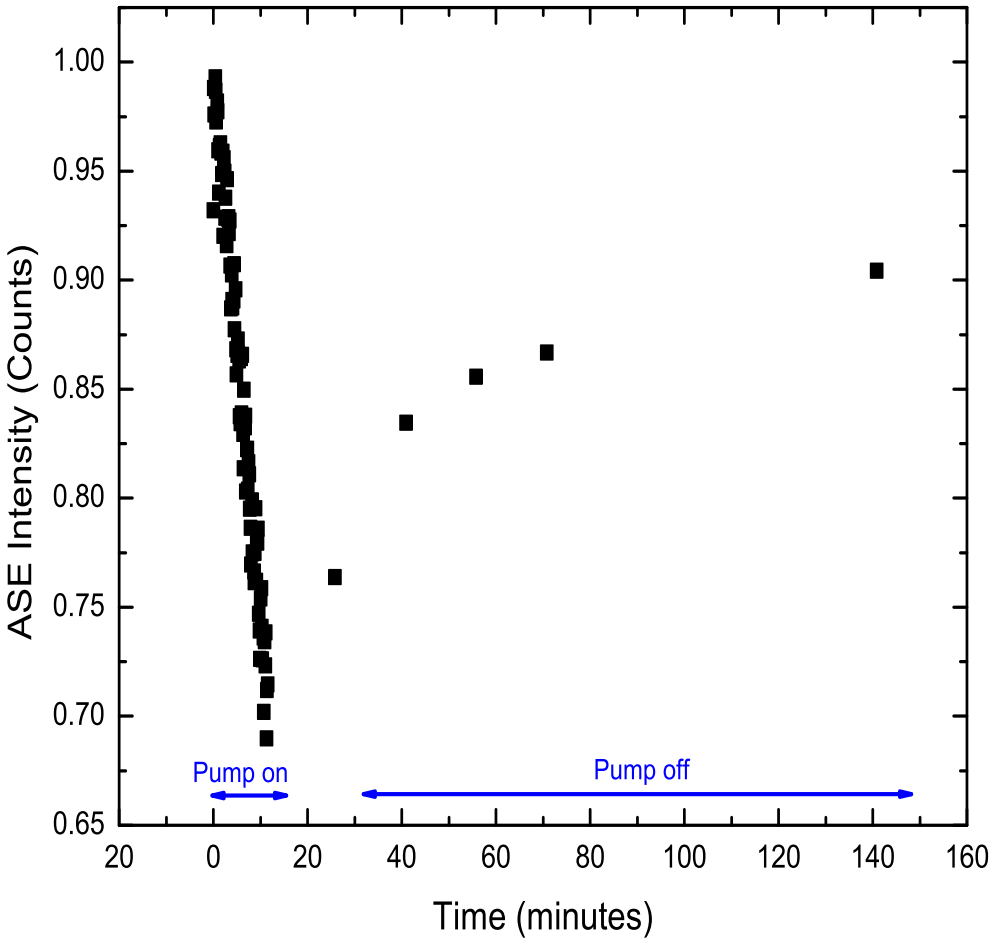

Figure 4.5: ASE intensity as a function of time with pump on and off for a 9g/l DO11/PMMA sample. The pump energy is 2mJ per pulse..

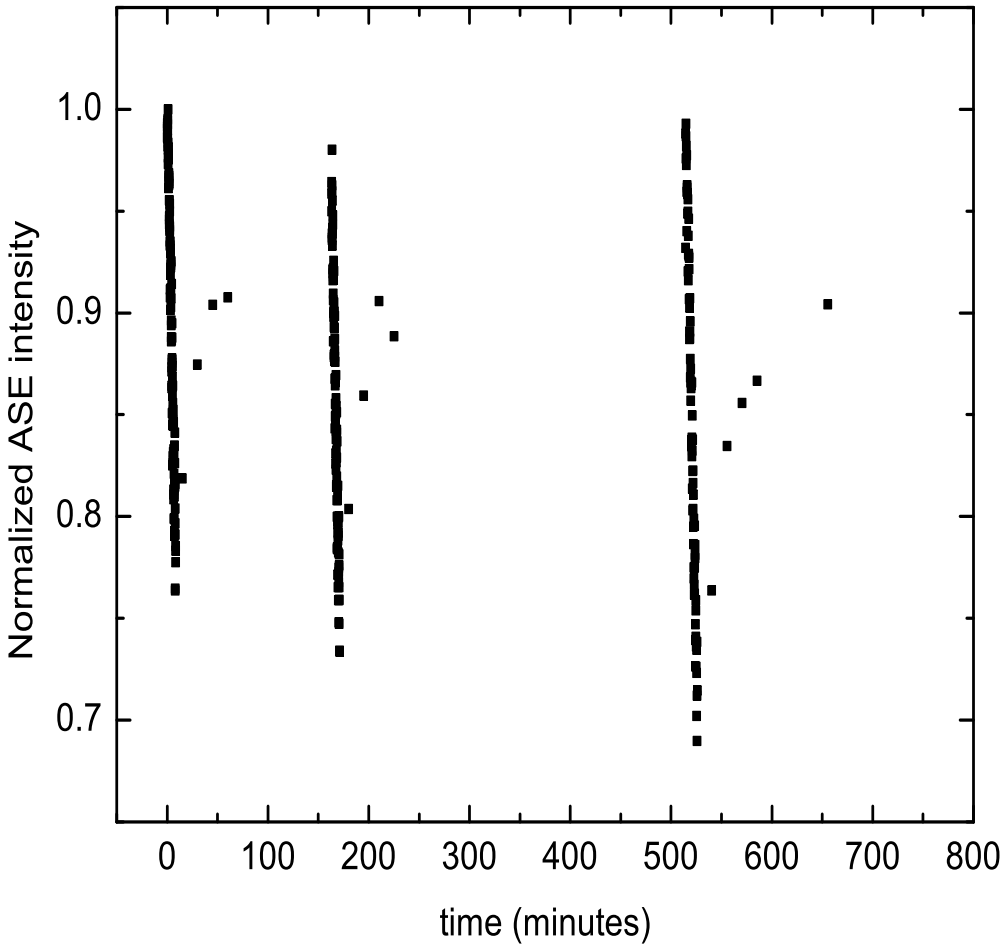

Figure 4.6: Photodegradation and recovery for a 9g/l sample of DO11/PMMA for three successive cycles of pumping and rest. The energy per pulse is 2mJ. Note that the sample will fully recover when allowed to heal for a long enough period of time.

9g/l for a small range of the pump energy. He found evidence of some aggregation at 6g/l and substantial aggregation at 9g/l. He also found that ASE saturate at about a 0.5mJ pump energy, which is the same result as ours as we showed in section 3.3. We have done a similar measurement as Howell for a broader range of concentrations and energies and similar results. Slight aggregation is found at 7g/l and substantial aggregation is found at 9g/l and 11g/l as shown in Figure 4.2.

The concentration dependent measurements determine if self-healing depends on the proximity between the DO11 molecules. We have found that the degree of recovery gets greater at higher concentrations as is shown in the progression from Figure 4.3 to Figure 4.6. The 3g/l sample shows no recovery while 5g/l shows a small degree of self-healing. These data clearly show that a high density of DO11 chromophores is required for self-healing to be observed.

4.3 Optical Anisotropy Measurement

Pump-induced optical anisotropy is measured by determining the change in absorbance of a probe beam when polarized along the pump polarization and perpendicular to it. In Disperse Red 1 (DR1) doped PMMA it is well known that photo-induced isomerization, a change in the molecular shape in response to light, followed by re-orientation in the direction perpendicular to the polarization of the pump laser [8, 9, 10]. A DR1 molecule, upon being excited by light or heat, changes its structure from the Cis to Trans isomer form as shown in Figure 4.7. We find

that the DO11 molecule in PMMA gives the same change in absorbance parallel and perpendicular to the pump polarization. Figure 4.8 shows the measured absorption change of DO11/PMMA for these two different polarizations. The pump intensity is 2.55×10^9 W/m^2 for about 200 minutes. We see from the graph that the change for both polarizations is the same within experimental error. Thus, the DO11 does not reorient in response to the pump light, so reorientation is not the cause of the observed photodegradation, nor the healing process.

4.4 Temperature Dependent Measurement

The cause of photodegradation is the formation of a state that does not produce fluorescence, resulting in a drop in ASE. Based on the fact that recovery requires a material at high concentration, we postulate that this non-fluorescing state is a dimer. Thus, if the energies of the difference in dimer and monomer energies is on the order of kT, temperature dependent spectroscopy would be a good probe. We apply temperature as another method of excitation that changes the populations of relaxation rates between states. Questions that we address are:

1. How are the monomer and dimer populations change as a function of temperature?

2. How is ASE emission affected by changes in the populations? and

3. How does the population distribution affect the self-healing?

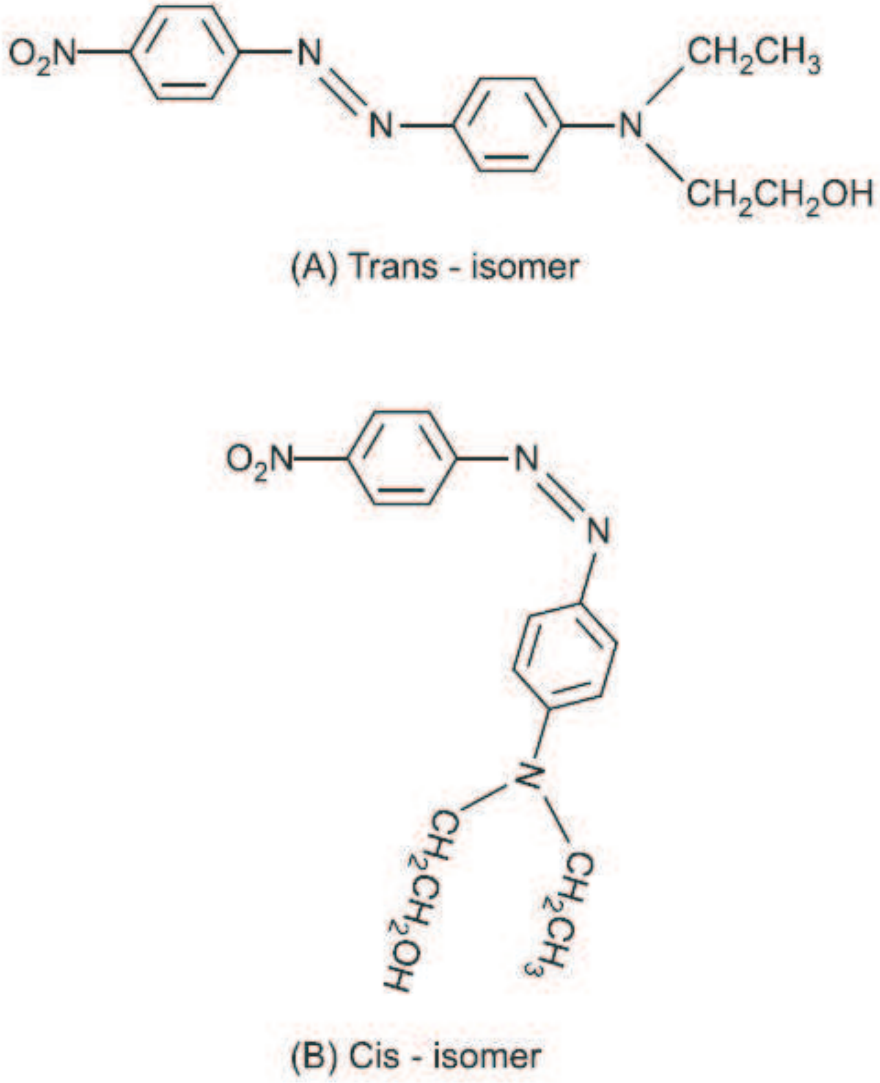

Figure 4.7: The cis and trans isomers of the DR1 molecule.

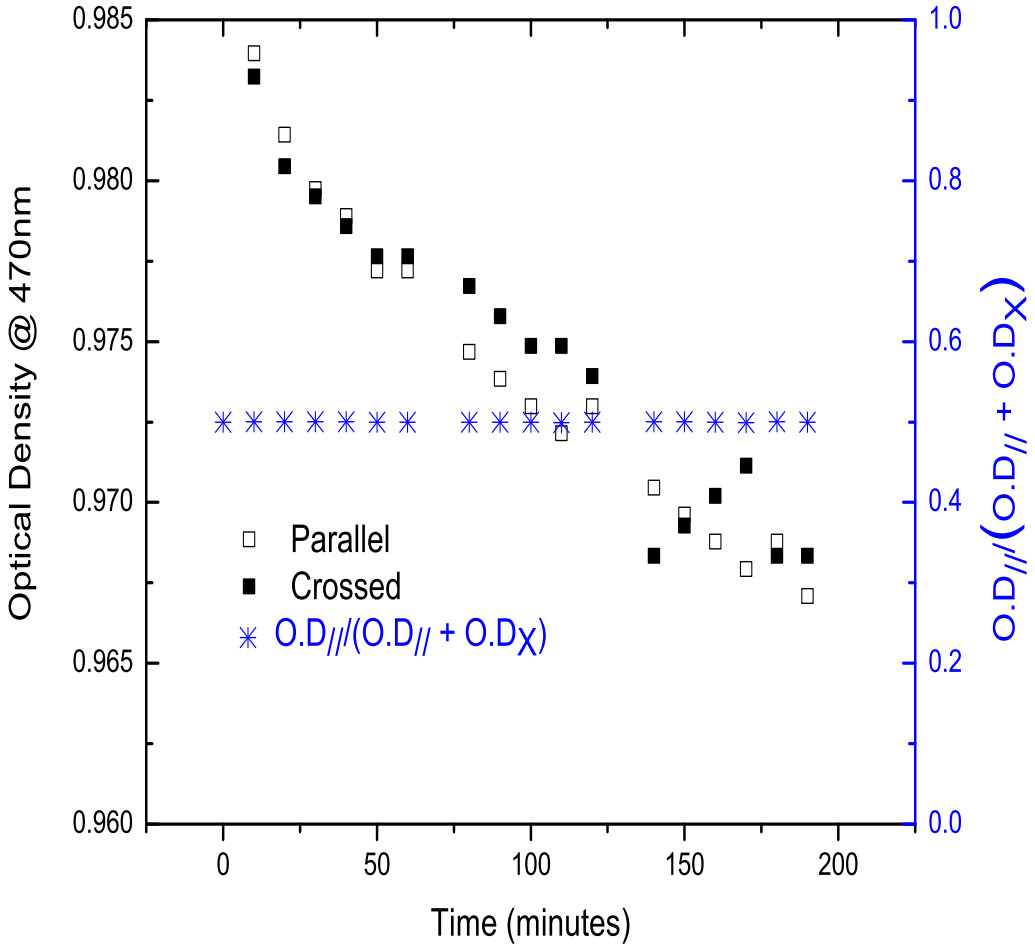

Figure 4.8: Absorbance of DO11/PMMA parallel and perpendicular to the pump beam polarization and the anisotropy parameter.

Figure 4.9 shows the absorption spectrum of DO11/PMMA as a function of temperature and Figure 4.10 shows the absorbance change relative to the spectrum at $T = 19^0C$. The plot shows three local extrema corresponding to the depletion of the monomer(center dip) and the formation of dimers(side peaks). There are several explanations for the red shift of the monomer dip. One is that the temperature changes the density of the polymer and hence the local fields at the molecule. Alternatively, at elevated temperature the relative strengths of the states can change. Or, the superposition of two peaks function can lead to an apparent shift in one of the peaks even though the underlying peaks have not shifted. Finally, the shift may be due to changes in how the polymer interacts with the dye. An example of a spectrum redshift due to the host material is given in reference [11].

Whatever the cause, the dip at 510nm can be associated with the monomer population and the two side peaks with the dimer. The conclusion is that as the temperature increased, the dimers population increases as the monomer population decreases. This measurement thus sheds light on the population dynamics and suggests that the hypothesis for dimer formation is a reasonable one.

We have also measured the fluorescence at fixed pump intensity as a function of temperature. The fluorescence decreases with increasing temperature as shown in Figure 4.11. This is consistent with the temperature dependent absorbance where we probe the increase of the dimers population, which we postulate is the cause of photodegradation. Since the dimers does not fluoresce, their presence is detectable by

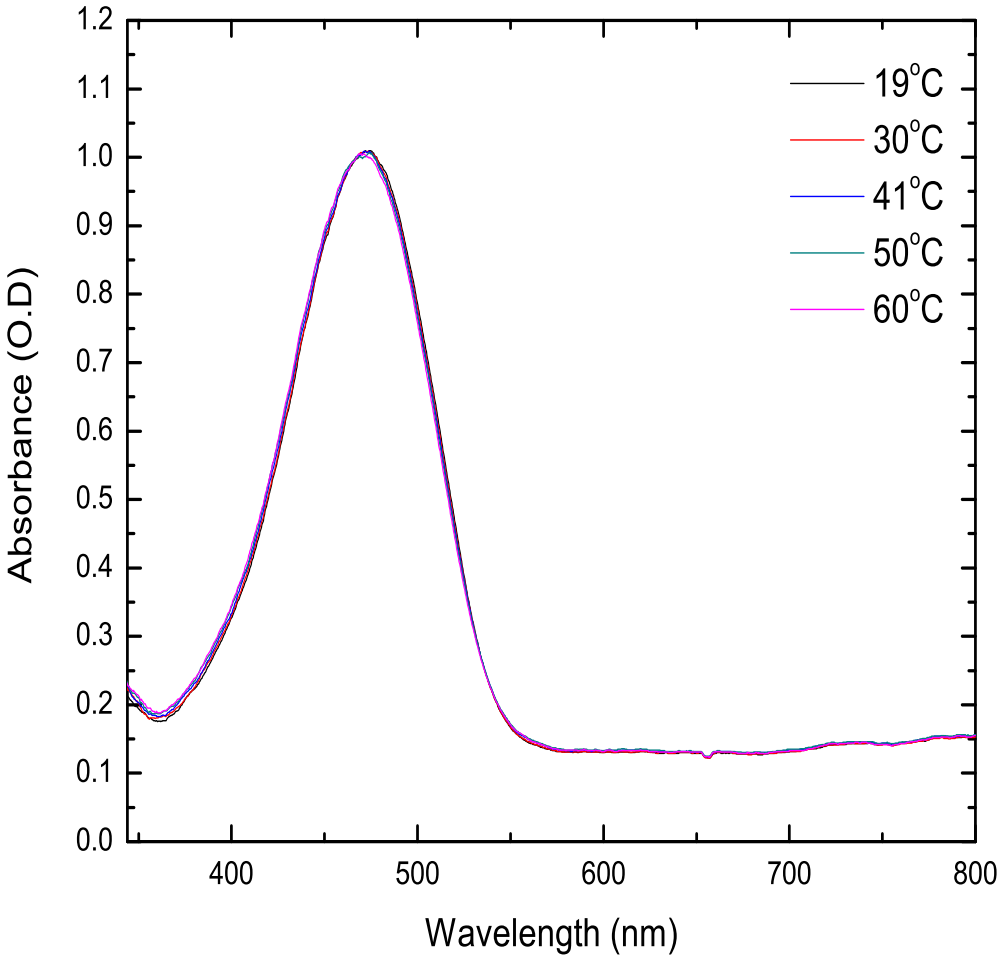

Figure 4.9: Absorbance as a function of temperature of DO11 dye.

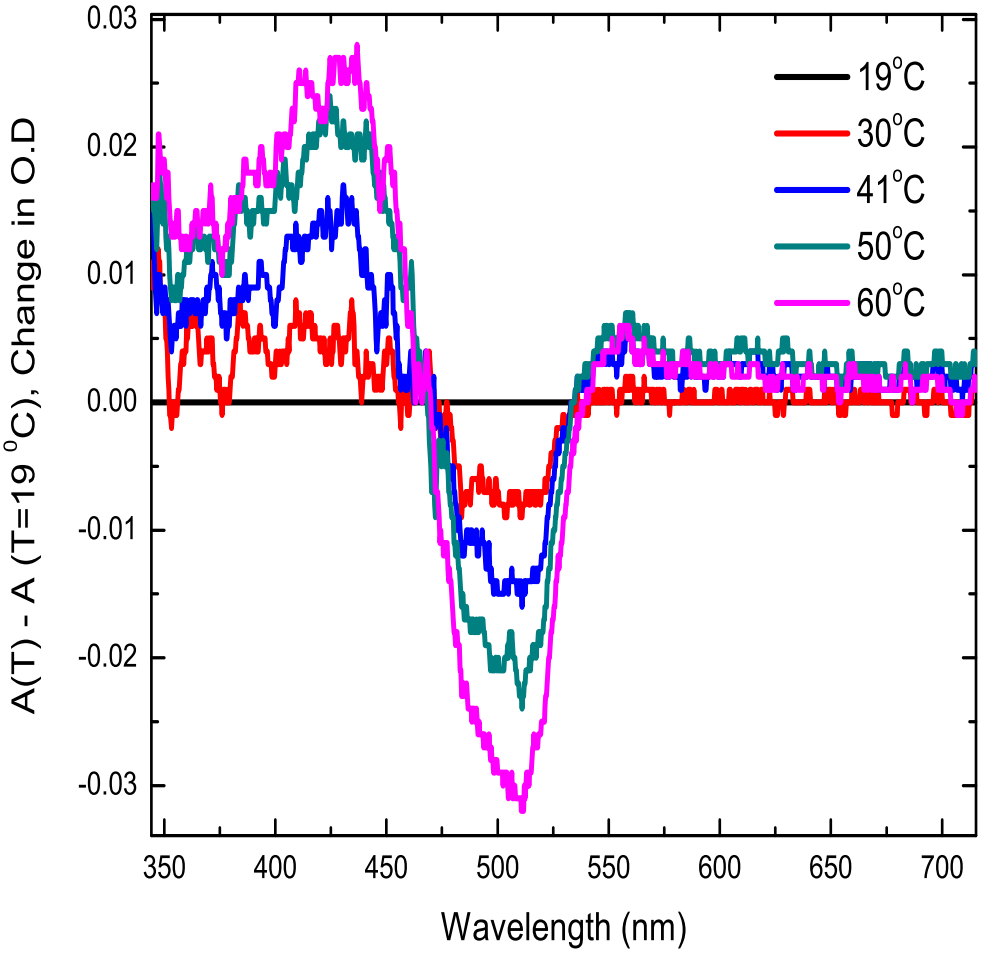

Figure 4.10: Absorbance change relative to T=19^0C as a function of temperature.

linear absorption but no new structure is observed in the fluorescence spectrum, as we would expect. Our temperature dependent experiment suggests that the dimer state (made from two tautomers), which is lower in energy than the tautomer molecule, is of higher energy than the DO11 molecule. Thus, the dimer can decay back to a DO11 molecule. Because of these energy assignments, we would expect that at T=0K, the system would be made of all DO11 molecules. As the temperature is raised, the dimer population increases first, followed by an increase in the tautomer population. Since the process of ASE leads to a large population of dimers, which are not in thermal equilibrium, the dimer population decays into the monomer state. Thus, the rate of decay increases as the temperature of the polymer is decreased. So, self-healing that results in increased ASE can be accelerated by cooling the sample for the given range of temperatures. This behavior has been observed in the literature [12].

4.5 Intensity Dependent Measurements

To make many nonlinear effects observable requires intense monochromatic radiation. However, such high intensities can cause photochemical reactions in the material. In our experiments, we expose our samples to high-intensity for long duration and probe their response using linear absorption and ASE as a function of time as it is described in Sections 4.5.1 and 4.5.2. The intensity induces changes in the physical properties of the sample. We have proposed that a population change between two species is responsible, and the species are consistent with being monomers DO11 molecules) and

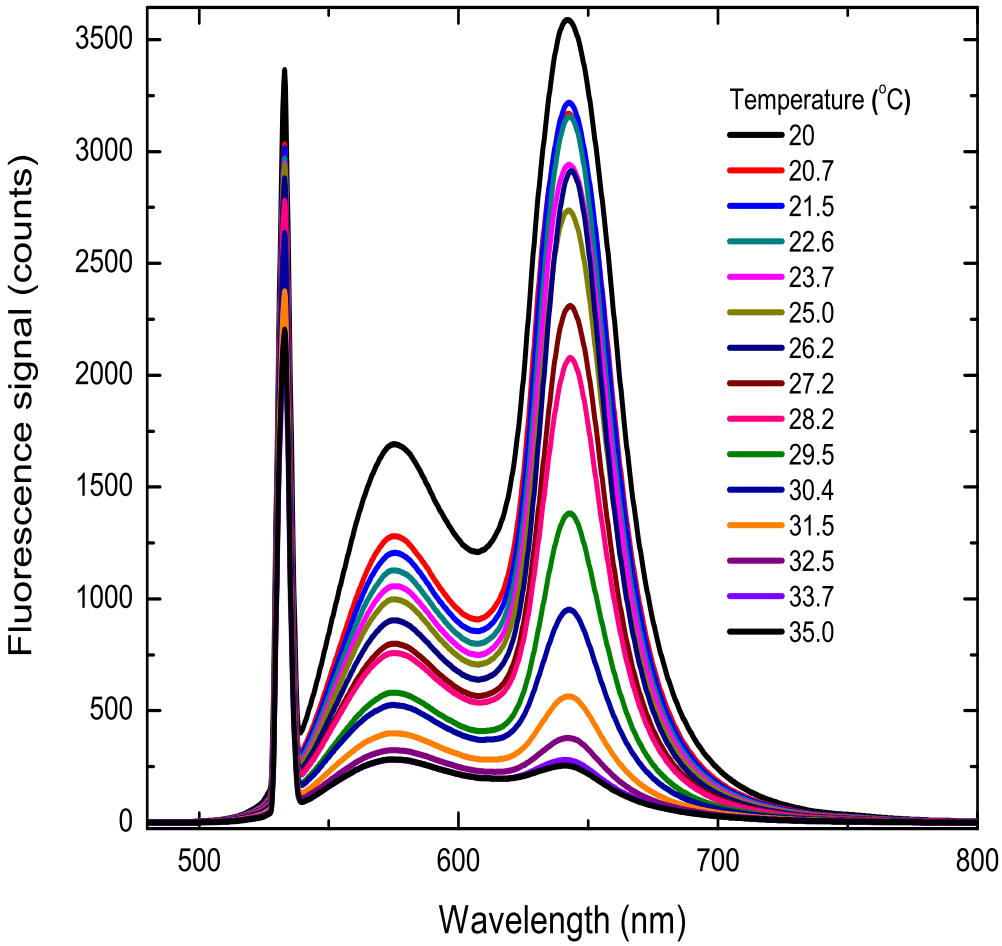

Figure 4.11: Fluorescence at fixed pump intensity as a function of temperature.

dimers (a pair of coupled DO11 tautomer molecules). The absorbance change or the decrease in ASE is proportional to the intensity for a fixed-duration experiments, but also dependent on the time integrated intensity or total number of pulses absorbed by the sample. We investigate both of these cases.

4.5.1 Absorption Measurement: Fixed Intensity and Room Temperature

This measurement was done to understand the population dynamics using absorbance as a probe when the sample is pumped at constant intensity. The absorption spectrum identifies states of a system by positions and areas of peaks. Though the spectrum is continuous, it can be used to determine the energy eigenvalues and transition moments of a species of molecules. Therefore, a change in absorbance spectrum is associated with a change in the eigenfunctions.

Figure 4.12 shows the absorption spectrum at room temperature under constant pumping as a function of time. Figure 4.13 shows the difference in the spectrum at time t and the absorbance at time t=0. The two points at 426nm and 541nm on the graph that don't change with time are called isobestic points. Changes in the absorbance peaks occur at 390nm, 475nm and 557nm wavelengths. The decrease at 475nm represents the destruction of monomers (DO11 molecules) and the increase at 390nm and 557nm represents the creation of dimers (pairs of DO11 tautomers).

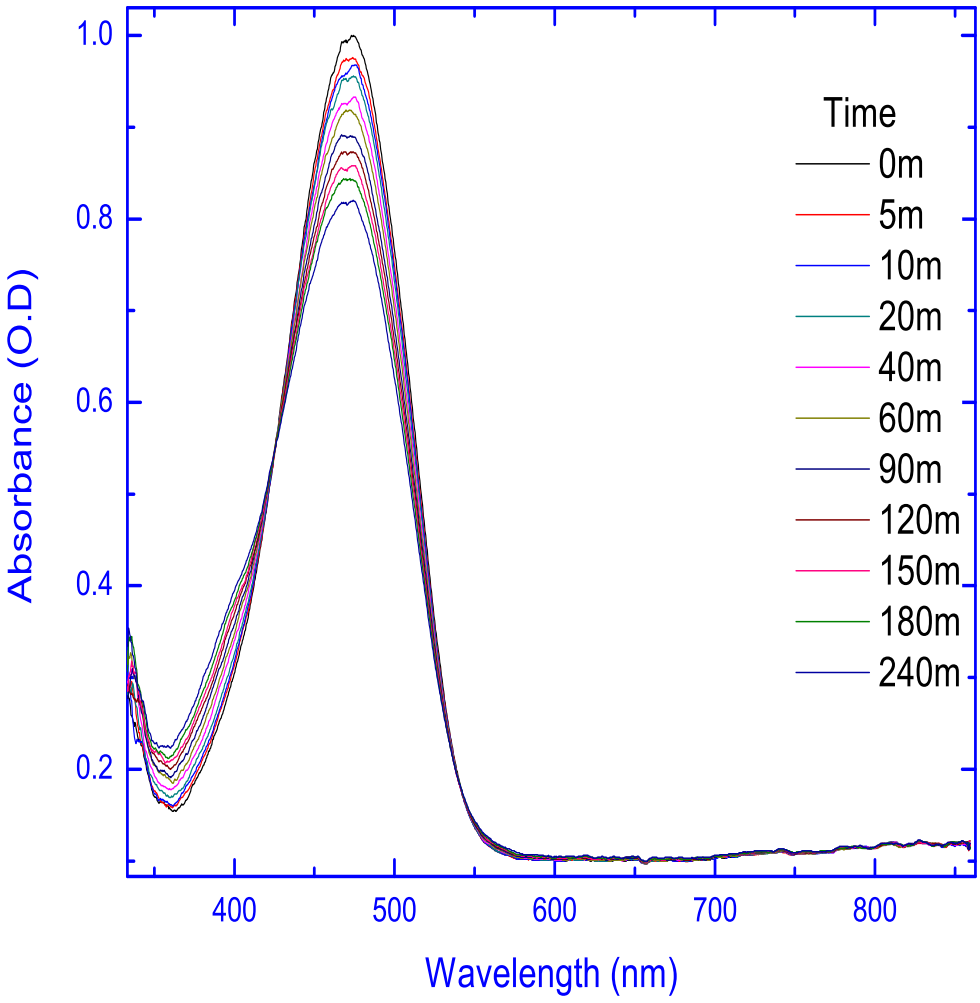

Figure 4.12: Absorbance as a function of time at fixed pump intensity (3.11 $\times 10^{10} W/m^2$) and room temperature for a sample concentration of 9g/l.

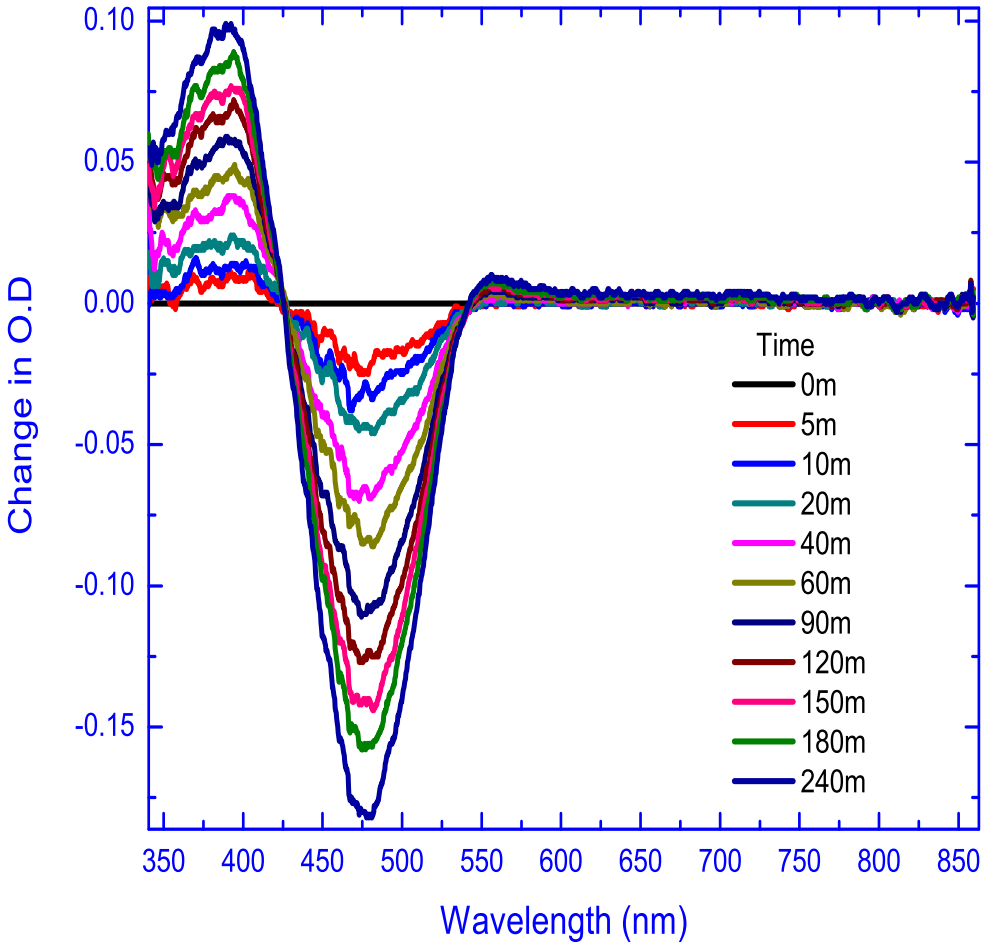

Figure 4.13: Absorbance change relative to t=0 absorbance at fixed intensity and room temperature. The pump intensity used is 3.11 $\times 10^{10} W/m^2$. The sample concentration is 9g/l.

4.5.2 ASE Measurement as a Function of Time for Various Intensities at Room Temperature

Figure 4.14 shows a plot of the ASE intensity over time scales that are long enough to observe the equilibrium condition that the photodegradation process equals the recovery process. Figure 4.15 shows ASE as a function of time and pump intensity when the degradation process exceeds the recovery process. Our theoretical model given by Equation[2.19] to Equation[2.23] agrees well with the experiment at various intensities. Furthermore, we find that the degradation rate is a linear function of the intensity as shown Figure 4.16. Note that the points in Figure 4.16 are determined from the fit parameters from Figure 4.15. This linear dependence is attributed to one-photon absorption, which agrees with our assumptions that a one photon absorption excites the molecules, an assumption we have used to formulate our theory. The recovery process, however, is independent of the intensity as shown in Figure 4.17 as assumed by our model. Our theory also predicts the ASE time dependence at very long times were the signal reaches a nonzero equilibrium, as shown in Figure 4.14 where the ASE recovery and photodegradation process are comparable.

4.5.3 Recovery Measurements

Figures 4.18 and 4.19 show self-healing of ASE as a function of time and a fit to our population dynamics theory for samples with two different histories. This method was used to get the parameters shown as in Figure 4.17 to yield the intensity dependence

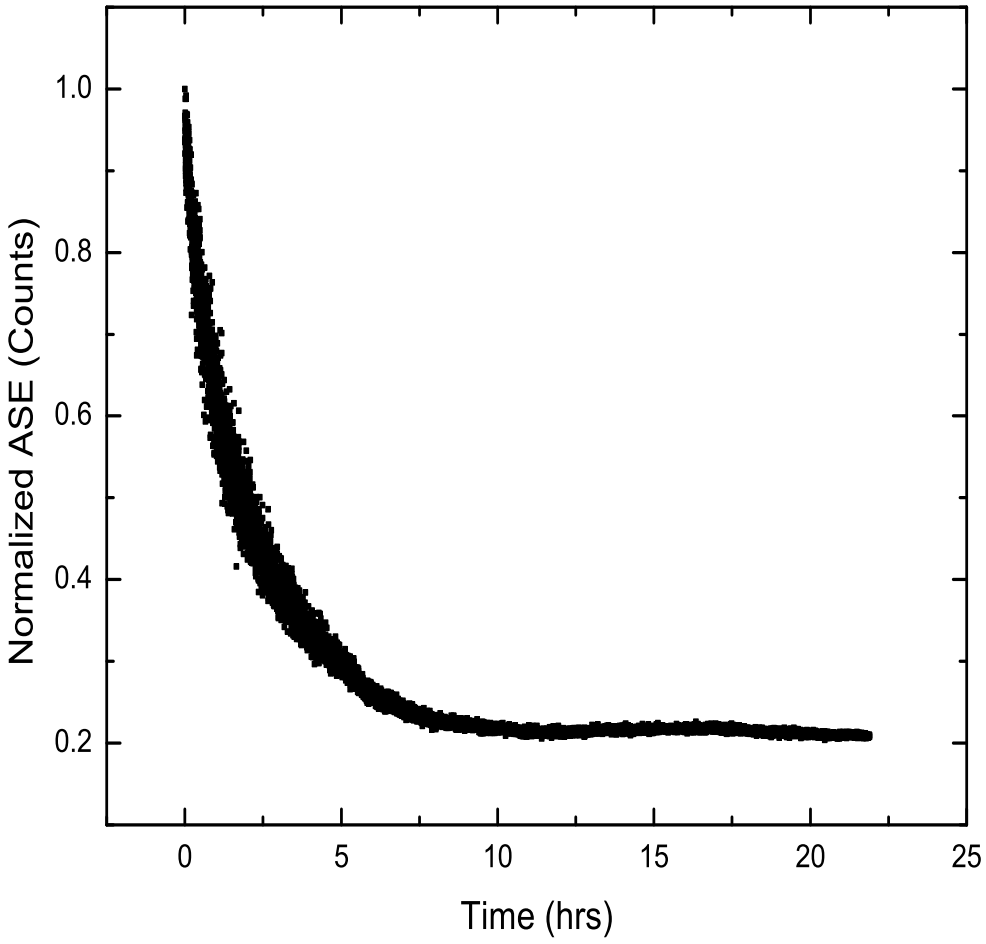

Figure 4.14: Photodegradation as a function of time over time scales that are long enough to show the equilibrium condition when the photodegradation rate matches the recovery rate.

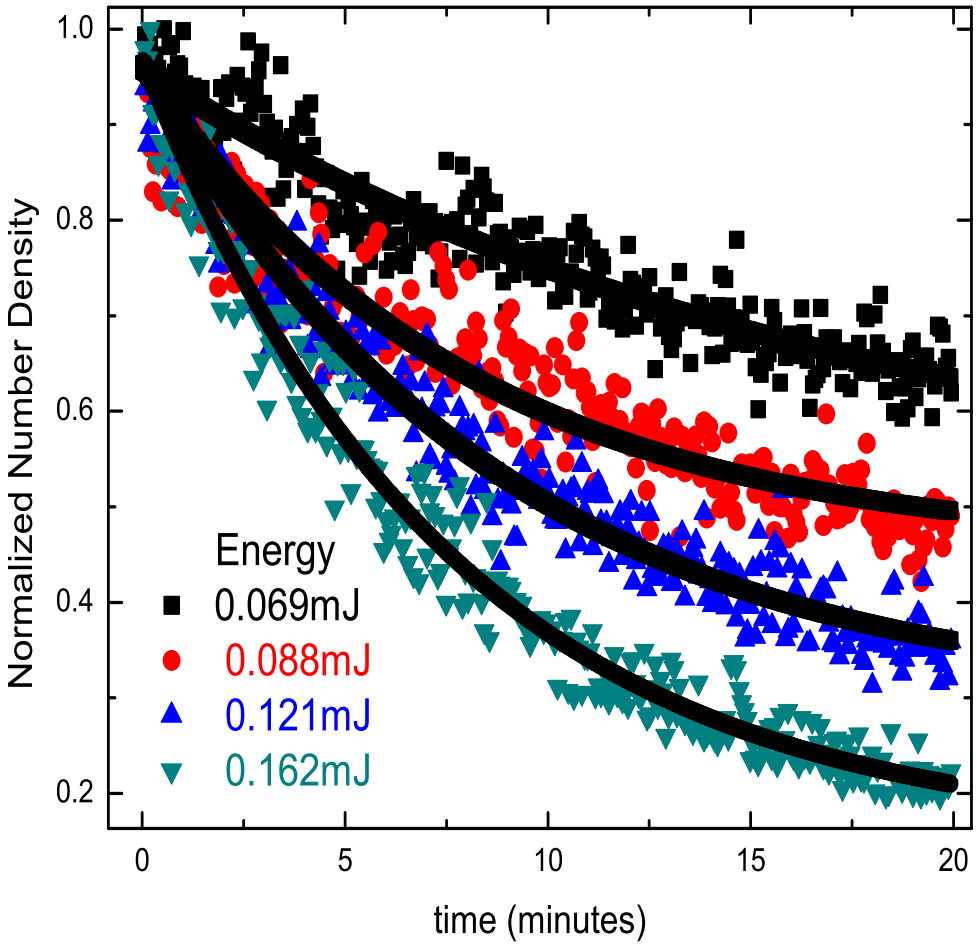

Figure 4.15: Photodegradation as a function of time and intensity fit to Equation[2.21].

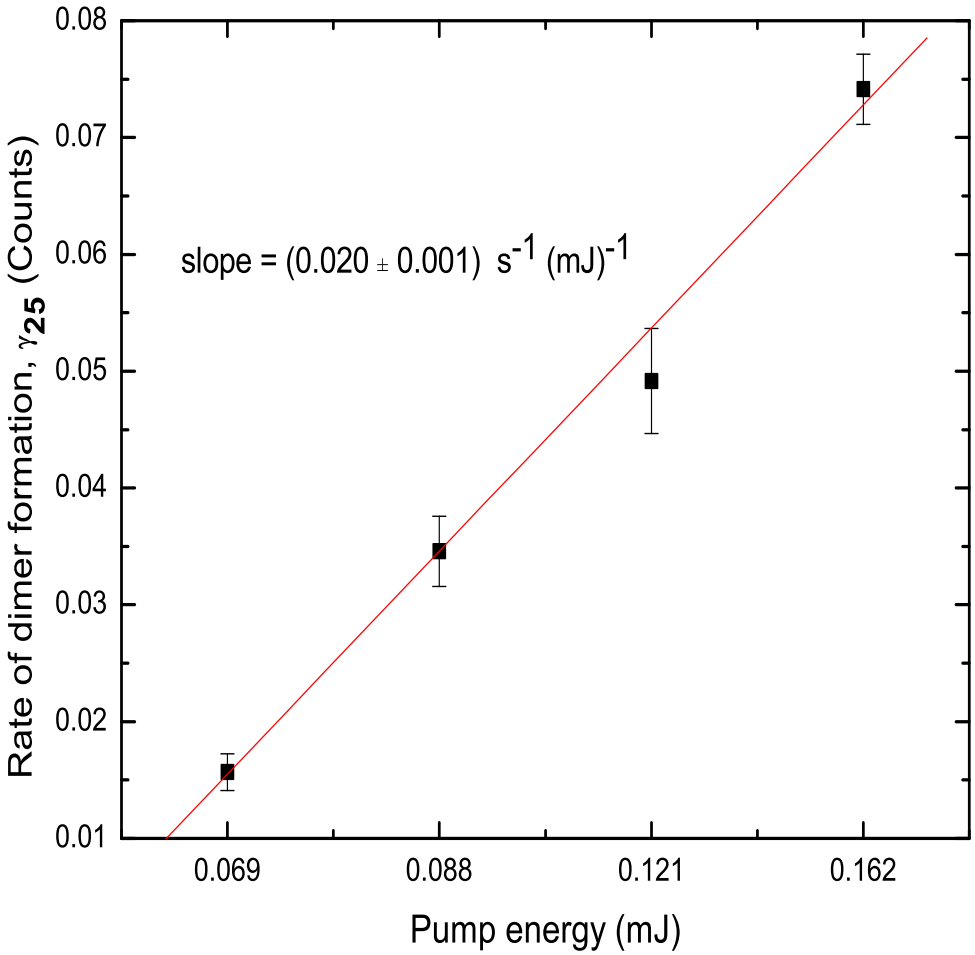

Figure 4.16: Degradation rate as a function of pump energy.

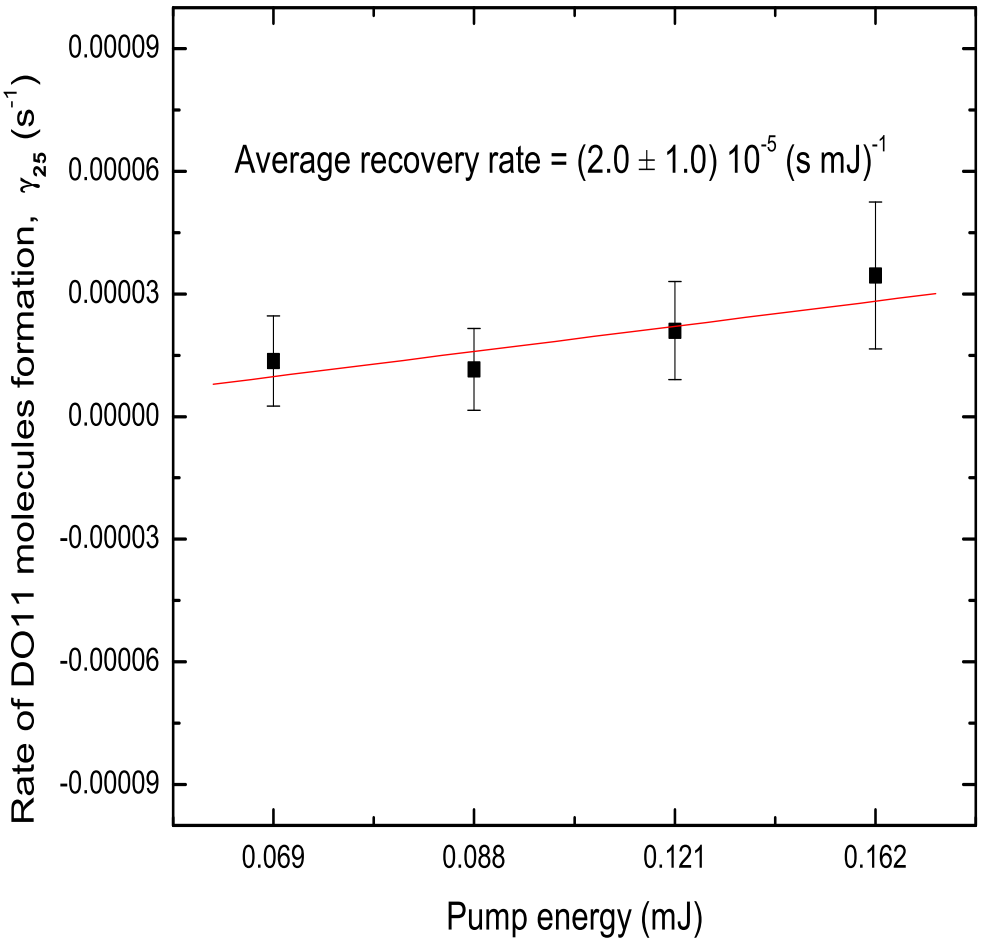

Figure 4.17: Recovery rate as a function of pump energy.

of ASE during recovery for samples pumped with different intensities. This shows that the self-healing process is independent of the pump intensity history.

4.5.4 Gamma Irradiation and Self-Healing

Preliminary studies show that self-healing may improve with gamma ray irradiation. Figure 4.20 and 4.21 shows photodegradation and recovery before and after gamma irradiation. The degree of self-healing appears better after the irradiation. The combination of laser and gamma radiation cycling is potentially a new avenue for making even better materials.

4.6 Proposed Energy-Level Diagram

In this section, we bring all the results together in the form of an energy-level diagram that describes all the observed phenomena in one unified picture. Figure 4.22 shows the energy-level diagram. From our photodegradation dynamical studies, we found that the ASE intensity levels off to a nonzero value after a long irradiation time. This suggests that after long periods of irradiation an equilibrium state is reached where the degradation process matches the recovery process. Since the degradation rate depends on the pump intensity, the equilibrium level also depends on the pump intensity. Figure 4.14 shows that when the pump intensity is high, the equilibrium ASE intensity is low. From our population dynamics results, we have found that the time constants for degradation and recovery are different, i.e., the decay time constant

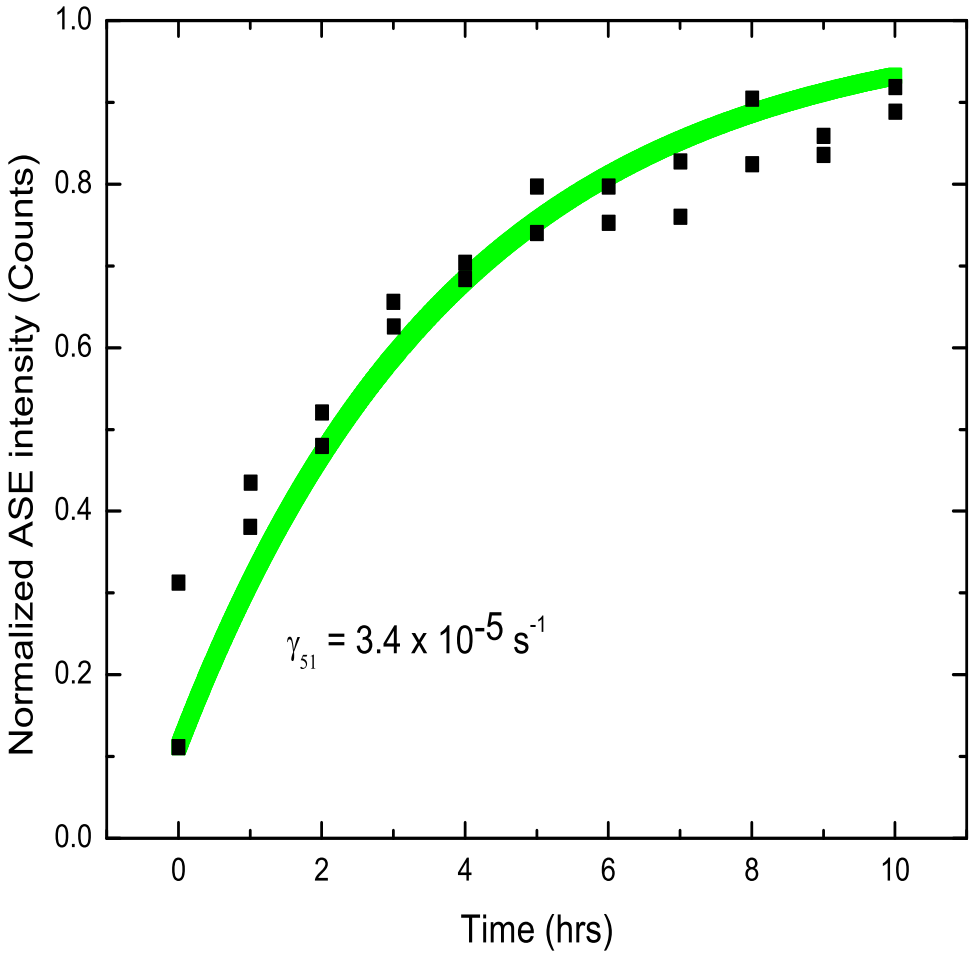

Figure 4.18: ASE signal as a function of time during self-healing for sample originally pumped with an intensity of I= 1.67 $\times$ 10^{10} W/m^2.

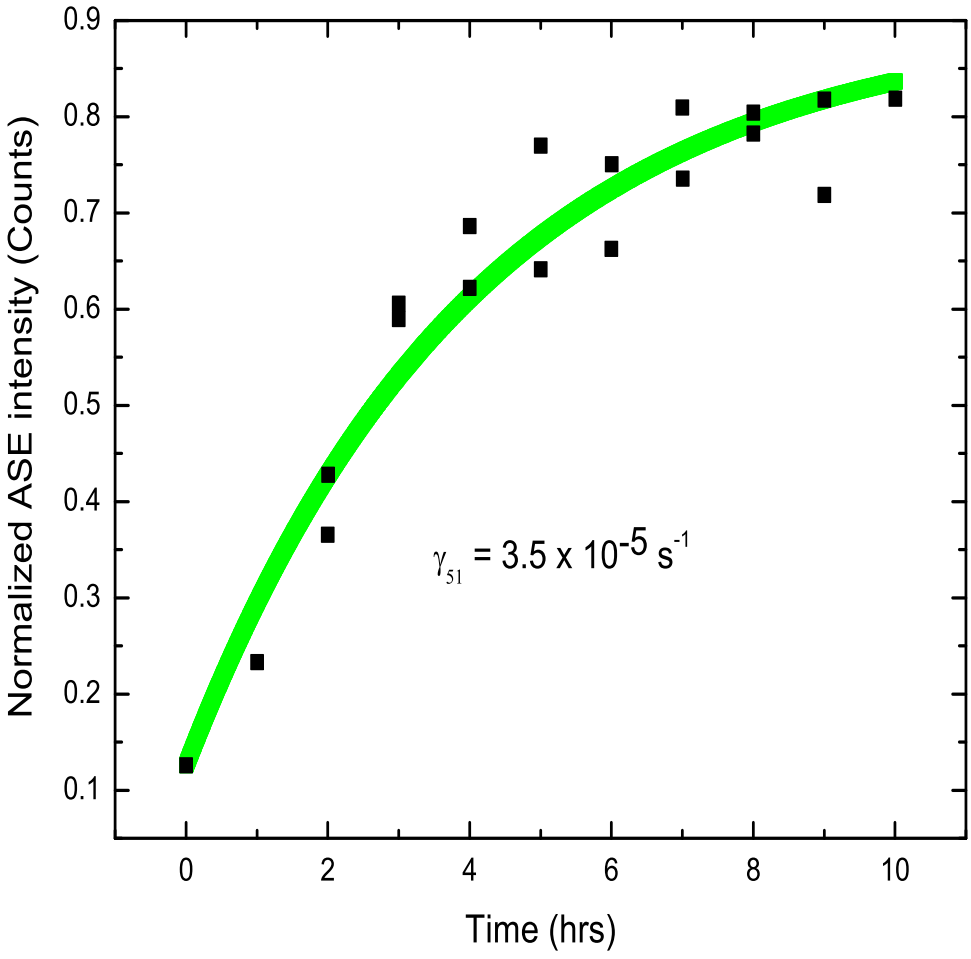

Figure 4.19: ASE signal as a function of time during self-healing for sample originally pumped with an intensity of I= 2.21 $\times$ 10^{10} W/m^2.

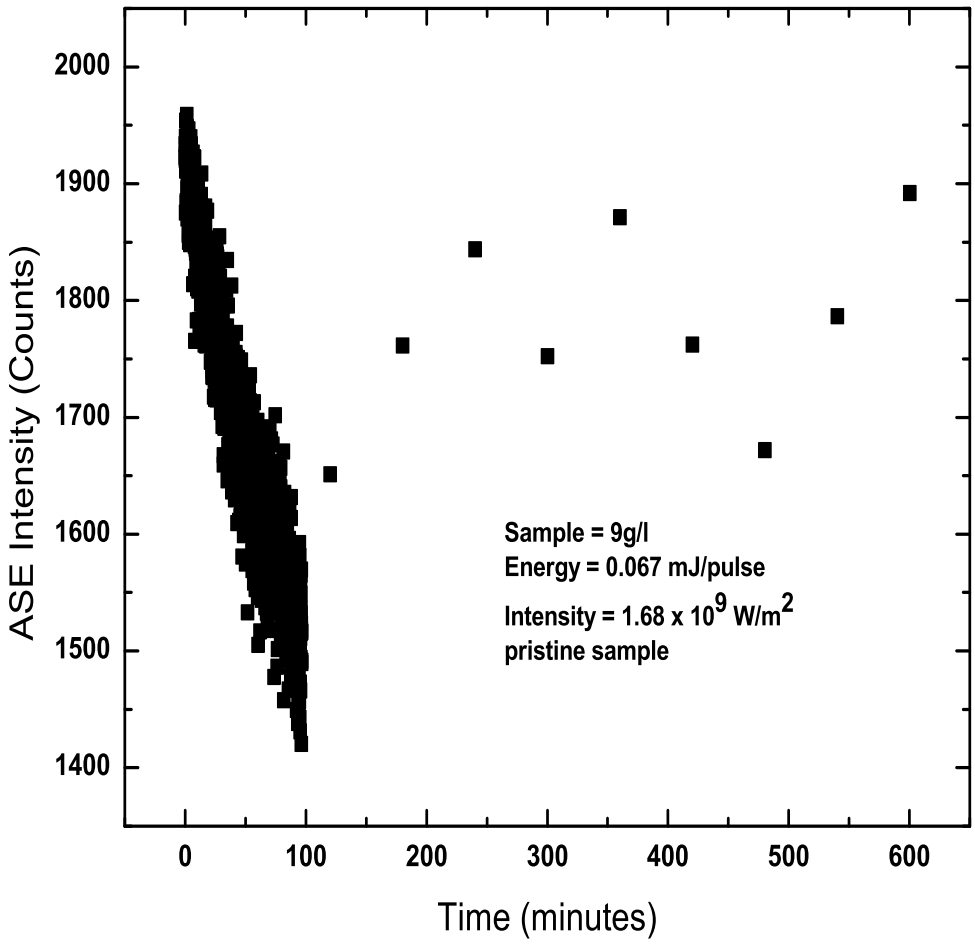

Figure 4.20: Photodegradation and recovery in 9g/l of a DO11/PMMA sample. The pump energy is 2mJ per pulse.

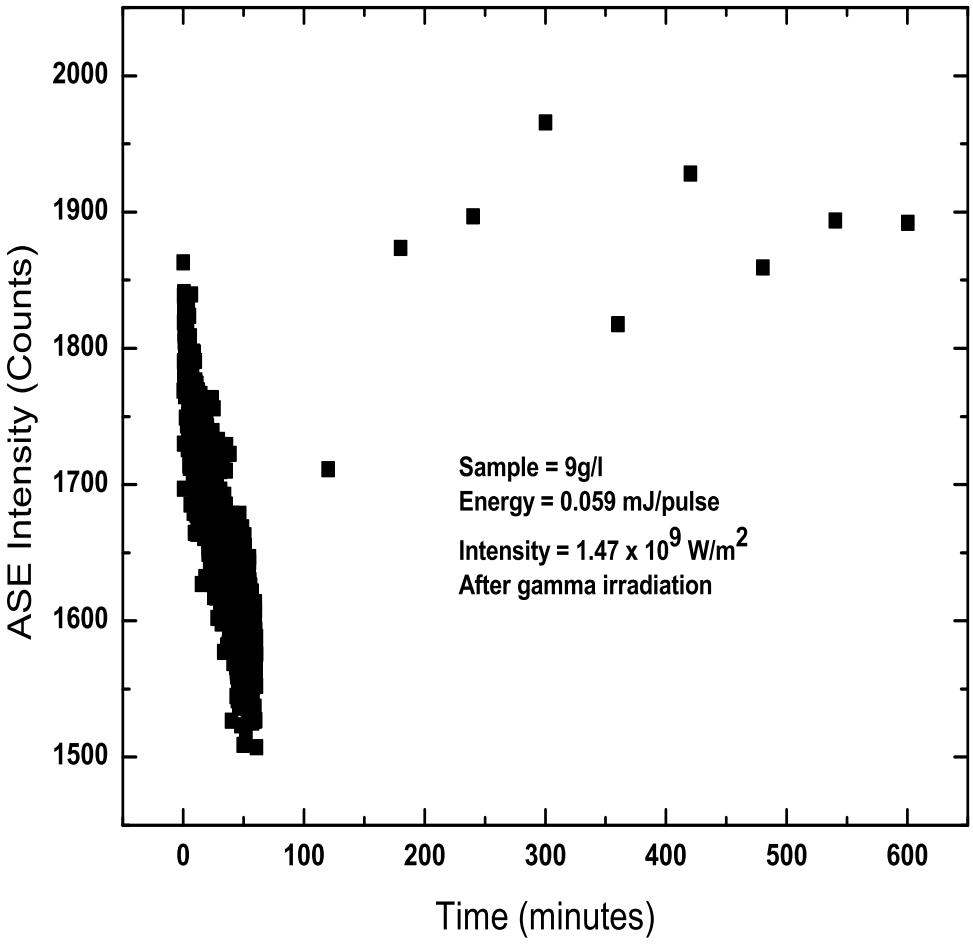

Figure 4.21: Photodegradation and recovery for a 9g/l DO11/PMMA sample (same sample as used in Figure 4.20) after gamma irradiation.

$\frac{1}{\gamma_{25}}$ is faster than the recovery time constant $\frac{1}{\gamma_{51}}$ which is shown as in Figure 4.16 and Figure 4.17. Thus, this implies that the degradation forms a metastable species with an energy higher than the non-degraded material.

From our absorption measurement, we have found that the first singlet excited state of the DO11 molecule in PMMA is at 2.64 eV. The molecular structure of DO11 falls in a class of materials that is known to phototautomerize, that is, light can cause a proton to jump to a nearby site. Furthermore, the large Stokes Shift of the fluorescence is consistent with a tautomer being responsible. At low pump intensity, the fluorescence spectrum peaks at 2.16 eV, and at high pump intensity, the ASE peak is at 1.92 eV. The fact that ASE is observed implies that an inverted population is excited which requires a long-lived state away from the excitation light. Again, this is consistent with the formation of a long-lived excited state tautomer that decays to a ground state tautomer.

The self-healing effect is only observed when the dye concentration is high, but is not observed in liquid solutions which only degrade[14]. This observation motivates us to propose that a dimer of two tautomers forms due to strong polar interactions between nearby molecules. Since the dimer has a different energy spectrum than the DO11 molecule and the tautomer, it would be reasonable to speculate that it may not form an inverted population when excited by the laser light. To test this hypothesis, we did linear absorption spectroscopy during photodegradation in the solid DO11/PMMA sample and find that the DO11 peak gets depleted and two new

peaks form. This observation is consistent with interacting tautomers that form dimers. The two observed energy levels at 3.18 eV and 2.23 eV are consistent with dimers.

From this picture, the photodegradation and the self-healing cycle can be viewed as follows. When a DO11 molecule is excited, one possible outcome is for the excited state to non-radiatively decay to the tautomer state. The observed fluorescence is due to de-excitation of this tautomer to its ground state. The ground state tautomer, due to the strong dipole interactions forms a dimer (which has an energy level between the DO11 molecule and the tautomer molecule) which we conclude from the observation that the ground state can decay into either a dimer or a DO11 molecule; and , the dimer can decay into two separate DO11 molecules. The dimer decay to DO11 molecule by thermal agitations as it was confirmed experimentally by the observation of accelerated decay at increased temperature. We find that at high enough temperatures, the three states can become equally populated, so at some point, raising the temperature decreases the DO11 molecule population. We found this result in certain temperature regime. The net effect is that once the system returns to singlet DO11 molecules, the material has healed and ASE returns.

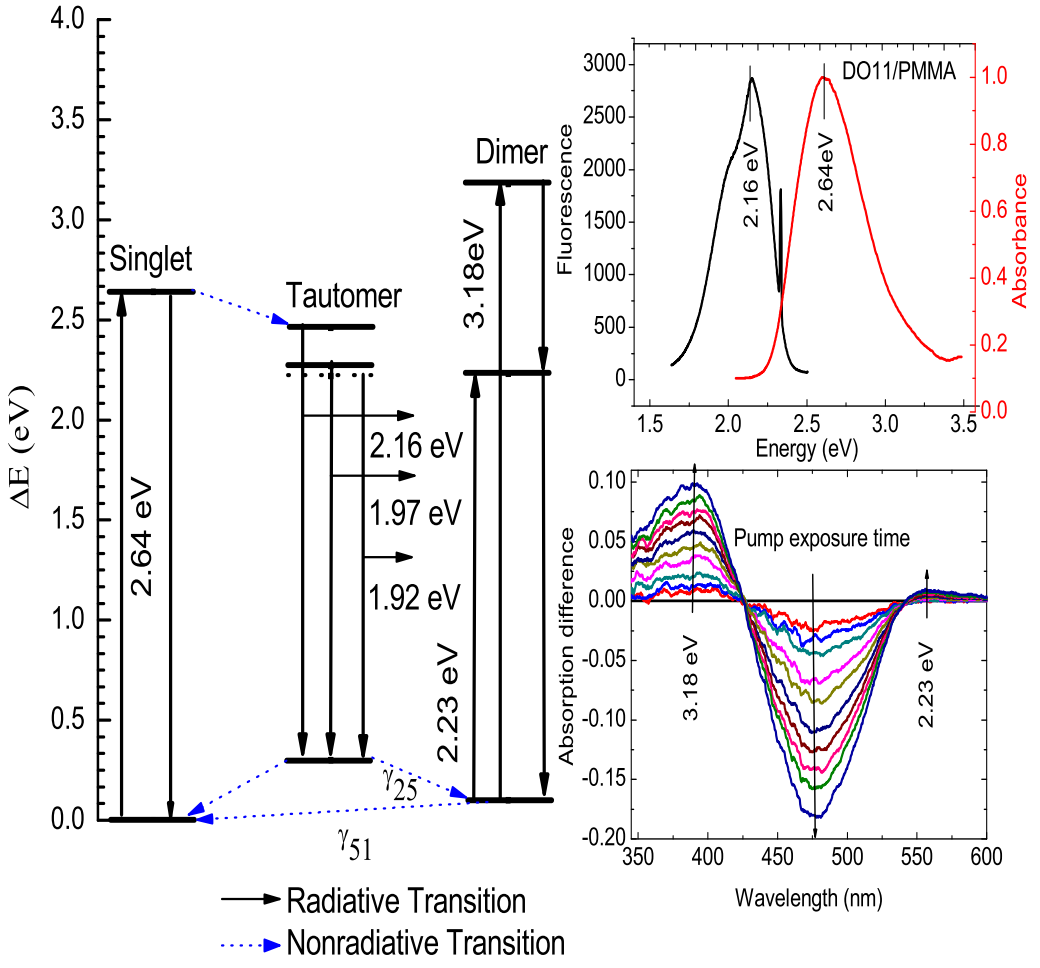

Figure 4.22: The proposed energy level diagram (left portion) and some of the data used in its construction (right).

Bibliography

[1] K.H. Drexhage, *Structure and Properties of Laser Dyes in Topics in Applied Physics, Dye Lasers*, pp. 171, 176, SpringerVerlag, Berlin, Germany 1990.

[2] Benniston, A. C.;Harriman, A.; Lawrei, D. J.; Mayeux, A. Phys. Chem. Chem. Phys. **6**, 51-57, **2004**.

[3] Kaneda, K.; Arai, T. Photochem Photobiol. Sci. **2(4)**, 402-406, **2003**.

[4] W. West and S. Pearce, J. Phys. Chem. **69**, 1894, 1965.

[5] M. E. Lamm and D. M. Neville, J. Phys. Chem. **69**, 3872, 1965.

[6] D. L. Akins and J. W. Macklin, J. Phys. Chem. **93**, 5999, 1989.

[7] B. Howell and M. G. Kuzyk, J. Opt. Soc. Am. B **19**, 1790 (2002).

[8] Weiya Zhang, *Effect Of A Thin Optical Kerr Medium On A Laguerre-Gaussian Beam And The Application*, Doctoral dissertation, Washington State University, 2006.

[9] S. Bian, D. Robinson, and M. Kuzyk, *Optical activated cantilever using photomechanical effects in dye-doped polymer fibers*, J. Opt. Soc. Am. B 23, 697 (2006).

[10] J. J. Park, *Photo-induced molecular reorientation and photothermal heating as mechanisms of the intensity-dependent refractive index in dye-doped polymers*, Doctoral dissertation, Washington State University, 2006.

[11] K.H. Drexhage, *Structure and Properties of Laser Dyes in Topics in Applied Physics*, Dye Lasers, pp. 171, SpringerVerlag, Berlin, Germany 1990.

[12] Duarte, F. J. and Hillman, L.W., *Dye Laser Principles With Application*, pp. 263, Academic Press, Inc. San Diego, CA 1990.

[13] Duarte, F. J. and Hillman, L.W., *Dye Laser Principles With Application*, pp. 324, Academic Press, Inc. San Diego, CA 1990.

[14] B. Howell and M. G. Kuzyk, Appl. Phys. Lett. **85**, 1901 (2004).

[15] B. Howell, *Transient Absorption and Stimulated Emission of the Organic Dye Disperse Orange 11*, Master's thesis, Washington State University, 2001.

Chapter 5

Conclusion

We studied the mechanisms of reversible photodegradation of amplified spontaneous emission in the organic dye 1-amino-2-methylanthraquinone (Disperse Orange 11 or DO11) doped into solid polymethylmethacrylate (PMMA) using the second harmonic of an Nd:YAG laser in a transverse pumping configuration to excite the molecules. From polarization-dependent linear spectroscopy measurements, we have determined that the bulk material remains isotropic when pumped with a polarized laser. This shows that the molecule does not reorient, so molecular re-orientation is not responsible. However, the fact that the absorption decreases suggests that the pump beam changes the sample.

Since the degree of self-healing increases with dye concentration, we studied the concentration dependence of the ASE signal for 3, 5, 7, 9, and 11g/l samples and found that the PMMA polymer is saturated with DO11 molecules at a concentration

of 9g/l, the concentration where photodegradation is fully reversible.

Absorbance change measurements of the DO11/PMMA sample pumped with light at room temperature shows changes in the spectrum at 390nm, 480nm, and 557nm. In particular, the new peaks that are observed at 390nm and 557nm with pumping are due to the formation of dimers, made of pair of DO11 tautomers. The decrease of the peak at 480nm is associated with a decrease of the population of DO11 molecules when dimers are formed. In the dimer state, ASE is quenched, leading to photodegradation. Note that the tautomers, which have a large dipole moment compared with the DO11 molecules is the source of emission that gives the ASE. We propose that the dimers form the tautomers due to strong dipole interactions.

Absorbance measurements as a function of temperature but fixed intensity spectrum that changes in a way similar to what is observed with pumping, i.e, dimers are forming as the temperature is increased. We note that the temperature-dependent data yield peaks that are in slightly different positions that what is observed for the spectra of an optically-pumped material. The difference arises mostly likely because the temperature-dependent measurements populate the ground state tautomer while the intensity-dependent measurements do not. We find that the ASE intensity as a function of temperature also decreases with increasing temperature, consistent with our absorption results.

ASE photodegradation and recovery at different intensities and room temperature shows that the rate of photodegradation, (i.e, dimer formation) increases with increas-

ing intensity. But the recovery rate or the formation of the molecules back from the dimer state is independent of the intensity. This combination of measurements are consistent with our proposed model of excitation → tautomer formation → emission → dimer formation → breakup of dimers as responsible for photodegradation and recovery.

Future Work

We have added gamma irradiation as yet another factor for improving material self-healing and find that the molecule recovers to a higher ASE efficiency after irradiation than for the pristine sample. At this point the mechanism is unknown. But the observation suggests the potentially interesting prospect of applying laser cycling and gamma irradiation to make more robust materials for high-intensity application. Understanding the mechanisms of self-healing at the microscopic level will undoubtedly lead to many avenues for making novel materials.

Appendices

Appendix A

Absorption cross section σ

The intensity that exits a material of thickness l and absorption coefficient α is given by

$$I(l) = I(0) \exp(-\alpha l), \tag{A.1}$$

where I(0) is the incident intensity. The absorbance A is defined as the log of the ratio of the transmitted intensity to the incident intensity,

$$A = -\log\left[\frac{I(l)}{I(0)}\right]. \tag{A.2}$$

Using equation[A.1] and equation[A.2], we get an expression for the absorption coefficient α

$$\alpha = \frac{A}{l \log[e]} \tag{A.3}$$

The absorption cross section is related to α by

$$\sigma = \frac{\alpha}{N}, \tag{A.4}$$

where N is the number density of molecules. Using Equation[A.4] and linear absorption of the DO11/PMMA sample, we can estimate the absorption cross section as in the Figure A.1.

To calculate the number density N, we use the equation by Kuzyk[1]. Using the density of PMMA, $\rho = 1.19 g/cm^3$, the molecular weight of DO11, $m_d = 237$, and 0.95Wt% of DO11(9g/l), we get the number density $N = 2.4 \times 10^{16}$.

Estimation of the Parameters

- The number of photons absorbed per unit time by the sample , ω_p, is estimated using the equation

$$\omega_p = \frac{\sigma I}{\hbar \omega}, \tag{A.5}$$

  where $\omega = \frac{c}{\lambda}$, c=3 $\times$ 10^8 m/s, λ=532nm, σ=6 $\times$ 10^{-20} m^2, $\hbar = 1.1 \times 10^{-34}$ Js, and typicaly I = 1.67 $\times$ 10^{10} W/m^2. This yields $\omega_p = 1.5 \times 10^{10}$ per second.

- The radiative decay rate γ_{32} from T_0-T_1 is estimated using the CEO given by

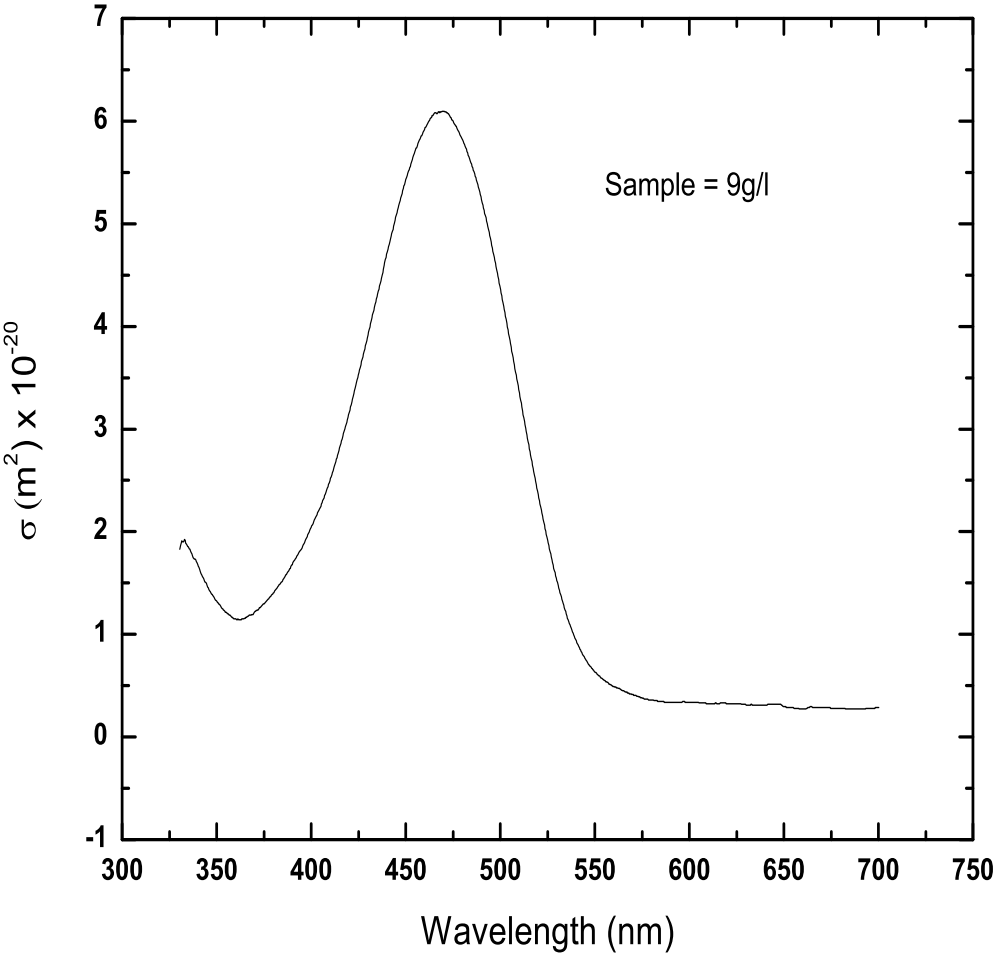

Figure A.1: Absorption cross-section of DO11 in PMMA.

Equation 2.13 and the value found is 4ns, where e = 1.6 $\times$ 10^{-19}C, ϵ_0 = 8.85 $\times$ 10^{-12} F/m, m_e=9.1 x 10^-31 kg, λ_0=595nm and n=1.49. This yields γ_{32} = 2.5×10^8 per second.

- The radiative decay rate γ_{41} from S_0-S_1 is estimated the same way as γ_{32} except that λ_0=470nm. This yields $\gamma_{41} = 4.0 \times 10^8$ per second

- γ_{43} is the phototautomerization rate and it is in the picosecond time range.

- γ_{21} is also rate of phototautomerization but slower than γ_{43} due to dimer formation.

Appendix B

The Mathematica Code for

Modeling Population Dynamics

Model For The Degradation Process

```
Needs["BiokmodSysModel"];

Needs["BiokmodFitmodel"];

SetDirectory["D:\1aNatnael\analysis"];

data1 = Import["A02199g1.dat"];

I1 = 1.67 * 10^10;

nn = Dimensions[data1]//First;

ω = 3 * 10^8/(532 * 10^(-9));

hbar = 1 * 10^(-34);
```

$\sigma = 6 * 10\text{^}(-20);$

$\omega_p = \sigma \text{I1}/(\text{hbar}\omega);$

$\gamma_{32} = 2.5 * 10\text{^}8;$

$L = 10\text{^} - 2;$

$a = 10\text{^} - 5;$

$\gamma_{21} = 1.0 * 10\text{^}10;$

$\gamma_{43} = 1.0 * 10\text{^}11;$

$\gamma_{41} = 4.0 * \ 10\text{^}8 \ ;$

$\omega_s = \gamma_{32} \ \left(\frac{a^2}{4L^2} e^{x_3[t] \ \sigma L} - \frac{a^2}{4L^2}\right);$

$\text{datax} = \text{data1};$

$\text{datax}[[\text{All}, 2]] = 0;$

$\text{For}[i = 1, i \leq \text{nn}, \text{datax}[[i, 2]] = 1/(\sigma L)$

$\text{Log}[1 + \left(\frac{\text{data1}[[i,2]] 4 \sigma L\text{^}2}{\gamma_{32} \text{hbar} \omega a\text{^}2}\right)]; i{+}{+}];$

$\text{data1} = \text{datax};$

$\text{datax1} = \text{datax};$

$\text{datax1}[[\text{All}, 2]] = 0;$

$\text{For}\left[i = 1, i \leq \text{nn}, \text{datax1}[[i, 2]] = \frac{\text{datax}[[i,2]]}{\text{datax}[[1,2]]}; i{+}{+}\right];$

$\text{data1} = \text{datax1};$

$\text{Model5} = \text{CoefMatrix}\left[5, \left\{\{1, 1, -\omega_p\}, \{1, 2, \gamma_{21}\}, \{1, 4, \gamma_{41}\},\right.\right.$

$\left.\left.\{1, 5, 2\gamma_{51}\}, \{2, 2, -\gamma_{21} - \gamma_{25}\}, \{2, 3, \omega_s + \gamma_{32}\},\right.\right.$

$\{3,3,-\gamma_{32}-\omega_s\},\{3,4,\gamma_{43}\},\{4,1,\omega_p\},\{4,4,-\gamma_{43}-\gamma_{41}\},$

$\{5,2,\gamma_{25}\},\{5,5,-2\gamma_{51}\}\}];$

$\text{bb}=\{0,0,0,0,0\};$

$\text{IC}=\{\text{data1}//\text{First}//\text{Last},0,0,0,0\};$

$\text{ShowODE}[\text{Model5},\text{IC},\text{bb},t,x]\backslash\backslash\text{MatrixForm}$

$$\begin{pmatrix} x_1'[t]==-\omega_p x_1[t]+\gamma_{21}x_2[t]+\gamma_{41}x_4[t]+2\gamma_{51}x_5[t] \\ x_2'[t]==(-\gamma_{21}-\gamma_{25})\,x_2[t]+(\gamma_{32}+\omega_s)\,x_3[t] \\ x_3'[t]==(-\gamma_{32}-\omega_s)\,x_3[t]+\gamma_{43}x_4[t] \\ x_4'[t]==\omega_p x_1[t]+(-\gamma_{41}-\gamma_{43})\,x_4[t] \\ x_5'[t]==\gamma_{25}x_2[t]-2\gamma_{51}x_5[t] \\ x_1[0]==1 \\ x_2[0]==0 \\ x_3[0]==0 \\ x_4[0]==0 \\ x_5[0]==0 \end{pmatrix}$$

$\text{X1}[\text{t1\_},\text{c1\_}?\text{NumericQ},\text{c2\_}?\text{NumericQ}]:=x_3[t]/.$

$\text{SystemNDSolve}[\text{Model5}/.\{\gamma_{25}\to\text{c1},\gamma_{51}\to\text{c2}\},$

$\text{IC},\text{bb},\{t,0,\text{data1}//\text{Last}//\text{First}\},$

$t,x(*,\text{MaxSteps}\to 1000000*)]/.t\to\text{t1}$

$\text{Timing}[\text{fittedparameters}=\text{FindMinimum}[\text{X2Fit}[\{\text{c1},\text{c2}\},$

$\text{data1},\text{X1}[t,\text{c1},\text{c2}],t],$

{c1, 0.01, 0.02}, {c2, 0.0001, 0.0002}]]

Plot[Evaluate[X1[t, c1, c2]/.fittedparameters

[[2]], {t, 0, data1//Last//First},

PlotRange → All, Prolog:>Map[{Orange,

PointSize[.04], Point[##]}&, data1]]]]

Model for The Recovery Process

Needs["BiokmodSysModel"];

Needs["BiokmodFitmodel"];

SetDirectory["D:\Research\Dissertation

\Natnael\analysis"];

data21 = Import["GA02249g1R.dat"];

I1 = 0;

ω = 300000000/(532 * 10^(−9));

hbar = 1 * 10^(−34);

σ = 6 * 10^(−20);

ω_p = σI1/(hbarω);

γ_{32} = 0; L = 10^ − 2;

a = 10^ − 5;

$\gamma_{21} = 0;$

$\gamma_{43} = 0;$

$\gamma_{32} = 0;$

$\gamma_{25} = 0;$

$\gamma_{41} = 0;$

$\omega_s = \gamma_{32} \left(\frac{a^2}{4L^2} e^{x_3[t]\sigma L} - \frac{a^2}{4L^2}\right);$

$\text{Model5} = \text{CoefMatrix}[5, \{\{1, 1, -\omega_p\}, \{1, 2, \gamma_{21}\},$

$\{1, 4, \omega_p + \gamma_{41}\}, \{1, 5, 2\gamma_{51}\}, \{2, 2, -\gamma_{21} - \gamma_{25} - \omega_s\},$

$\{2, 3, \omega_s + \gamma_{32}\}, \{3, 2, \omega_s\}, \{3, 3, -\gamma_{32} - \omega_s\},$

$\{3, 4, \gamma_{43}\}, \{4, 1, \omega_p\}, \{4, 4, -\gamma_{43} - \omega_p - \gamma_{41}\},$

$\{5, 2, \gamma_{25}\}, \{5, 5, -2\gamma_{51}\}\}]; \text{bb} = \{0, 0, 0, 0, 0\};$

$\text{IC} = \{\text{data21//First//Last}, 0, 0, 0, \text{data21}$

$\text{//Last//Last}\};$

$\text{ShowODE}[\text{Model5}, \text{IC}, \text{bb}, t, x]\text{//MatrixForm}$

$$\begin{pmatrix} x_1'[t] == 2\gamma_{51}x_5[t] \\ x_2'[t] == 0 \\ x_3'[t] == 0 \\ x_4'[t] == 0 \\ x_5'[t] == -2\gamma_{51}x_5[t] \\ x_1[0] == 0.12564 \\ x_2[0] == 0 \\ x_3[0] == 0 \\ x_4[0] == 0 \\ x_5[0] == 0.77793 \end{pmatrix}$$

X1[t1_, c1_?NumericQ]:=$x_1[t]$/.SystemNDSolve[Model5/.

$\{\gamma_{51} \to$ c1$\}$, IC, bb, $\{t, 0,$ data21//Last//First$\}$,

$t, x]/.t \to$ t1

Timing[fittedparameters = NMinimize[{X2Fit[{c1}, data21,

X1[t, c1], t], 0 < c1 < 0.1}, {c1}]]

Plot[Evaluate[X1[t, c1]/.fittedparameters[[2]],

$\{t, 0,$ data21//Last//First$\}$, PlotRange $\to \{\{-1000, 35500\},$

$\{0, 1\}\}$, Prolog:>Map[{Orange, PointSize[.04],

Point[##]}&, data21]], FrameLabel $\to \{t$[seconds],

"Recovered ASE[Normalized]"}, Frame $\to$ True]

Bibliography

[1] M. G. Kuzyk, *Polymer Fiber Optics: Materials, Physics, and Applications*, Vol. **117** of Optical Science and Engineering (CRC Press, 2006).